SCOUR AROUND A CIRCULAR PILE
DUE TO OSCILLATORY WAVE MOTION

A Thesis

by

DONALD RAYMOND WELLS

Submitted to the Graduate College of
Texas A&M University in
partial fulfillment of the requirement for the degree of

MASTER OF SCIENCE

January 1970

Major Subject: Civil Engineering

SCOUR AROUND A CIRCULAR PILE

DUE TO OSCILLATORY WAVE MOTION

A Thesis

by

DONALD RAYMOND WELLS

Approved as to style and content by:

_____
(Chairman of Committee)

_____ _____
(Head of Department) (Member)

_____ _____
(Member) (Member)

January 1970

ABSTRACT

Scour Around a Circular Pile Due to Oscillatory Wave Motion. (January 1970)

Donald R. Wells, B.S.C.E., University of South Carolina

Directed by: Dr. Robert M. Sorensen

Incipient motion and scour caused by a circular cylindrical pile are studied using a two-dimensional wave flume and natural sands. Through dimensional analysis the influential parameters are developed and the data collected are studied to determine the functional relationships between the parameters. The primary objective of the study was to determine the parameters that control ultimate scour depth and their influence on the resulting scour patterns.

ACKNOWLEDGMENTS

The author wishes to express his sincere gratitude to Dr. R. M. Sorensen whose advice, encouragement and continual support throughout the preparation of this report was greatly appreciated. A note of thanks is also due Dr. J. B. Herbich whose words of advice and wisdom were freely given.

A special note of thanks is also due to the U.S. Navy Civil Engineer Corps and their parent organization, the Naval Facilities Engineering Command who gave the author the opportunity to increase his knowledge and gain new insight into the coastal and ocean engineering discipline.

And finally a special note of thanks is due to the author's wife for her continual encouragement and advice throughout the preparation of this report. And to my children who have done without their fair share of my time in the past two years.

TABLE OF CONTENTS

LIST OF TABLES

LIST OF FIGURES

CHAPTER I

INTRODUCTION

The primary objective of this research was to study the effects of scour around a circular pile caused by oscillatory motion. The study was begun by observing incipient motion which is the beginning of any scour phenomena and concluded with the studies on scour.

Incipient motion and scour have been studied extensively with regard to open channel flow but it has only been in the last two decades that research has been carried out on these subjects in oscillatory motion. It is extremely difficult to formulate mathematical equations that represent accurately the phenomena of incipient motion and as yet no one has been able to formulate equations that will govern incipient motion in every case. The data obtained for incipient motion in this study was compared with the results obtained by others and no attempt will be made at describing the motion mathematically.

The remainder of the research was concentrated on studying by experiment in a uni-directional two-dimensional flow the scour around a circular pile and the ultimate depth reached by the scour. The experiments were conducted using one pile of 1.5 inch diameter and three natural sands. Two water depths of 1.25 ft. and 0.666 ft. and

---

"The citations on the following pages follow the style of the Journal of the Hydraulics Division, Proceedings of the American Society of Civil Engineers."

three waves of different characteristics were used in the experimentation. An attempt was made at correlating the scour patterns obtained and the vortex flow around the cylinder. The study will be carried out using several natural sands of various mean diameters.

CHAPTER II

REVIEW OF LITERATURE

INCIPIENT MOTION

Definition

It becomes obvious when reading papers on incipient motion that there is no single universally excepted definition for incipient motion. Because of this it is sometimes difficult to compare the results obtained by various authors. For the purposes of this study the definition put forth by Eagleson and Dean, (8) is best suited and will be used. They defined incipient motion as "an instantaneous condition reached when the resultant of all the active forces on the particle intersects the line connecting the bed particle contact points." The term "active" means all the forces due to water particle motion and gravity.

Review of Previous Work

Incipient motion has been studied as far back as 1753 when Brahms (15) presented his formula for the critical velocity necessary for incipient motion as:

$$U_{cR} = KW^{1/6} \qquad (1)$$

where

U_{cR} = critical velocity necessary to cause incipient motion,

W = submerged weight of the particle, and

K = coefficient.

The equation was not used extensively mainly because of the difficulty in evaluating the constant which is a function of numerous variables. In 1816, L. G. du Buat (15) presented a listing of pick up velocities for various types of granular materials. The majority of the research conducted up until the 1950's was concentrated in open channel flow. However in 1946, Bagnold (3) paved the way for the study of incipient motion in oscillatory flow. An excellent review of the literature on sediment transport and incipient motion is presented by Abou-Seida (1).

The first major work on incipient motion caused by oscillatory motion was done in 1954 by Li (10). Using an oscillating bed in a still fluid, Li investigated the boundary layer caused by oscillatory motion. He found that the transition from laminar to turbulent boundary layer occurred at a Reynolds number of 800 for a hydrodynamically smooth boundary and that the Reynolds number for the transition point was a function of roughness. Vincent (24) conducted a similar study; however, he used a wave flume so as to more naturally duplicate the conditions found in nature. From his studies, he found that the Reynolds number for the laminar to turbulent transition point of a smooth boundary was much less than that reported by Li. In both studies, Reynolds' number was defined as

$$N_R = d_1\sqrt{\frac{\omega}{\nu}} \tag{2}$$

where

ω = angular velocity of oscillation,

ν = kinematic viscosity, and

d_1 = max. amplitude of horizontal displacement at the bottom.

Using a first order wave theory approximation

$$d_1 = 2\left(\frac{H}{2 \text{ Sinh } \frac{2\pi h}{L}}\right) \tag{3}$$

where

H = wave height,

h = still water depth, and

L = wave length.

Vincent also concluded that the transition point was a function of roughness and would vary depending on the characteristics of the bed material. The discrepancy between the results of the two investigators can most probably be attributed to the differences in experimental set up. It is felt that the results obtained by Vincent are more correct as they more nearly duplicate nature.

Eagelson and Dean (8) continuing work initiated by Ippen and Eagleson (12) made a rigorous mathematical analyses of incipient motion and sediment transport and presented equations for both. Their equation for the velocity necessary for incipient motion to occur is

$$U^2 = \frac{4/3 \text{ gd}}{C_D}\left(\frac{S_s - S}{S}\right)\tan \phi \tag{4}$$

where

U = free stream velocity just above the boundary layer,

g = acceleration of gravity,

d = mean sediment particle diameter,

C_D = coefficient of drag,

S_s = specific gravity of sand,

S = specific gravity of water, and

ϕ = angle of repose of the sediment.

Several other authors have presented equations for incipient motion notably Goddet (19), Ko (14), Vincent (24), and Chepil (5).

All of the equations presented are accurate within certain limits but none of them will predict the exact occurrence of incipient motion. This is primarily due to the inability to evaluate the coefficients of drag and lift and the influences of the angle of repose, and bed particle geometry.

Raudkivi (19) presents a very good discussion of these problems. He points out that when the boundary layer thickness is approximately 5 or more times the surface roughness the flow around the individual exposed particles is laminar, eddies will not be shed and therefore the force being exerted on the particles will be fairly uniform across the bed. However when the boundary thickness becomes approximately less than the surface roughness dimension, the flow past the particles will be turbulent and eddies will be shed. The most exposed bed particles will form wakes and thus the hydrodynamic forces being exerted on the bed particles will be concentrated on the uppermost particles. Thus incipient motion can occur on a particular particle earlier than would be predicted by one of the equations for incipient motion. Coleman (6) recently has developed relationships between the drag coefficient C_D, the lift factor, K, which is similar to the lift coefficient C_L, and the Reynolds number. His results appear to have considerable merit. His equations, although for steady state

conditions, do give a representation for the lift on a bed particle. Using steel and plastic spheres and varying the viscosity of the liquid he was able to obtain data over a broad spectrum. Analyzing the data and arranging into a dimensionless force term

$$\frac{f}{\Delta\gamma d^3} \tag{5}$$

where

f = measured drag force,

$\Delta\gamma$ = differential of weight density between the particle and a fluid, and

d = particle diameter

and plotting it against Reynolds number, N_R (see Fig. 1), he found that the data for both the steel and plastic spheres plotted on the same curve. He has concluded that all other materials should also plot on approximately the same curve. The functional dependency between the lift factor K, the drag coefficient C_D, the Reynolds number N_R and the relative boundary layer thickness, d/δ, are readily apparent by observing Fig. 2. Examining Fig. 2, it can be seen that when the boundary layer thickness, δ, is larger than the mean bed particle diameter there is negative lift on the particle and when the boundary layer shrinks to a thickness less than the mean particle diameter the lift factor becomes positive and there exists a force trying to lift the bed particle into suspension.

Reference (22) presents an excellent discussion on incipient motion including an analysis and comparison of the results of several

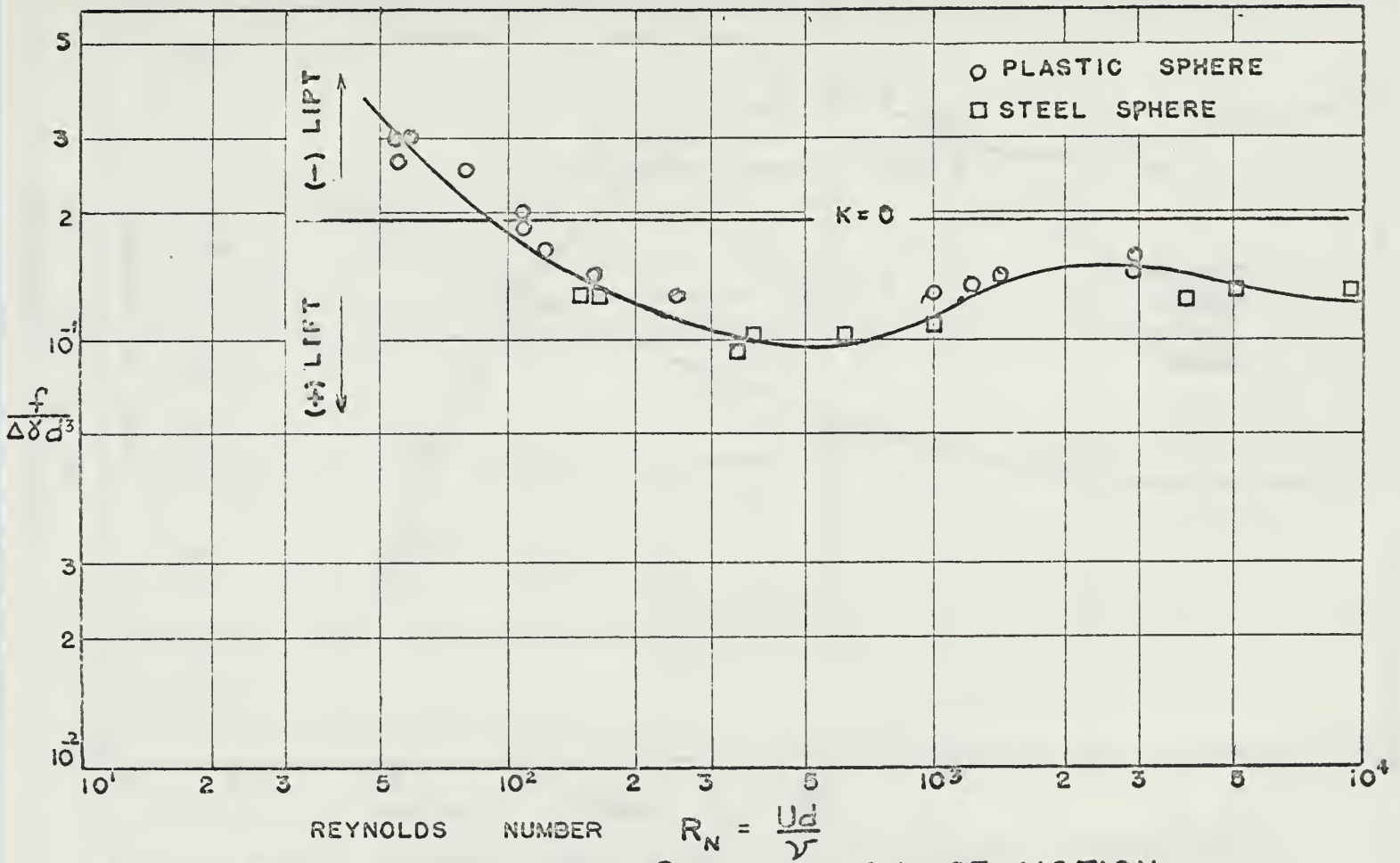

FIG. I. FORCE FUNCTION AND INITIATION OF MOTION

AFTER (COLEMAN)

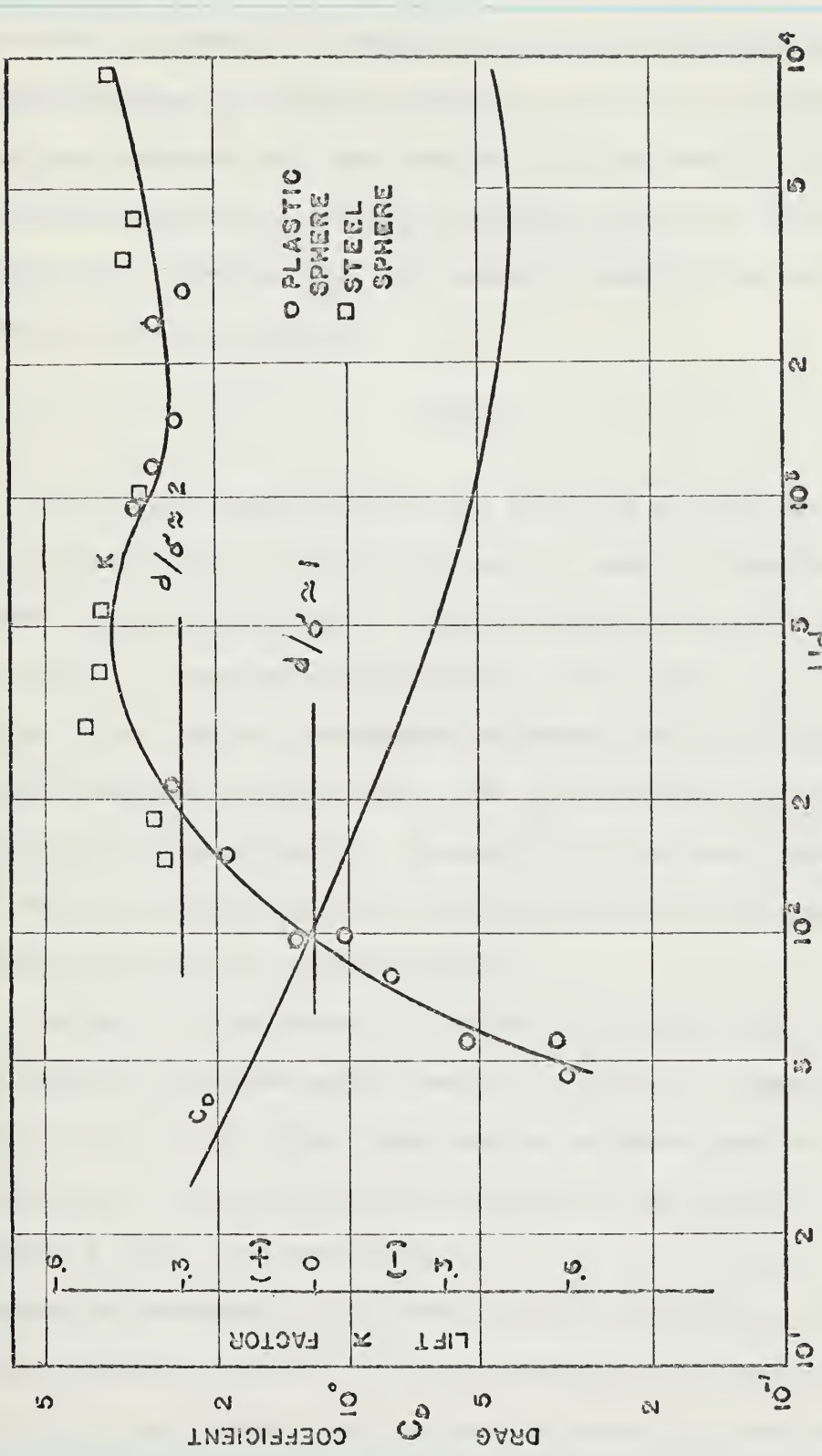

FIG. 2. LIFT FACTOR AND DRAG COEFFICIENT FUNCTIONS

AFTER (COLEMAN)

authors. In general the committee on sedimentation has found many inconsistencies in critical velocities necessary for incipient motion and have concluded that when studying incipient motion critical shear stresses should be the governing parameter instead of critical velocities. Reference (22) also presents equations for incipient motion from various authors.

SCOUR

Very little experiment work has been done on scour due to oscillatory wave motion, however there exists a wealth of knowledge on scour in open channel flow. Since the forces that cause scour are virtually the same for oscillatory flow as for open channel (steady state) flow, that is, hydrodynamic in nature, the knowledge gained from experiments in open channel flow can be applied with reservations to oscillatory motion. The majority of the work done on scour in oscillatory motion has been concerned primarily with scour of beaches and littoral sediment transport.

Murphy (17), Van Weele (23) and Ko (14) studied scour in front of seawalls of various angles, and their results are summarized by Herbich et al. (9). They found that the ultimate depth of scour is a function of wave characteristics as well as the number of waves passing a given point where scour occurs and scour approaches its maximum value asymptotically after initially increasing very rapidly. Roper, Schneider and Shen (20) have shown that for steady state conditions in open channel flow the depth of scour is a function of the

pier Reynolds number. The pier Reynolds number is defined as

$$N_{RP} = \frac{UD}{\nu} \tag{6}$$

where

U = horizontal free stream velocity,

D = pile diameter, and

ν = kinematic viscosity.

They have further shown that the scour is influenced by the type of vortex system caused by the pier. For a circular pile a horseshoe vortex system is most generally formed. The vortex system gets its name from the physical similarities between it and a horseshoe. Slugs of bed particles have been observed to be scoured from around a pile when the vortex is periodically shed. For nonsteady state conditions (oscillatory motion) this horseshoe vortex system may not have time to build up to such an intensity that it is shed and therefore the vortex system formed by oscillatory wave motion may not influence the scour.

The influence of the bed particle size on scour is not generally known, however studies conducted by Roper, Schneider and Shen (20) show that when the bed particle size is greater than 0.52 millimeter, the particle size influences scour depth and when the particle size is less than 0.52 millimeter scour depth is independent of particle size. Studies conducted by Richardson, Zaki, and Bagnold and reported by Raudkivi (19) have shown that the concentration, C, equal to the ratio of grain occupied space to whole space has an influence on the drag coefficient and thereby could influence scour depth.

Carstens (4) in a report on scour has made extensive studies of the scour associated with different types of obstacles. From his study he has shown that the rate of scour caused by an object in the flow path is a function of the sediment number N_s, sediment grain geometry, and the ratio of the scour depth to the obstacle size. The sediment number is defined as

$$N_s = \frac{U}{\sqrt{(S_s-1)gd}} \tag{7}$$

where

U = free stream velocity,

S_s = specific gravity of sediment,

g = acceleration of gravity, and

d = mean sediment particle diameter.

His studies were primarily conducted in steady flow. He presents equations for the ultimate scour depth associated with a vertical cylinder obstacle and for the relative scour depth as a function of the sediment number, however all his equations are based on the supposition that the scour hole formed will have the appearance and form of an inverted frustum of a right circular cone having a base diameter equal to the pile diameter and a side slope equal to the angle of repose.

To mathematically describe scour in oscillatory flow is extremely difficult. The parameters involved that influence scour are troublesome to analyze and are interrelated in a complex way.

CHAPTER III

THEORETICAL CONSIDERATIONS

The forces that influence or cause motion of bed particles, whether it be at the initial stages of motion (incipient) or well into defined scour are hydrodynamic. The water particle motions, velocities and accelerations, and the forces they in turn produce will be calculated using Stokes third order wave theory. This theory was chosen to be used after studying papers by Dean (7) and Le Méhaute, Divoky and Lin (16) and comparing the wave characteristics with the results published by the aforementioned authors.

STOKES THIRD ORDER WAVE THEORY

To present a complete discussion of his theory is beyond the scope of this report and only the pertinent equations related to this study will be presented. A complete discussion of Stokes theory can be found in Wiegel (25), Ippen (11) and others.

Stokes theory is an infinite series solution obtained by expanding the velocity potential about the still water line. It merely includes more terms in the series solution than does the Airy theory which uses only the first term of the series. Stokes theory can be expanded into any order theory but the third and fifth order theories are the most stable.

A close inspection of the equations of the third order theory shows that all the equations contain repeating constants and that the

theory can be somewhat simplified by tabulating these constants for various values of wave characteristics. This has been done by Skjelbreia (21).

The repeating functions associated with the wave profile as defined by Skjelbreia are

$$A_1 = \frac{a}{L} \tag{8}$$

$$A_2 = \pi A_1^2 \cdot f_2 \left(\frac{h}{L}\right) \tag{9}$$

and

$$A_3 = \pi^2 A_1^3 \cdot f_3 \left(\frac{h}{L}\right) \tag{10}$$

where

a = wave amplitude,

L = wave length,

h = still water depth, and

where

$$f_2\left(\frac{h}{L}\right) = \frac{\left(2 + \cosh \frac{4\pi h}{L}\right) \cosh \frac{2\pi h}{L}}{2 \sinh^3 \frac{2\pi h}{L}} \quad \text{and} \tag{11}$$

$$f_3\left(\frac{h}{L}\right) = \frac{3}{16} \quad \frac{1 + 8 \cosh^6 \frac{2\pi h}{L}}{\sinh^6 \frac{2\pi h}{L}} \tag{12}$$

The common factors associated with water particle velocity and accelerations are

$$F_1 = \frac{2\pi a}{L} \cdot \frac{1}{\sinh \frac{2\pi h}{L}} \tag{13}$$

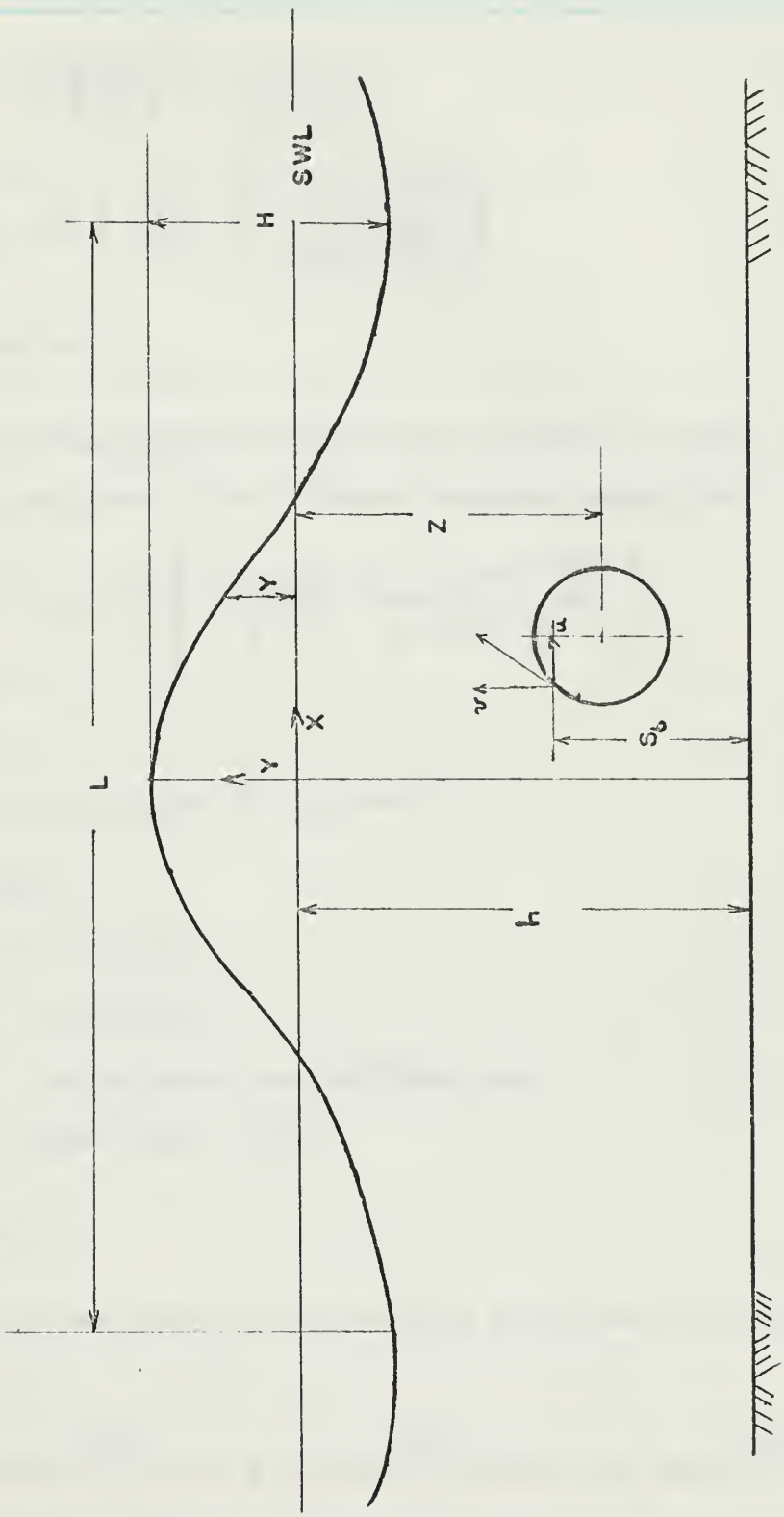

FIG. 3. DEFINITION SKETCH

$$F_2 = \frac{3}{4}\left(\frac{2\pi a}{L}\right)^2 \cdot \frac{1}{\sinh^4 \frac{2\pi h}{L}} \tag{14}$$

$$F_3 = \frac{3}{64}\left(\frac{2\pi a}{L}\right)^3 \cdot \left(\frac{11-2\cosh \frac{4\pi h}{L}}{\sinh^7 \frac{2\pi h}{L}}\right) \tag{15}$$

Wave Characteristics

The wave length, wave velocity and wave profile for Stokes third order theory are given by the following equations respectively:

$$L = \frac{gT^2}{2\pi} \tanh \frac{2\pi h}{L}\left[1 + \left(\frac{2\pi a}{L}\right)^2 \frac{14 + 4\cosh^2 \frac{4\pi h}{L}}{16 \sinh^4 \frac{2\pi h}{L}}\right] \tag{16}$$

$$C = \frac{L}{T} \tag{17}$$

$$\frac{y}{L} = A_1 \operatorname{Cos} \theta + A_2 \operatorname{Cos} 2\theta + A_3 \operatorname{Cos} 3\theta \tag{18}$$

In the equations

T = wave period,

C = wave celerity,

y = instantaneous wave amplitude, and

θ = phase angle of wave.

Particle Velocity

The horizontal water particle velocity is defined by the equation

$$\frac{u}{C} = F_1 \cosh \frac{2\pi S_b}{L} \cos \theta + F_2 \cosh \frac{4\pi S_b}{L} \cos 2\theta + F_3 \cosh \frac{6\pi S_b}{L} \cos 3\theta \tag{19}$$

and the vertical water particle velocity is defined by the equation

$$\frac{v}{c} = F_1 \sinh \frac{2\pi S_b}{L} \sin \theta + F_2 \sinh \frac{4\pi S_b}{L} \sin 2\theta + F_3 \sinh \frac{6\pi S_b}{L} \sin 3\theta \qquad (20)$$

where u = instantaneous horizontal water particle velocity,

v = instantaneous vertical water particle velocity, and

S_b = distance from the bed to the water particle in question.

HYDRODYNAMIC FORCES

The forces influencing bed particle motion are hydrodynamic and consist of the forces of drag, lift , and inertia. However since the force due to inertia is a function of d^3 whereas the force due to drag is a function of d^2 and because inertia forces will never predominate due to the small particle size, the force of inertia will be neglected. The total hydrodynamic force will therefore be the combination of the lift force and the drag force. The hydrodynamic forces are opposed by the force of gravity and influenced by bed particle geometry.

Drag

In an ideal fluid, that is one having no viscosity and the flow being irrotational, the flow around an object will be as shown in Fig. 4a and the drag force on the object will be zero. However, there are no ideal fluids in nature, and consequently due to viscosity

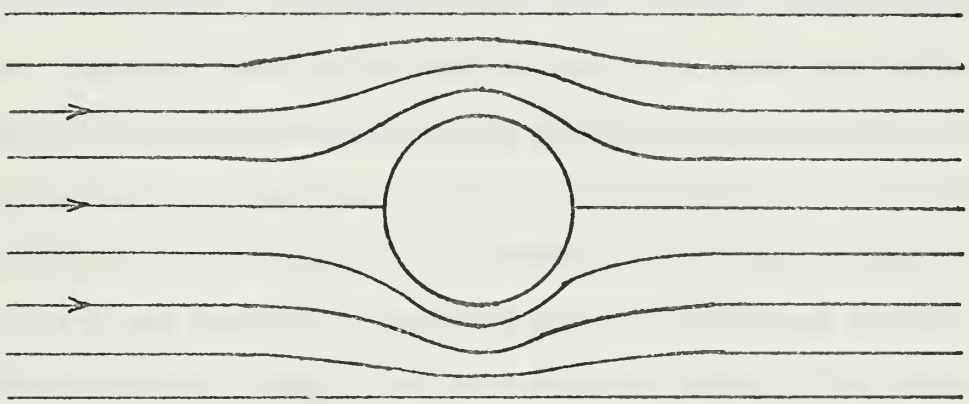

A. IDEAL FLOW

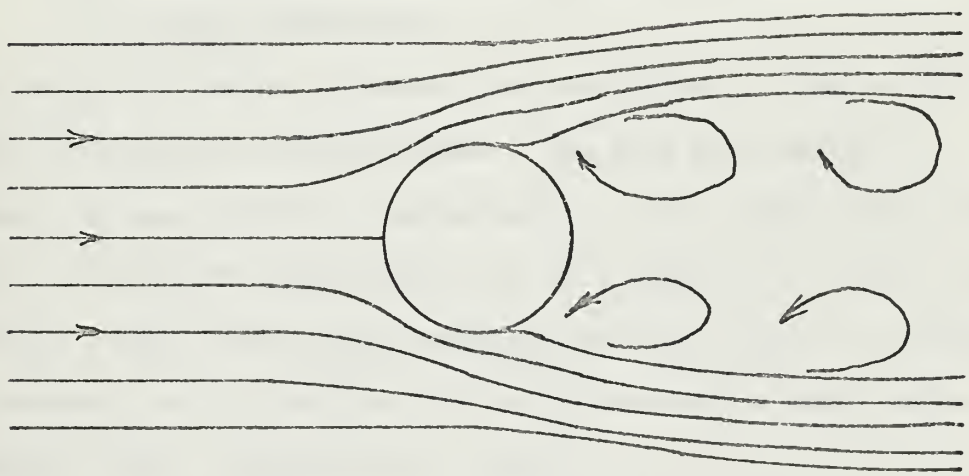

B. WITH SEPARATION

FIG. 4. FLOW AROUND A SPHERE

and boundary layer effects a separation of flow occurs on the boundary of the object and a wake is formed (Fig. 4b). The point of separation is a function of the shape of the object and the local Reynolds number. The drag force is the combination of the form drag due to pressure differential and the viscous drag due to skin function. The point through which the drag force acts is not necessarily the center of gravity of the bed particle but depends on the relative magnitude of the lift and drag force components which are functions of bed particle geometry, location and local Reynolds number. The steady force due to drag as developed in any elementary fluid mechanics text can be shown to be equal

$$F_D = \frac{C_D}{2} \rho A U^2 \tag{21}$$

where

A = projected area of object normal to flow direction

C_D = drag coefficient

Since drag is a viscous phenomena, the coefficient of drag is primarily influenced by Reynolds number. The drag coefficient for spheres has been studied by various authors under steady state conditions by letting the spheres free fall in a liquid in a large circular cylinder. Under steady state conditions the fall velocity is called the terminal velocity and the drag on the particle is equal to the submerged weight. Therefore for a sphere

$$C_D = \frac{4/3\ gd}{V^2} \left(\frac{\rho_s - \rho}{\rho} \right) \tag{22}$$

where

V = fall velocity at steady state conditions,

ρ_s = density of the sediment, and

ρ = density of the fluid.

Alger and Simons (2) studied the fall velocity for irregular shaped particles using a shape parameter

$$SF\ {}^{d}A/d_n \tag{23}$$

where

SF = Corey shape factor = $\frac{C}{\sqrt{ab}}$

C = minimum dimension of particle

a = maximum dimension of particle

b = intermediate dimension of particle

d_A = diameter of a sphere having the same surface area as that of the particle

d_n = diameter of a sphere which has the same volume as that of the particle.

Plotting C_D versus Reynolds number they found that as the shape factor increased the value of C_D increased for a constant Reynolds number. It was also found that an increase of the shape parameter indicates a decrease in the sliding-tipping motion and an increase in particle rotation. As reported by Eagleson and Dean (8), Carty studied the drag coefficient for various size spheres falling in an infinite fluid and rolling on an inclined plane. Eagleson and Dean (8) corrected Carty's data to take into account the effect of non-uniform free stream velocity and a plot of these data can be found in

reference (8). Because of the nonuniform shapes of sand grains and their angularity there will be a variance from the theoretical values of C_D for a sphere. Coleman (6) found in experiments where the forces were measured electronically and C_D was calculated for spheres of plastic and steel that the data had considerable scatter but tended to group around the theoretical curve of C_D versus N_R for fall velocity.

The drag coefficient therefore is not simply related to Reynolds number but is a function of Reynolds number, particle geometry, and is also influenced to some unknown extent by adjacent particles causing anomalies in the flow patterns.

Lift

The relationship for the force due to lift is similar to that for form drag and is given by

$$F_L = \frac{C_L}{2} \rho A U^2 \qquad (24)$$

where

C_L = coefficient of lift

A = projected area perpendicular to flow direction.

The lift force is the resultant due to the pressure differential above and below the particle. The pressure differential is caused when the fluid velocity is increased as it passes over the top of the particle thereby decreasing the pressure and since the pressure below the particle remains fairly static there is a pressure differential

or lift force. A significant number of the studies conducted on forces related to particle movement has neglected the lift force however the proof that it does exist and is significant has been reported (6) (22).

The coefficient of lift has not been studied as extensively as the coefficient of drag primarily due to the difficulty in evaluating it. Coleman's (6) work appears to give the best indications of its value.

GRAVITY

The hydrodynamic forces are opposed by the weight of the particle, friction and the intergranular reactions. The friction and intergranular reaction are difficult to evaluate but the gravity force can be represented by the equation

$$F_g = \frac{\pi d^3}{6} (\gamma_s - \gamma_f) \tag{25}$$

where

γ_s = specific weight of the sand, and

γ_f = specific weight of the fluid.

MECHANICS OF MOTION

It is very difficult to study the motion of sand grains primarily due to their varying sizes, angularity, and distribution in a bed. Therefore the problem must be simplified. This can be done by considering the sand grains to be spheres of uniform size. Referring

to Figs. 5 and 6 it can be seen that the total hydrodynamic force, F_T, is the combination of the lift and drag force. Referring to Fig. 2 it can be seen that the lift factor K and consequently the lift force will be negative for Reynolds number less than approximately 100. It is therefore possible for the particle to be pushed into the bed rather than be lifted out or rolled along it.

For motion to occur the sum of the moments about point R must be zero or in other words, F_T times its moment arm, d, must equal F_g times its moment arm, dsin θ. When this condition exists incipient motion can occur.

In Fig. 6 the total hydrodynamic force is shown acting through the center of gravity of the particle. This will not always be true and the point through which the force will act will depend on whether the flow around the particle is laminar or turbulent. However, for this study with shallow water waves the flow will be parallel to the bed and therefore the force, F_T, can be considered to act through the center of gravity.

The velocity, U, used in evaluating the results of these experiments will be the maximum water particle velocity that occurs at the bed and is the velocity associated with the wave crest for shallow water waves. Some authors include the entrainment velocity but that will not be done in these experiments.

FLOW AROUND THE PILE AND ITS RELATIONSHIP TO SCOUR

Any obstacle inserted into the region of a flowing medium will

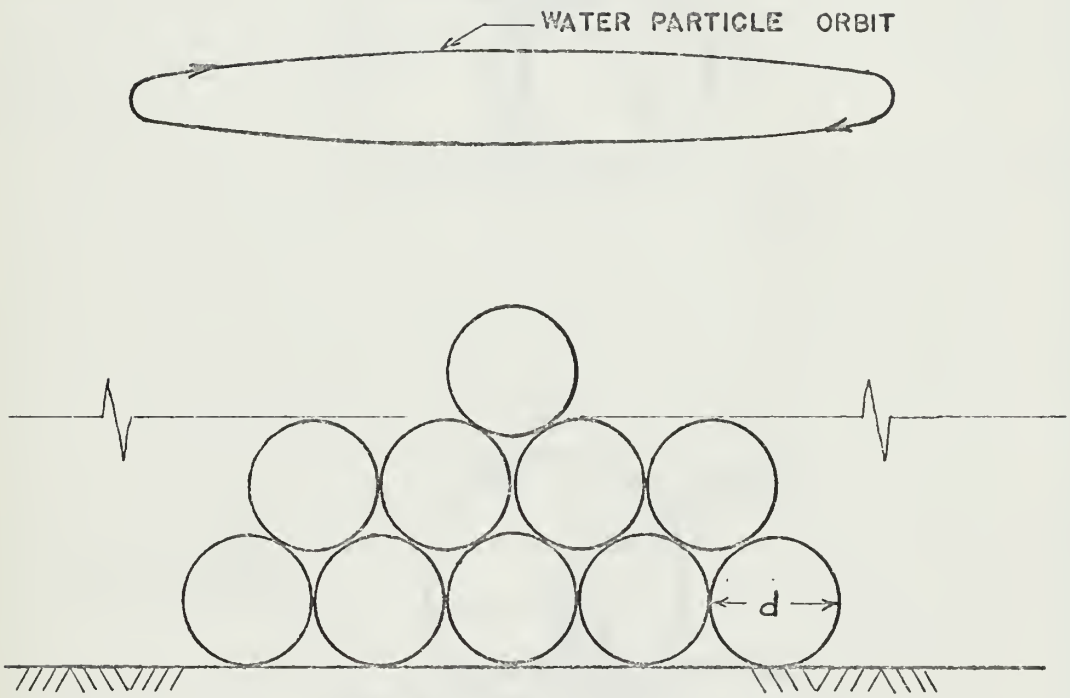

FIG. 5. HYPOTHETICAL BED OF SPHERICAL SAND GRAINS

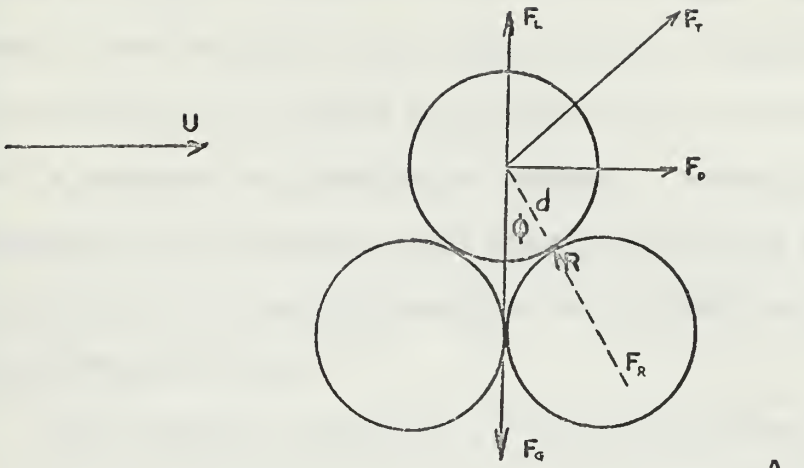

A.

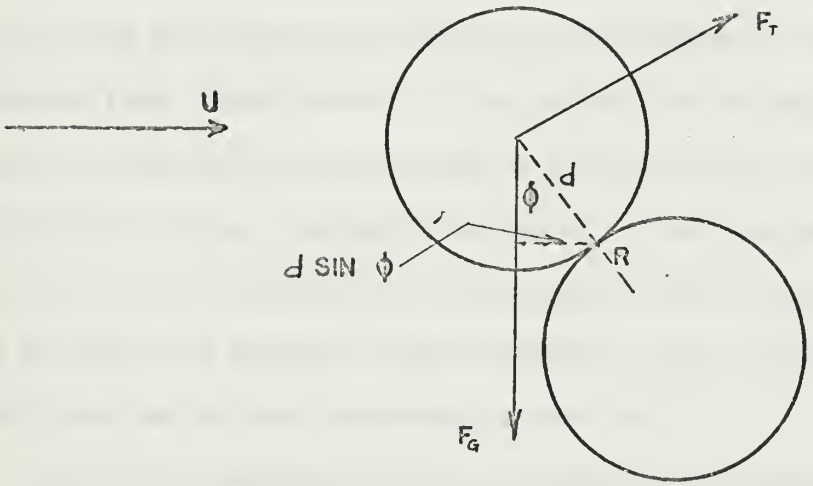

B.

FIG. 6. MECHANICS OF MOTION

cause the flow to be diverted around the obstacle. Depending on the shape of the obstacle, type of flow, and local Reynolds number, the flow velocity will increase as the flow deflects around the obstacle with a consequential reduction of pressure. Depending on surface roughness on the boundary, local Reynolds number and boundary layer thickness the flow can separate from the boundary causing a wake to occur behind the pile.

From potential flow theory, it can be shown that for flow around a cylinder the velocity of the flow at the points on the cylinder ninety degrees from the initial direction of flow will be twice the initial velocity of flow. In oscillatory flow where the direction of flow is changing periodically, the separation condition might not occur unless the distance the water particle moves is several pile diameters long. Also because of the periodic direction changes of the flow it is doubtful that the velocity of flow at the ninety degree points will be twice the initial velocity. From observations it is felt that if the distance the water particle moves is approximately five or more pile diameters then separation should occur and eddies should form and be shed periodically from the pile.

In studies conducted by Roper, Schneider, and Shen (20), it was shown that the vortex system formed by flow around an obstacle was related to the shape and size of the obstacle. They concluded that the eddy structure formed is the basic mechanism of scour and that the depth of scour was a function of the pier or pile Reynolds number, N_{RP}

where $N_{RP} = \frac{UD}{\nu}$ and (26)

D = pile diameter, and

ν = kinematic viscosity.

Because of the difficulty in evaluating the parameters that influence scour and the ultimate scour depth, no formulation of mathematical equations will be attempted. However the interrelationships and interdependency of the parameters influencing scour will be studied using the tool of dimensional analysis.

CHAPTER IV

DIMENSIONAL ANALYSIS

INCIPIENT MOTION

The following are considered to be the significant variables influencing incipient motion:

Variable		Units	Dimensions
h	Still water depth	ft	L
H	Wave height	ft	L
T	Wave period	sec	T
μ	Viscosity of water	lb-sec/ft^2	$\frac{M}{LT}$
g	Acceleration due to gravity	ft/sec^2	L/T^2
ρ	Density of water	slugs/ft^3	$\frac{M}{L^3}$
ρ_s	Density of sand	slugs/ft^3	$\frac{M}{L^3}$
d	Mean diameter of sand particle (50% finer)	ft	L
ϕ	Angle of repose of sand particles	degrees	-

Employing the Buckingham pi theorem, the repeating variables selected are ρ, h, and T. The Mass-Length-Time (MLT) system was selected to be used. Nine variables and three dimensions result in six pi terms.

Formulating and solving the equations results in the six dimensionless pi terms which are

$$\pi_1 = \frac{H}{h} \qquad \pi_4 = \frac{\rho}{\rho_s}$$

$$\pi_2 = \frac{gT^2}{h} \qquad \pi_5 = \frac{d}{h}$$

$$\pi_3 = \frac{h^2\rho}{T\mu} \qquad \pi_6 = \phi$$

Rearranging and combining the terms results in the functional equation

$$f(\frac{d}{h}, \phi, \frac{H}{h}, \frac{h}{gT^2}, \frac{h^2}{\mu T}(\rho_s - \rho)) = 0 \tag{27}$$

Since these experiments will use sand as a bed material the density of sand ρ_s will not change; also the density and viscosity of water will remain constant. Therefore the parameter $\frac{h^2}{\mu T}(\rho_s - \rho)$ will be fairly constant and will vary as $\frac{h^2}{T}$ varies. Since h and T are included in the $\frac{h}{gT^2}$ parameter the $\frac{h^2}{\mu T}(\rho_s - \rho)$ parameter can be dropped as it is not significant. Also it is doubtful that the angle of repose will be a significant parameter in these experiments; therefore it will be discarded. That leaves the functional relationship

$$\frac{d}{h} = F(\frac{h}{gT^2}, \frac{H}{h}) \tag{28}$$

which is to say that for incipient motion the relative particle size is a function of relative depth and relative wave height.

SCOUR

The variables considered to be significant for scour contain those considered for incipient motion, h, H, d, T, μ, ρ, ρ_s, ϕ, g and

the additional variables listed below.

Variables		Units	Dimension
D	Pile diameter	ft	L
U	Free stream velocity	ft/sec	L/T
$\bar{S}_u$	Ultimate significant scour depth	ft	L
t	Elapsed time	secs	T

The variable U although not independent of those listed above was included so that the parameter N_s could be defined in its normally accepted form.

Using the Buckingham pi theorem with thirteen variables and three dimensions results in ten pi terms. Selecting H, U, and μ as repeating variables and formulating and solving the equations results in the following pi terms.

$$\pi_1 = \frac{H}{h} \qquad \pi_6 = \frac{\mu}{H\rho_s U}$$

$$\pi_2 = \frac{H}{D} \qquad \pi_7 = \frac{\mu}{H\rho U}$$

$$\pi_3 = \frac{H}{d} \qquad \pi_8 = \frac{H}{\bar{S}_u}$$

$$\pi_4 = \frac{H}{\mu T} \qquad \pi_9 = \frac{H}{\mu t}$$

$$\pi_5 = \frac{U^2}{Hg} \qquad \pi_{10} = \phi$$

Rearranging and combining the pi terms gives

$$\pi_{11} = \frac{1}{\pi_8} = \frac{\bar{S}u}{H}$$

$$\pi_{12} = \frac{\pi_3}{\pi_8} = \frac{\bar{S}u}{d}$$

$$\pi_{13} = \pi_4^2 \pi_5 = \frac{H}{gT^2}$$

$$\pi_{14} = \frac{\pi_4^2 \pi_5}{\pi_1} = \frac{h}{gT^2}$$

$$\pi_{15} = \frac{1}{\pi_2 \pi_7} = \frac{UD}{\nu} = N_{RP}$$

$$\pi_{16} = \pi_4 \pi_5 \pi_3 (\pi_6 - \pi_7) = \frac{\nu}{gd(S_s-1)T} \text{ where } \frac{\nu}{T} = ft^2/sec^2$$

Substituting U^2 for $\frac{\nu}{T}$

$$\pi_{16} = \frac{U}{\sqrt{(S_s-1)gd}} = N_s$$

$$\pi_{17} = \frac{\pi_4}{\pi_9} = \frac{t}{T}$$

Therefore the functional relationship for scour is

$$\frac{\bar{S}u}{H} = f\left(\frac{H}{gT^2}, \frac{h}{gT^2}, N_{RP}, N_s, \frac{\bar{S}u}{d}, \frac{H}{h}, \frac{t}{T}, \phi\right) \qquad (29)$$

CHAPTER V

EXPERIMENTAL APPARATUS AND EQUIPMENT

The experiments on incipient motion and scour were conducted using the 120 foot long, 3 foot deep and 2 foot wide two dimensional wind-wave channel. A false bottom 6 inches deep and 16 feet long was constructed in the channel. At each end of the 16 foot false bottom was a gradual slope to bring the wave up to the new depth at the top of the false bottom. The 16 foot false bottom was split into three sections, two 6 foot sections at each end with 4 feet of the test sand in the center between the 6 foot sections. The 1-1/2 inch diameter steel pile was placed in the center of the 4 foot sand test section and anchored to an aluminum frame above the wave tank that keeps the pile vertical and stable.

Fig. 7 shows the test facility schematically. There is a wave filter constructed of screen wire with 1/2 inch openings located approximately 20 feet in front of the forward edge of the test apparatus to smooth out irregularities in the generated waves.

Scour depth measurements were made using a depth probe that was attached to a device that could be rotated around the pile 360 degrees and extended up to 8 inches from the outer edge of the pile. The rotating ring was marked in degrees and the extended arm was marked in inches so that any scour measurement could be identified in polar coordinates.

A mechanical counter was attached to the wave generator so that

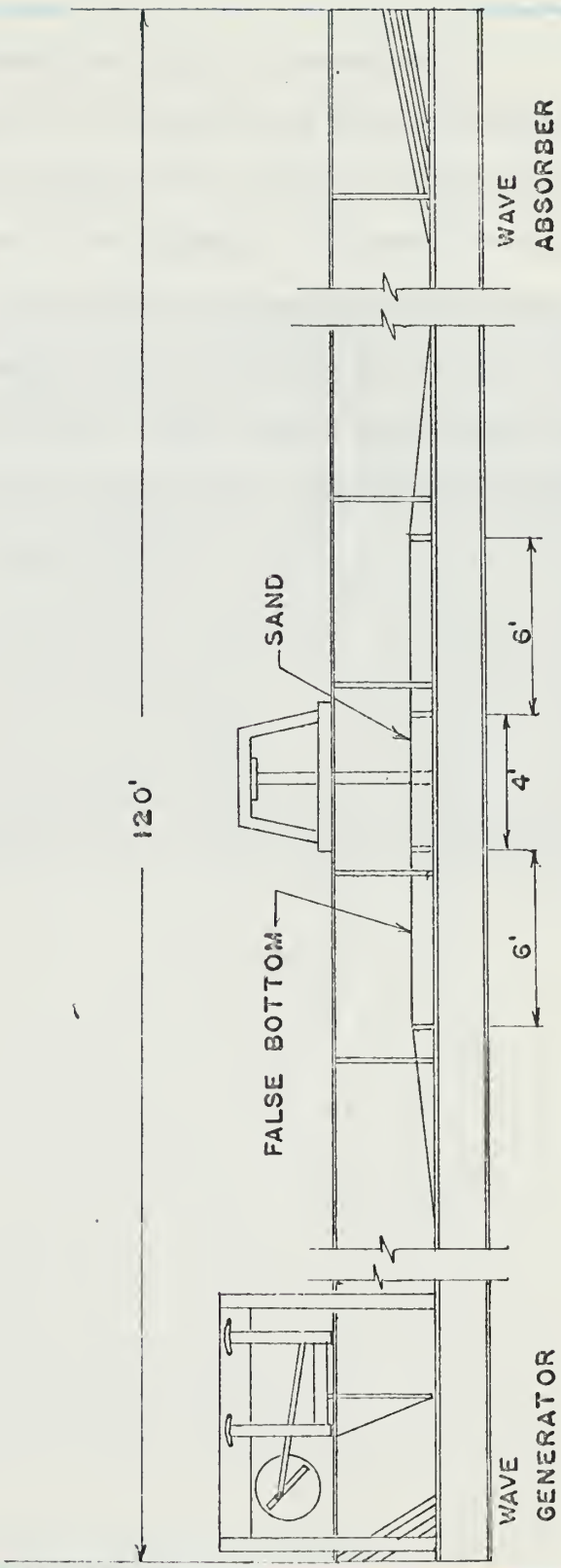

FIG. 7. TEST APPARATUS IN THE WIND-WAVE CHANNEL

the number of waves generated could be determined.

The wave generator is an oscillating pendulum type whose stroke and consequently wave height can be varied by adjusting the excentricity of the paddle arm on the flywheel. The period is varied through a variable rheostat that controls the speed of the flywheel. The rocker arms can be varied so as to vary the wave from a deep water wave to a shallow water wave. Wave heights and periods were measured by a capacitance wave gage connected to a Hewlett-Packard Dual Channel Carrier Amplifier recorder (Model No. 321).

FIG. 8. WAVE GENERATOR

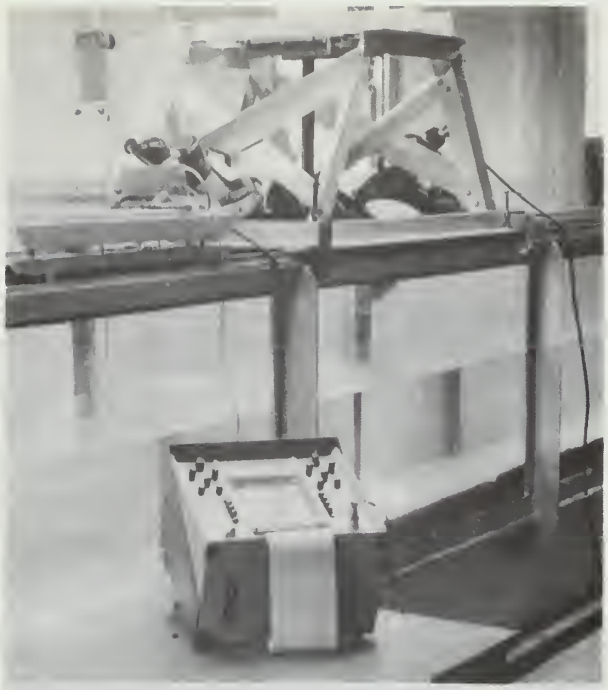

FIG. 9. HEWLETT-PACKARD DUAL CHANNEL RECORDER

FIG. 10. TEST FACILITY

FIG. 11. PILE RESTRAINING APPARATUS

CHAPTER VI

EXPERIMENTAL PROCEDURES

SIEVE ANALYSIS

Three sands were selected for use in the experiments. The sands were all standard Ottawa sands that are produced with a controlled size distribution. Each sand was subjected to a standard ASTM sieve analysis using sieve sizes 20, 30, 40, 50, 80, 100 and 200. A plot of the distribution of each sand is shown in Figs. 12, 13 and 14. The mean particle diameter (50% finer) for each sand was found from the sieve analysis. Twenty to thirty sand grains for each sand were collected as close to the mean diameter as possible and these grains were weighted and the average weight per sand grain tabulated.

Table 1 shows the sieve analysis data for the three experimental sands.

FALL VELOCITY

Fall velocity experiments were run to determine the C_D values for each sand. Although C_D was not used in evaluating incipient motion or scour, it was felt that the experiments would be worthwhile. Two experiments were conducted using mean diameter sand grains for each of the three sands. The sand grains were allowed to fall in an 8 ft long and 8 inch diameter cylindrical plexiglass cylinder filled with water. The grains were allowed to free fall over measured distances

TABLE 1.— EXPERIMENTAL SAND CHARACTERISTICS

Test Sand (1)	Manufacture trade name (2)	Mean grain diameter, d in millimeters (3)	Average weight per grain in grams (4)	Density in grams per cubic centimeter (5)
1	Sawing sand	0.62	2.314×10^{-4}	2.67
2	Crystal sand	0.325	1.310×10^{-4}	2.66
3	Bond sand	0.30	6.854×10^{-5}	2.665

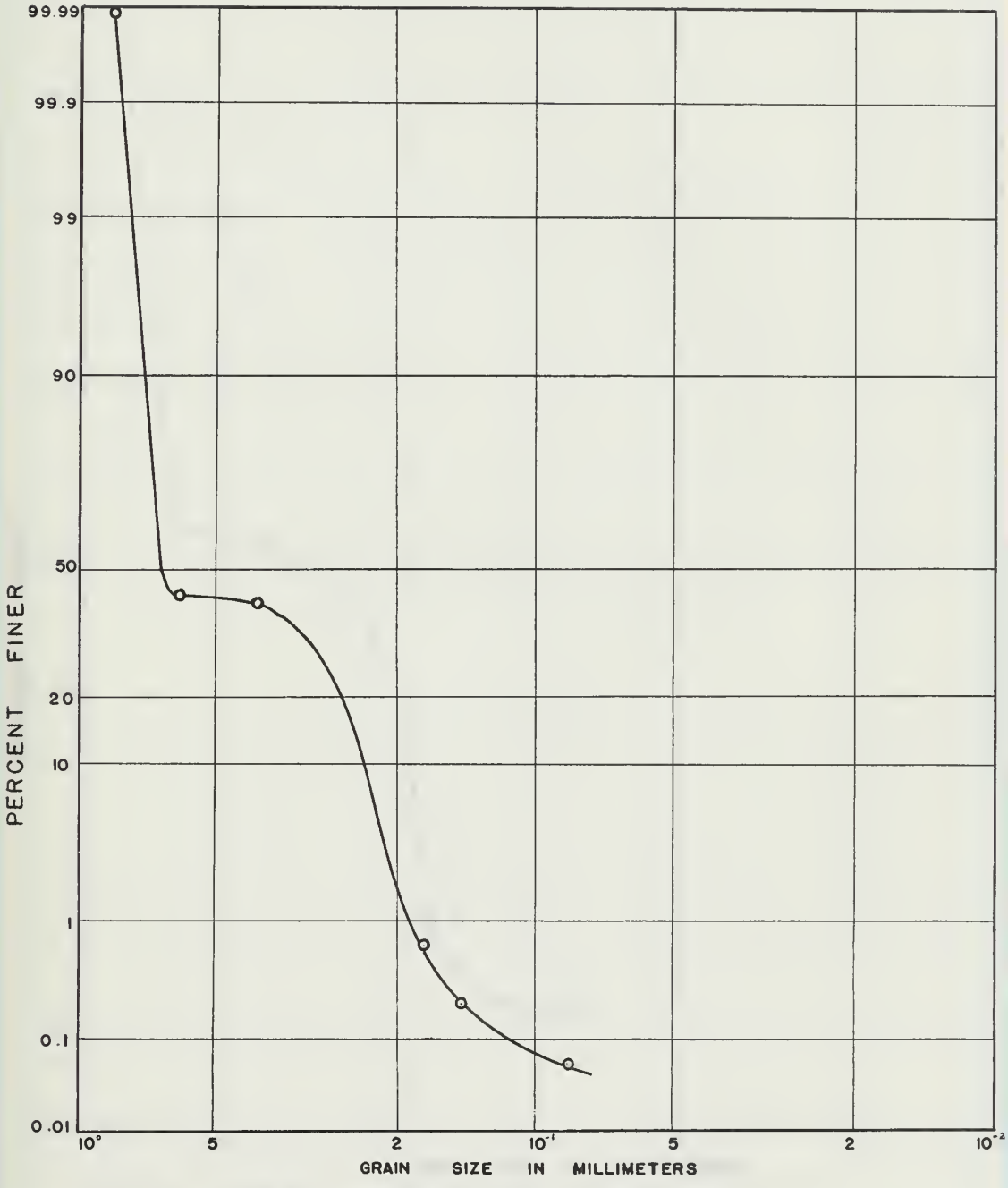

FIG. 12. SIEVE ANALYSIS OF SAND NO. 1

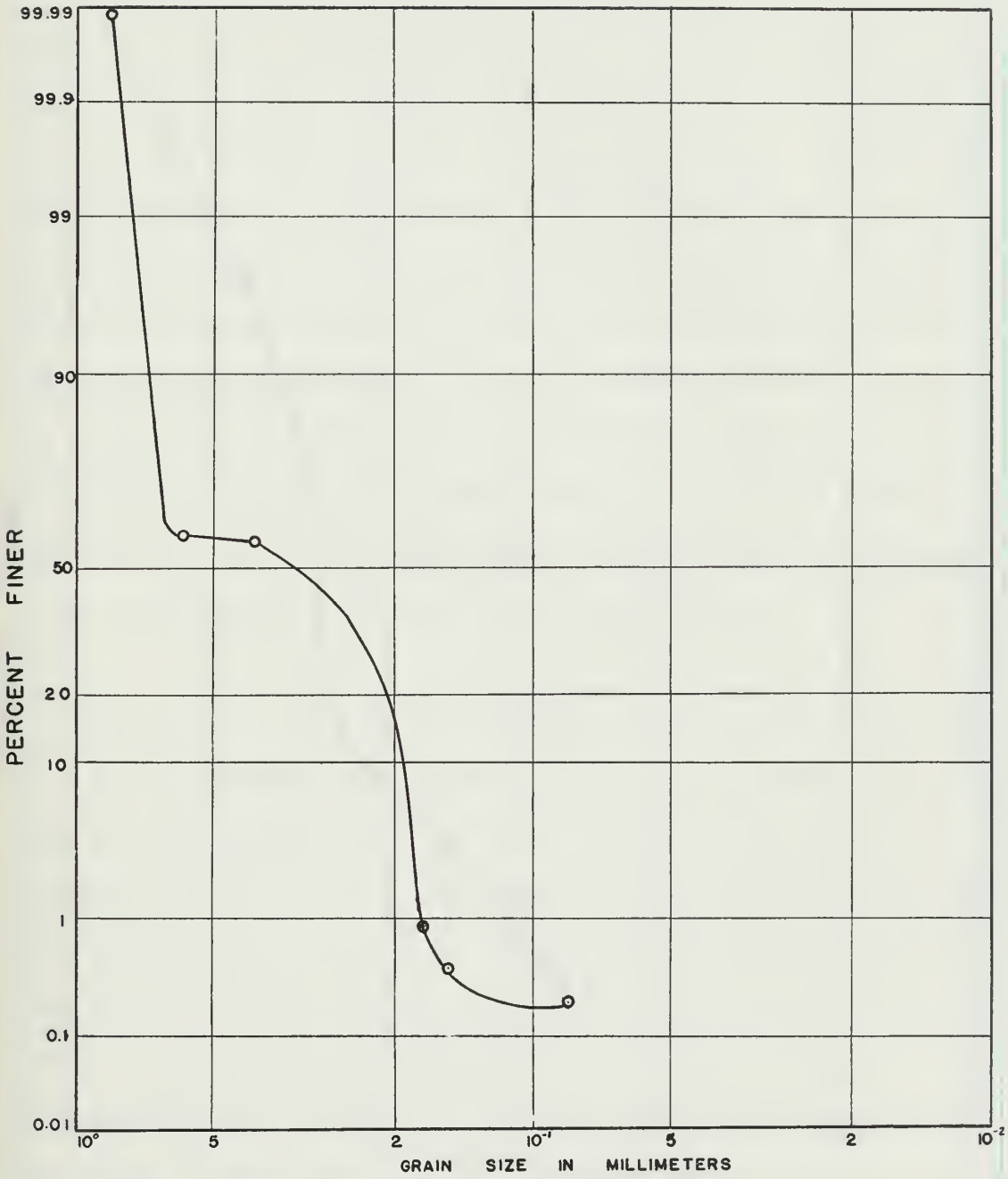

FIG. 13 SIEVE ANALYSIS OF SAND NO. 2

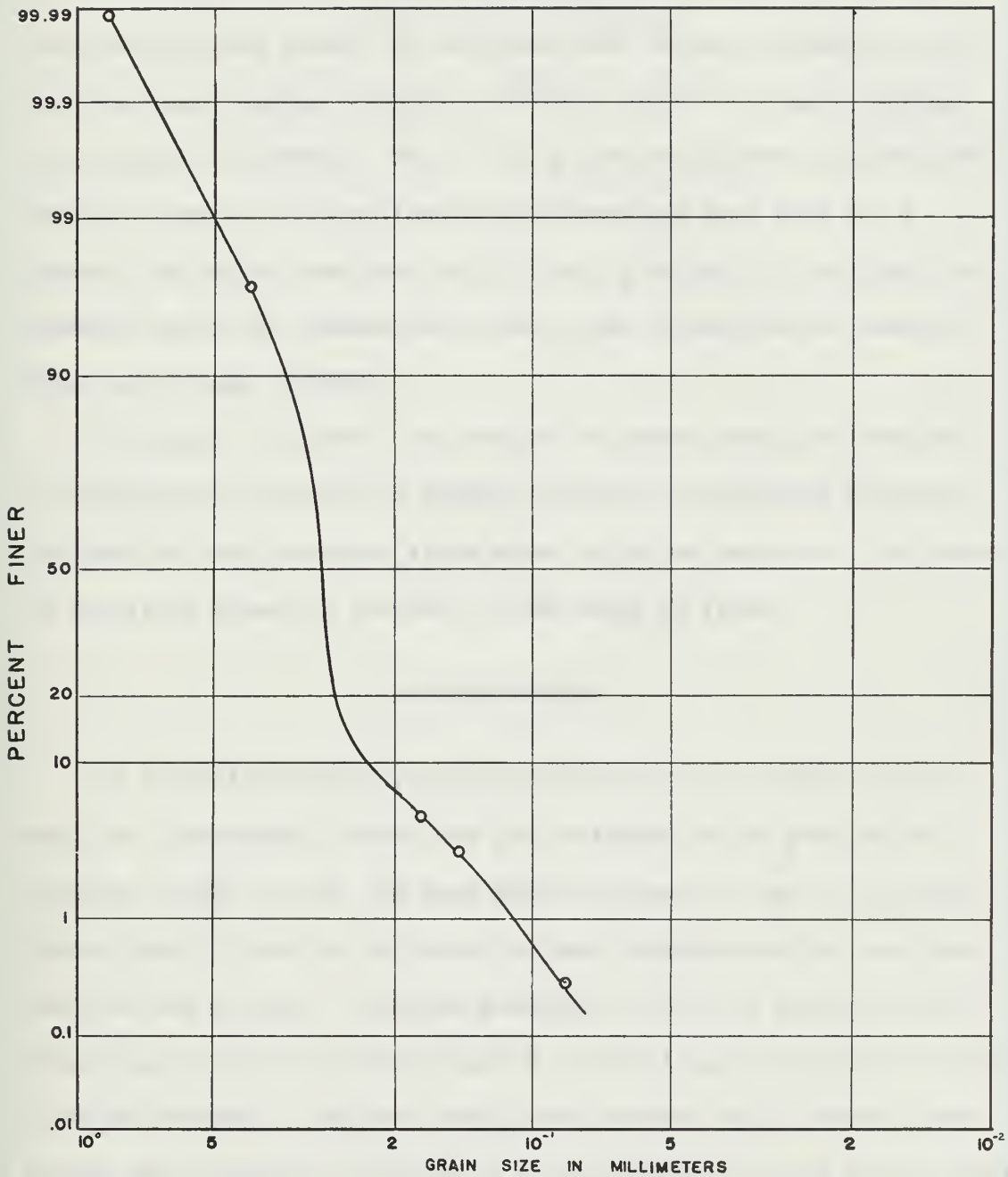

FIG. 14 SIEVE ANALYSIS OF SAND NO. 3

of 2 foot, 4 foot, and 6 foot and the time of fall was measured using a mechanical clock. The terminal velocity for each fall was calculated and all the values for each sand were averaged together to obtain the mean terminal velocity. Table 2 shows the mean C_D values and terminal velocities. Fig. 15 is a plot of all the runs for each sand as compared with the theoretical curve for free fall for a sphere. As can be seen from Fig. 15 the C_D values for each sand lie somewhat above the theoretical curve as can be expected as based on Alger and Simons (2) work.

The angle of repose ϕ for each of the three sands was measured by pouring each sand into a square container of water and allowing the sand to reach a stable slope whose angle was measured. The angle of the slope formed by the sand is the angle of repose.

INCIPIENT MOTION

As defined previously, incipient motion is that point in time when the hydrodynamic forces are just balanced by the gravity and friction forces so that the sand grain can just tip out of its position of rest. Prior to the start of each incipient motion run, the sand bed was leveled. The wave generator, set for a particular wave height and period, was started and the sand along the boundary of the pile was observed. The wave period was adjusted until several sand grains were observed to tip out of their position of rest and the wave characteristics were then recorded for that run. The wave period was then further adjusted to attempt to observe incipient motion on the

TABLE 2.— DRAG COEFFICIENT FOR EXPERIMENTAL SANDS FROM FALL VELOCITY EXPERIMENTS

Test sand	Mean particle diameter, d in millimeters	Mean fall velocity in feet per second	Mean drag coefficient C_D
(1)	(2)	(3)	(4)
1	0.62	0.2418	2.704
2	0.325	0.2096	2.738
3	0.30	0.1752	2.743

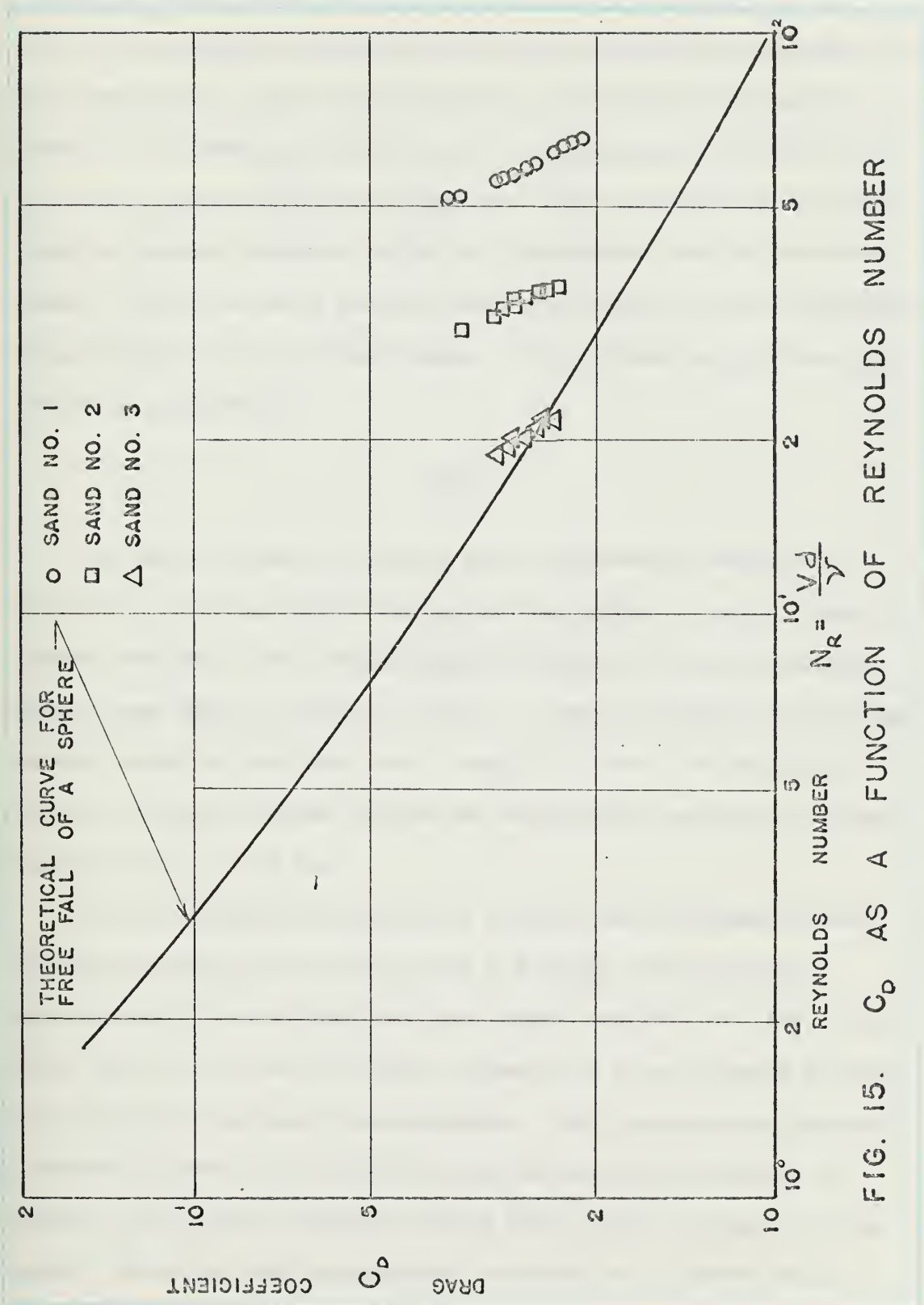

FIG. 15. C_D AS A FUNCTION OF REYNOLDS NUMBER

bed far enough away from the pile so that the pile had no influence on the sand grains. These experiments were run for all three sands at depths of 15 inches and 8 inches and for approximately fifteen runs per sand. Several paddle positions were used in making the runs in order to observe incipient motion for intermediate and shallow water waves. The bottom water particle velocity for each run was calculated using Stokes third order wave theory. The incipient motion data are tabulated in Appendix I.

SCOUR

For the experiments on scour, three experimental waves were selected of varying characteristics and two depths of water, 8 and 15 inches were used. The average characteristics for each experimental wave at each depth are shown in Table 3. Runs were made for each sand at each depth for each wave for a total of 18 runs. At the start of each run the sand bed was leveled and measurements were made to ascertain the level of the bed.

The wave generator adjusted for a particular experimental wave was then started and the wave period and height were recorded. Measurements of scour depth were made after each 200, 400, 800, 1200, 2000, 3000, etc. waves until there appeared to be no increase in scour depth after two successive measurements. This procedure was adjusted occasionally when it was felt that the run should be continued to observe scour pattern changes although there was no increase in scour depth. The scour depth measurements were made on a random basis,

TABLE 3.— EXPERIMENTAL WAVE CHARACTERISTICS

Test wave	Depth, h in feet	Average wave height, H, in feet	Average wave period, T, in seconds	Average wave length, L, in feet	Relative depth $\frac{h}{L}$	Wave steepness $\frac{H}{L}$
(1)	(2)	(3)	(4)	(5)	(6)	(7)
1	1.25	0.16	3.8	24.74	0.0506	.00647
	0.666	0.19	3.8	20.01	0.0333	.00950
2	1.25	.187	3.08	19.42	0.0644	.00963
	0.666	.13	3.08	15.14	0.0440	.00858
3	1.25	.275	1.875	10.85	0.1152	.02530
	0.666	.22	1.875	9.23	0.0721	.02380

measuring the deepest scour holes and trying to use the same holes for each measurement as a control basis. This could not always be done because when ripples formed on the bed a scour hole would occasionally be filled in. The relative significant scour depth and the relative ultimate significant scour depth were calculated by averaging the scour depths for the deepest one-third scour measurements and the latter being divided by the wave height. For each sequence point in a particular run, a collection of at least six data points was attempted but occasionally this could not be done due to the lack of scour holes. For each data point, the angle, distance from the pile and scour depth were recorded. At the completion of each run a number of data points were taken so as to be able to construct a contour map of the scour pattern. The data for the scour runs are tabulated in Appendix I.

CHAPTER VII

PRESENTATION AND DISCUSSION OF RESULTS

INCIPIENT MOTION

The occurrence of incipient motion was observed at the pile and on the bed so that an attempt of calculating the differences in the velocities between the two runs could be made and compared with the theoretical potential flow difference of two. Table 4 shows a comparison of the velocities and shows a mean velocity ratio of 1.691. The surface of the pile might be considered to be hydraulically rough since the paint blistered after being exposed to the water environment for several days. It is felt that the velocity ratio would not be 2.0 in the case of non-ideal fluids and non-steady state conditions; however, it is surprising to find the ratio as low as was calculated. Further experimentation should be done for various pile sizes and various roughnesses before any conclusions can be made as to what the velocity ratio will be and how it is influenced by roughness and pile size.

From the dimensional analysis results in Chapter IV it was assumed that incipient motion was a function of the relative depth, the relative wave height and the dimensionless particle size. These parameters were plotted on a log-log plot and are shown in Fig. 16 for incipient motion occurring at the pile boundary and Fig. 17 for incipient motion occurring on the bed. Referring to Fig. 16 it can be

TABLE 4.— VELOCITY RATIOS AS COMPARED WITH POTENTIAL FLOW THEORY[a]

Run number (1)	Sand number (2)	Incipient motion occurring at pile velocity in feet per second (3)	Incipient motion occurring on bed velocity in feet per second (4)	Ratio of velocities (5)	Mean velocity ratio[b] (6)
3	1	0.262		1.71	
3A	1		0.449		
4	1	0.279		1.39	
4A	1		0.388		1.653
9	1	0.246		1.56	
9A	1		0.384		
10	1	0.255		1.945	
10A	1		0.4965		
3	2	0.24		1.49	
3A	2		0.357		
4	2	0.291		1.61	
4A	2		0.467		1.594
5	2	0.269		1.625	
5A	2		0.437		
8	2	0.269		1.47	
8A	2		0.396		
10	2	0.269		1.18	
10A	2		0.317		
8	3	0.207		2.03	
8A	3		0.421		1.827
9	3	0.269		1.625	
9A	3		0.438		

[a] The velocity ratio for potential flow theory is 2.0.

[b] The average of the mean velocities is 1.691.

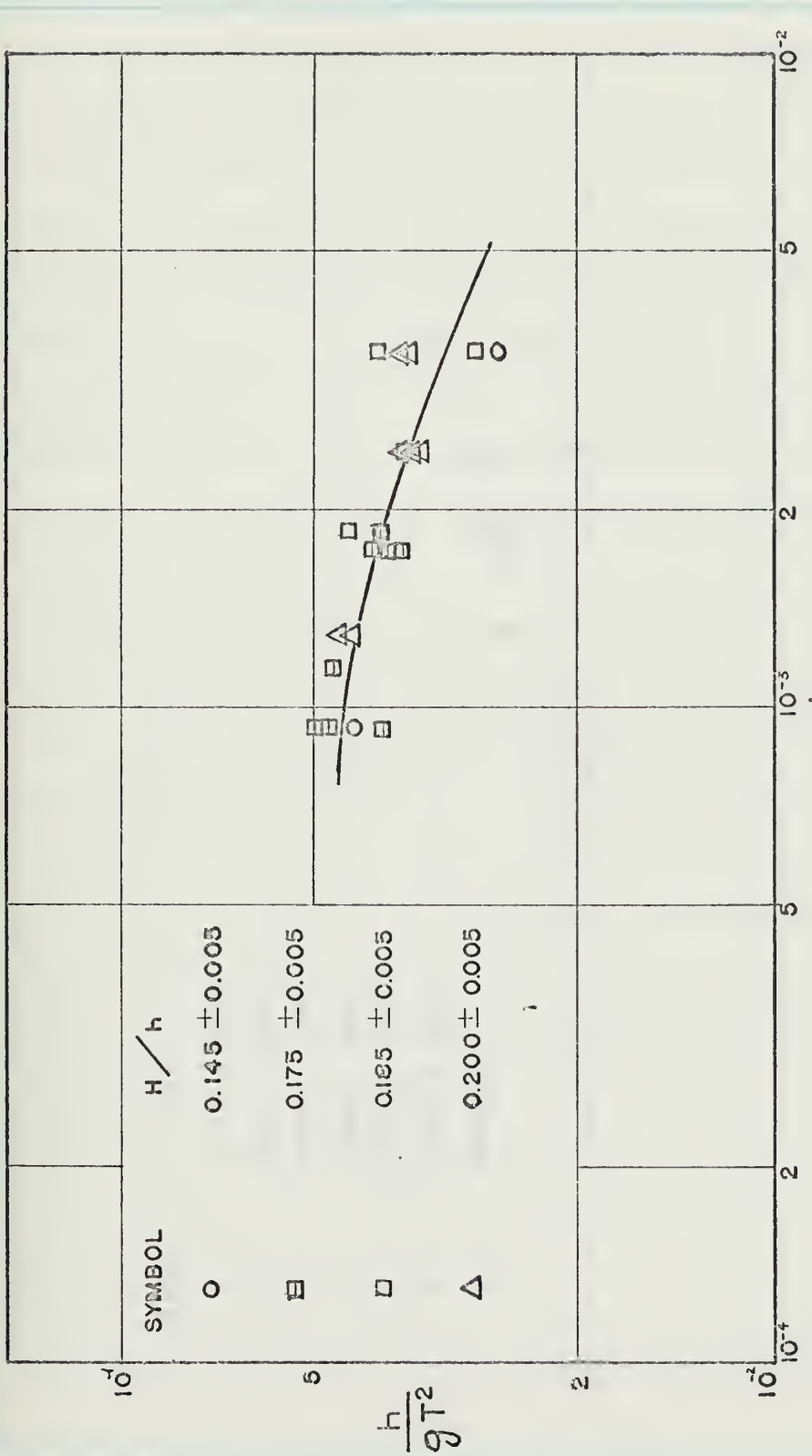

FIG. 16. INCIPIENT MOTION OCCURRING ON THE PILE BOUNDARY FOR VARIOUS VALUES OF RELATIVE WAVE HEIGHT

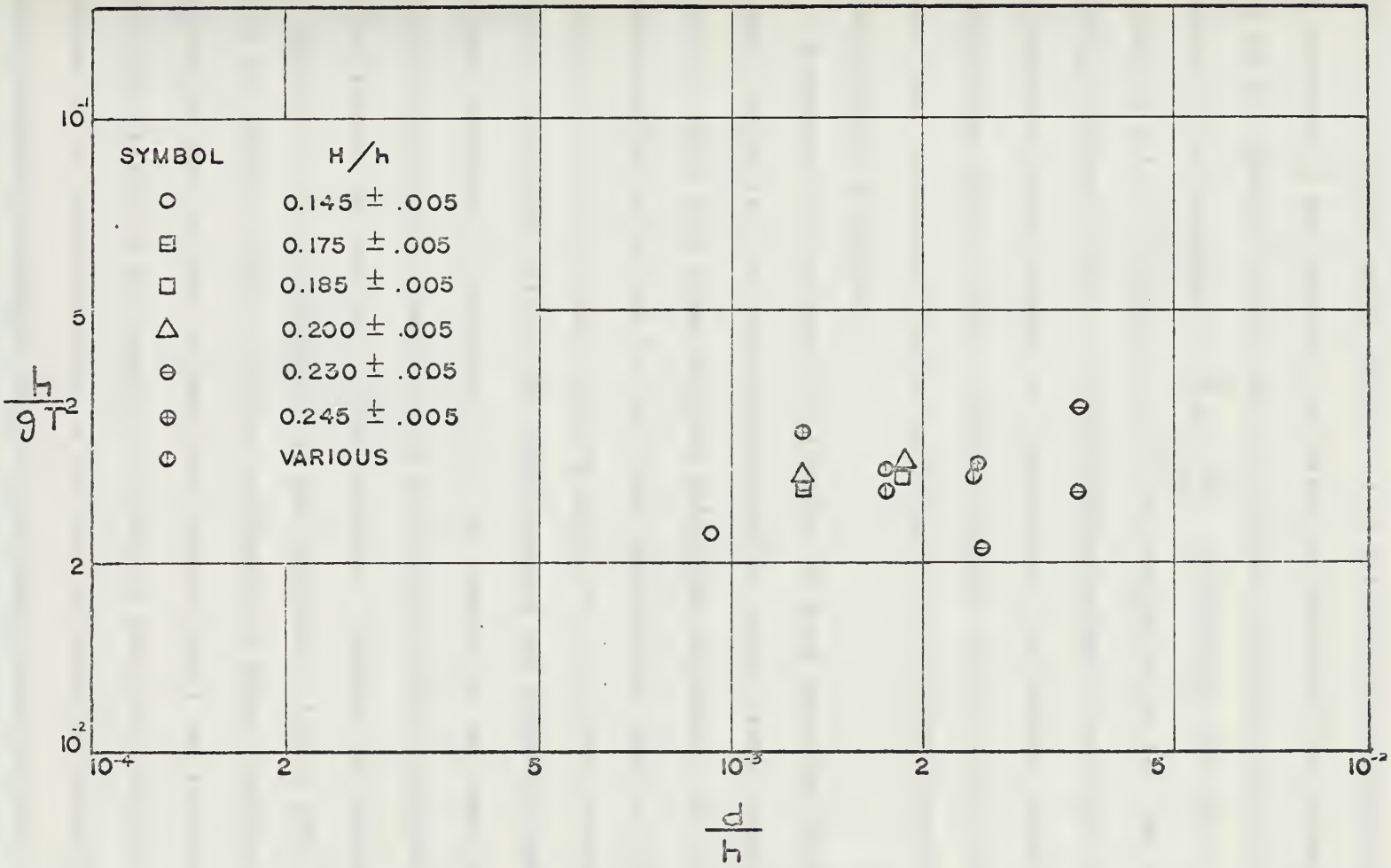

FIG. 17. INCIPIENT MOTION OCCURRING ON THE BED FOR VARIOUS VALUES OF RELATIVE WAVE HEIGHT

seen that incipient motion appears to be influenced only slightly by the parameter $\frac{H}{h}$ and appears to be directly related by the parameters $\frac{h}{gT^2}$ and $\frac{d}{h}$. However, in the case of incipient motion on the bed it appears to be independent of $\frac{H}{h}$ and $\frac{h}{gT^2}$. Considerably more data collection will be necessary before any conclusion can be drawn regarding incipient motion on a pile boundary except to say that the initiation of motion appears to a function of the relative depth and dimensionless particle size. This, of course, is only true for sands since these experiments did not investigate non-cohesive materials of other specific gravities.

Reference (22) presents a collection of data regarding the incipient velocities for various materials for steady state conditions. A plot of these data along with the velocities calculated for incipient motion on the bed for the three experimental sands is shown in Fig. 18. As can be seen from the graph, the incipient velocities for the three sands fall on the lower boundary and below the region of data presented by reference (22). The reason for the lower values is not known except to say that for oscillatory motion, incipient motion appears to occur at a lower velocity. However, as pointed out by Vanoni (22) in his discussion of the incipient velocity data, the curve for Shields (1936) data gave substantially higher incipient velocities than did that of Mavis and Laushey (1949) and the data of Hjulstrom (1935) did not compare to either of the other two curves. Because of the inconsistencies in the data for incipient velocities, Vanoni therefore recommends that critical shear stress be used as the

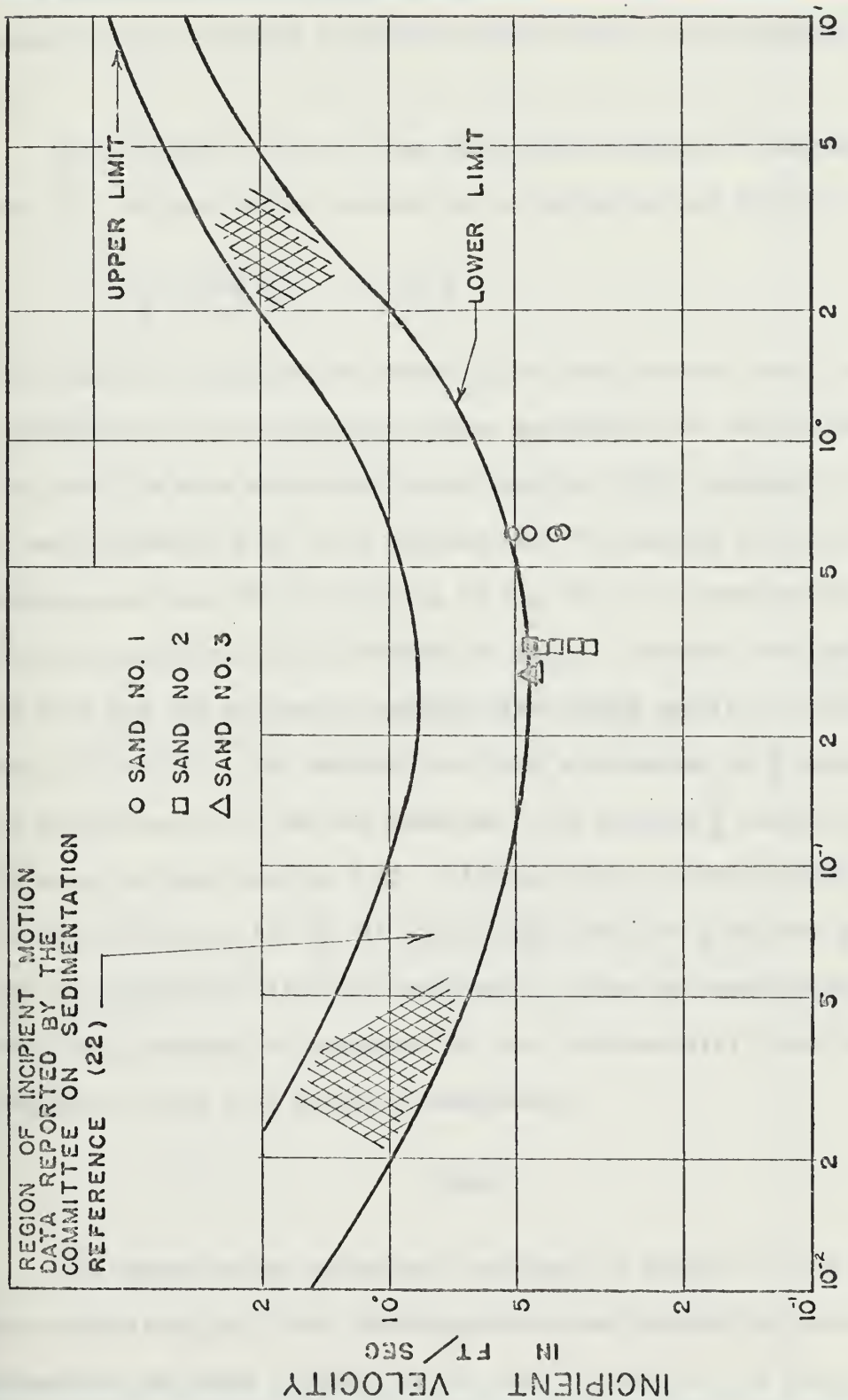

FIG. 18. INCIPIENT VELOCITY AS A FUNCTION OF GRAIN SIZE

parameter for comparing incipient motion rather than incipient velocity.

Using equation (4) for drag coefficient derived by Eagleson and Dean (8) and modified to account for a horizontal bed we have

$$C_D = \frac{4}{3} \frac{gd}{U^2} \left(\frac{S_s}{S} - 1\right) \tan \phi \qquad (30)$$

which has been verified experimentally in oscillatory flow. The drag coefficients for the incipient motion experiments on the bed away from the pile were calculated using equation (30), tabulated in Table 5, and plotted in Fig. 19 to compare with the results obtained by Eagleson and Dean (8). Referring to Fig. 19 it is apparent that very little correlation exists between the data. The data from Eagleson and Dean are for spheres of various size having specific gravities from 1.19 to 7.0. The authors also used a parameter of $\frac{d}{K}$ where K was the mean diameter of the bed material. The average $\frac{d}{K}$ value for the Eagleson and Dean data is 3.85. Although there is very little correlation of the data for C_D, it can be said that for a uniform graded sand in oscillatory flow the incipient C_D value is considerably less than that predicted by equation (30) and substantially less than that predicted by the fall velocity experiments.

SCOUR

The dimensionless parameters developed in Chapter IV for scour were calculated and their interdependency was studied by plotting the parameters as shown in Figs. 20, 21, 22, 23, and 24. In Fig. 20 the

TABLE 5.— DRAG COEFFICIENT RESULTS FROM INCIPIENT MOTION STUDIES

Run number	Sand number	Mean grain diameter, d, in feet	Incipient velocity in feet per second	Angle of repose, ϕ, in degrees	Reynolds number $R = \frac{Ud}{\nu}$	Drag coefficient C_D
(1)	(2)	(3)	(4)	(5)	(6)	(7)
3A	1	0.00235	0.449	30	105.4	.475
4A	1	0.00235	0.388	30	91.2	.638
9A	1	0.00235	0.384	30	90.3	.651
10A	1	0.00235	0.4965	30	116.8	.39
3A	2	0.00165	0.357	27	59.0	.468
4A	2	0.00165	0.467	27	77.0	.274
5A	2	0.00165	0.437	27	72.2	.312
8A	2	0.00165	0.396	27	65.4	.38
10A	2	0.00165	0.317	27	52.3	.593
8A	3	0.00117	0.421	26	49.3	.2285
9A	3	0.00117	0.438	26	51.3	.2105

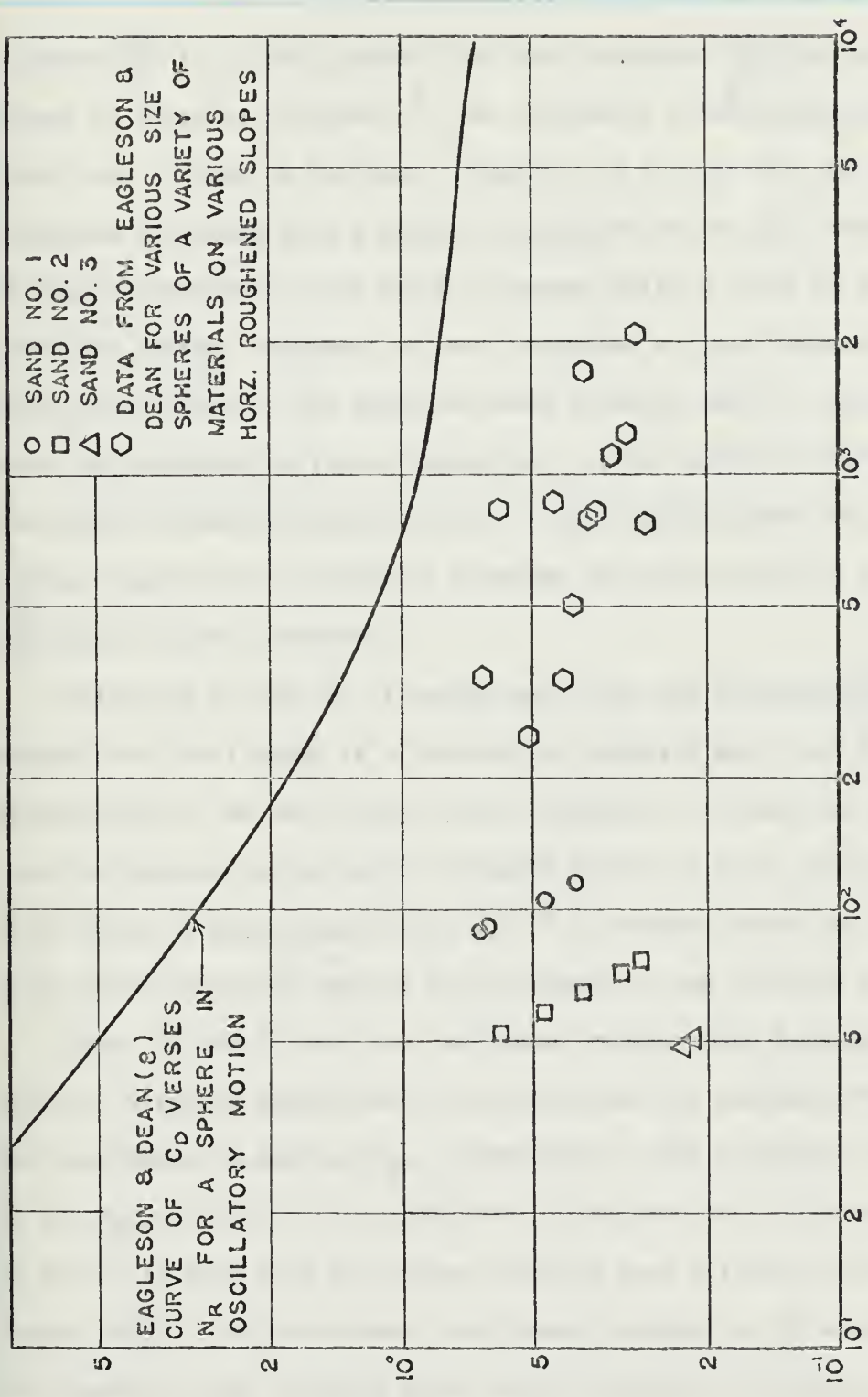

FIG. 19. DRAG COEFFICIENTS DEFINING INCIPIENT MOTION

parameter $\frac{\bar{S}u}{H}$ is plotted against the wave steepness $\frac{H}{gT^2}$ for various values of relative steepness $\frac{H}{h}$. No conclusive relationship can be drawn from a study of the plot. However, it is felt that as the wave steepness increases from a point of incipient motion the relative ultimate significant scour depth increases until a point is reached where for further increases in wave steepness a rapid decrease in scour depth occurs. The rapid decrease in scour depth is associated with the phenomena of ripple formation. It is conjectured that after the ripple formation becomes stable or well defined there will be no further significant increase or decrease in scour depth for further increases in wave steepness.

Referring to Fig. 21 it can be seen that the relative ultimate significant scour depth is a function of relative depth and bed particle size. As the relative depth decreases for each bed particle size the relative scour depth increases slowly at first until a relative depth of approximately 1.5×10^{-3} is reached where the relative scour depth increases rapidly for decreases in bed particle size.

Figs. 22 and 23 show the functional relationship between the relative ultimate significant scour depth and the sediment number, N_s, and pile Reynolds number, N_{RP}, respectively. The incipient values of N_s and N_{RP} for each of the sands were calculated and included on Figs. 22 and 23 to show that the curves actually have a rapid initial increase in $\frac{\bar{S}u}{H}$. The functional relationship appears to be similar in both cases in that relative scour depth increases very rapidly from the point where incipient motion occurs to a maximum relative scour depth.

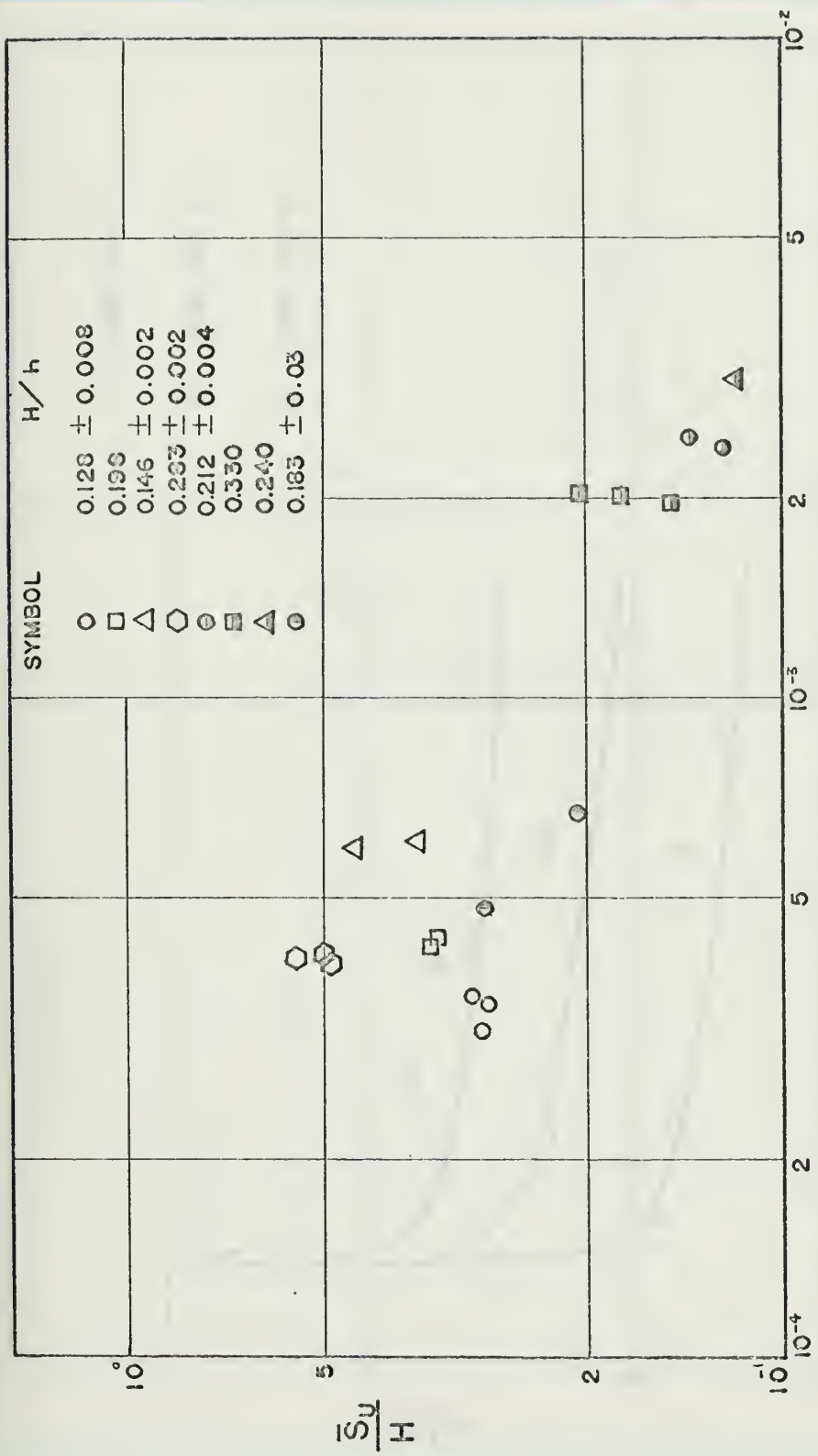

FIG. 20. RELATIVE ULTIMATE SIGNIFICANT SCOUR DEPTH AS A FUNCTION OF WAVE STEEPNESS FOR VARIOUS VALUES OF RELATIVE STEEPNESS

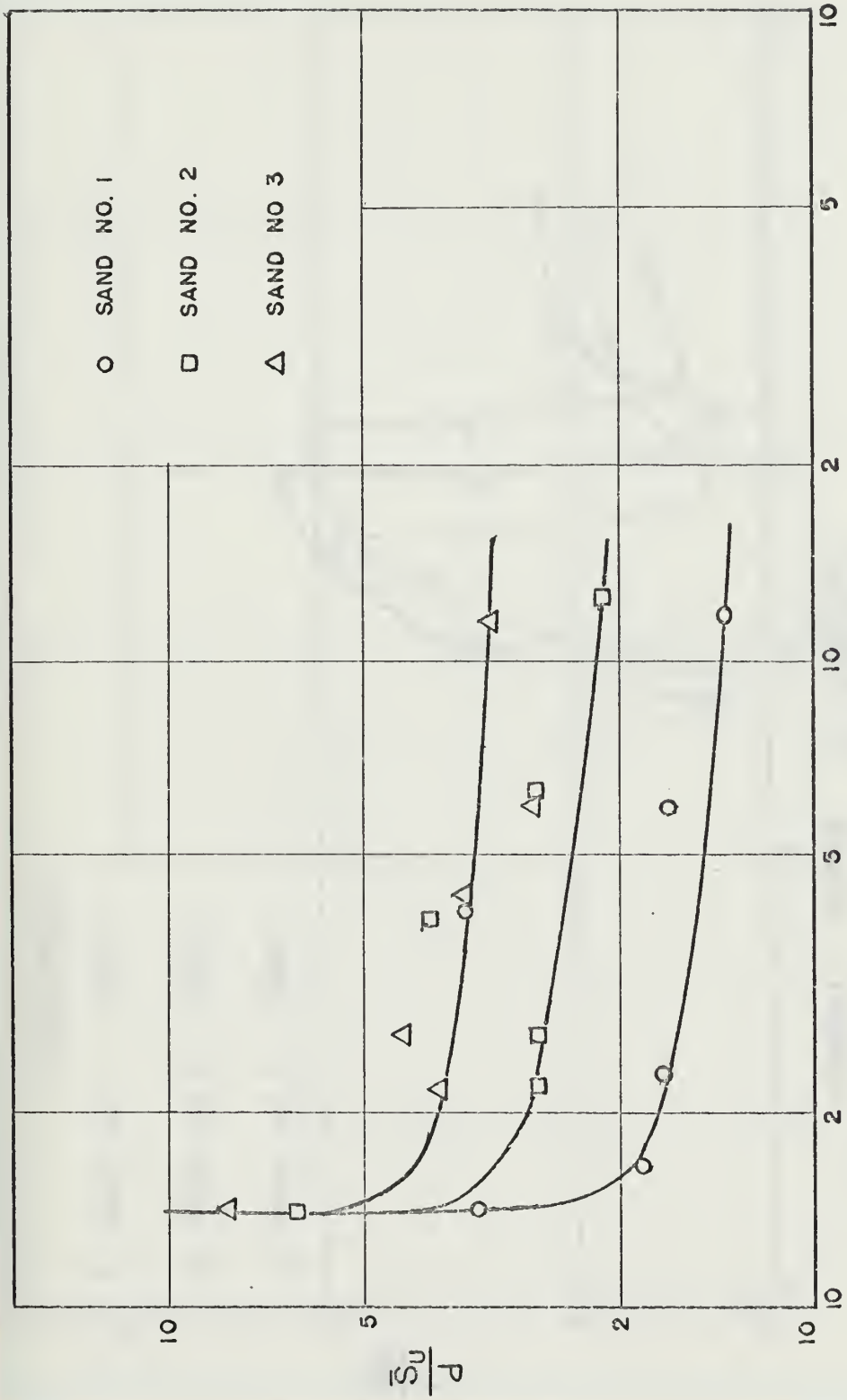

FIG. 21. RELATIVE ULTIMATE SIGNIFICANT SCOUR DEPTH AS A FUNCTION OF RELATIVE DEPTH

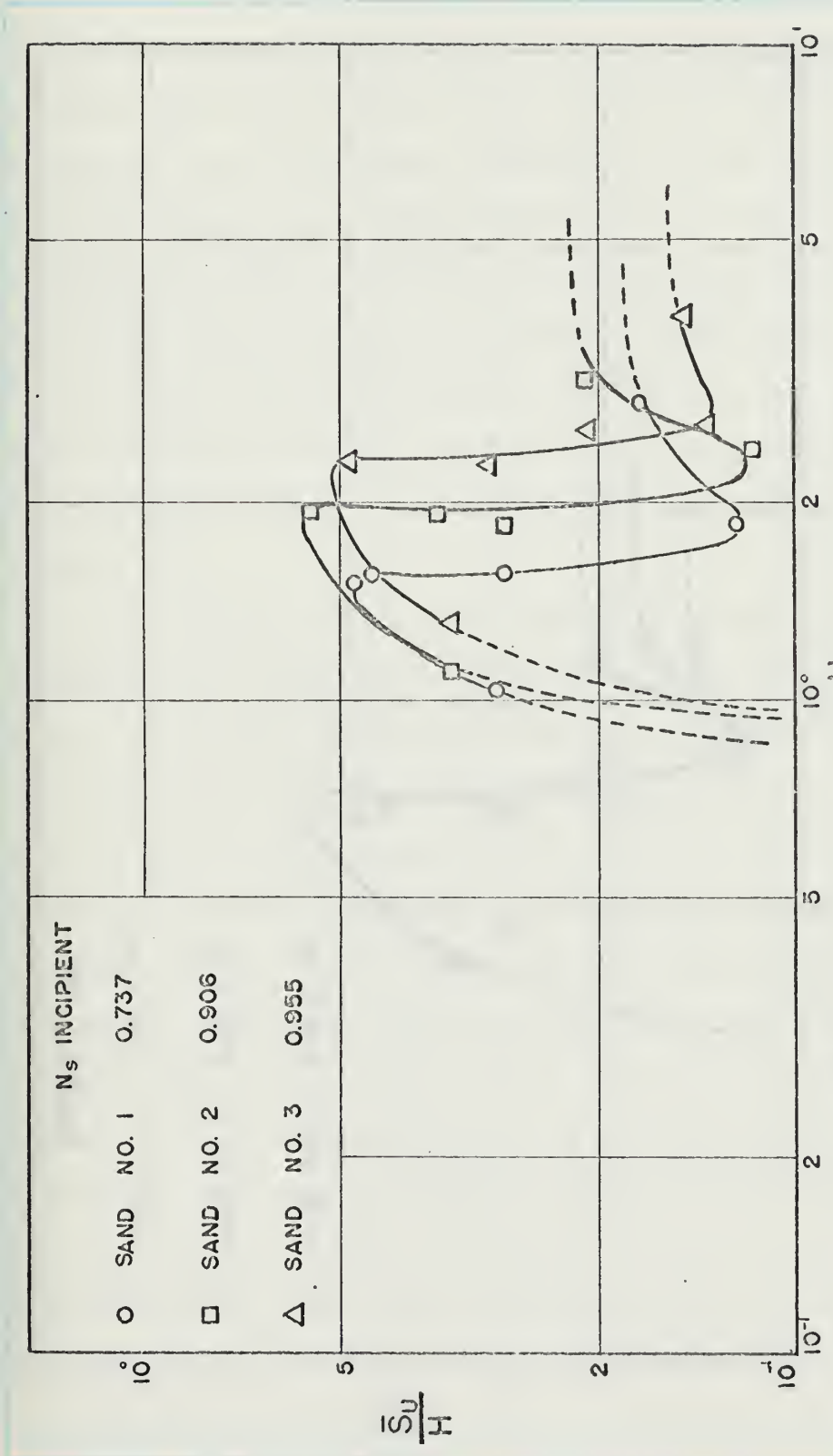

FIG. 22. RELATIVE ULTIMATE SIGNIFICANT SCOUR DEPTH AS A FUNCTION OF THE SEDIMENT NUMBER

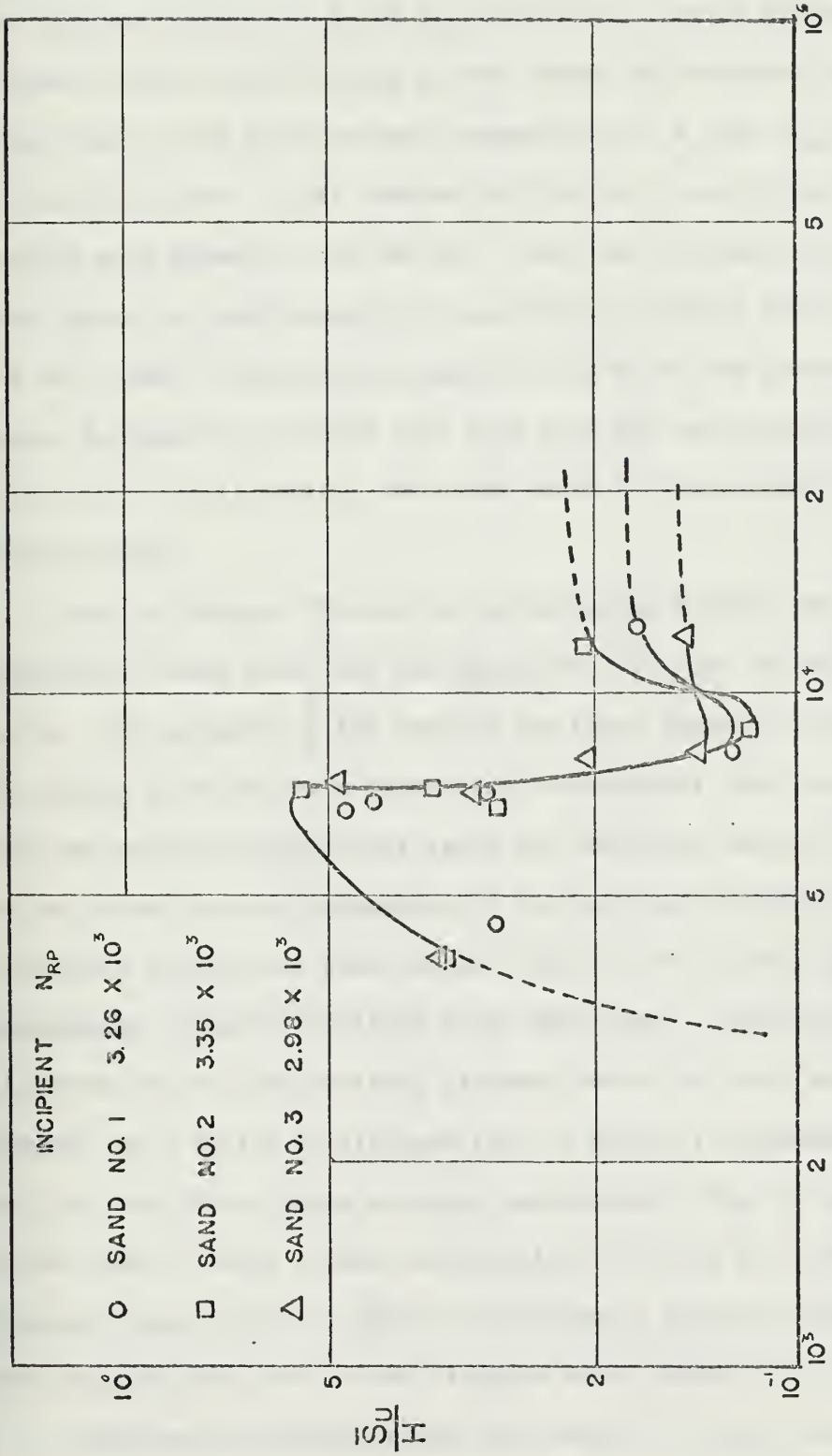

FIG. 23. RELATIVE ULTIMATE SIGNIFICANT SCOUR DEPTH AS A FUNCTION OF THE PILE REYNOLDS NUMBER

Any further increase in N_s or N_{RP} results in a rapid decrease in ultimate scour depth reaching a point where the relative ultimate significant scour depth becomes independent of N_s and N_{RP} but not of bed particle size. It is unknown why the No. 2 sand which has a smaller mean diameter than the No. 1 sand has the maximum ultimate scour depth and also levels off at a higher relative scour depth than the No. 1 sand. One possible answer could be as was pointed out by Roper, Schneider, and Shear (20) that when the bed particle size is less than 0.52 millimeter, the scour depth is independent of the bed particle size.

Figs. 24 through 29 show the relationship between the relative significant scour depth and the parameter t/T which is the number of waves. The parameter $\frac{\bar{S}}{H}$ for each of the three sands is plotted versus the number of waves for a particular experimental wave so as to compare the relative significant scour for the three sands. The majority of the curves have a characteristic initial rapid increase in the relatively significant scour depth. Most of the curves reach their apppoximate ultimate condition after 2000 waves. Also the majority of curves reach characteristic plateaus where the scour activity is dormant for a period of time and then it starts to increase again. For the runs where ripple activity was dominant (Fig. 26 and 29), the curves seem to reach a peak value rapidly followed by a decrease in relative scour depth for further increases in number of waves and then finally level off at the ultimate scour depth.

Intuitively one would think that Sand No. 1 would have the largest

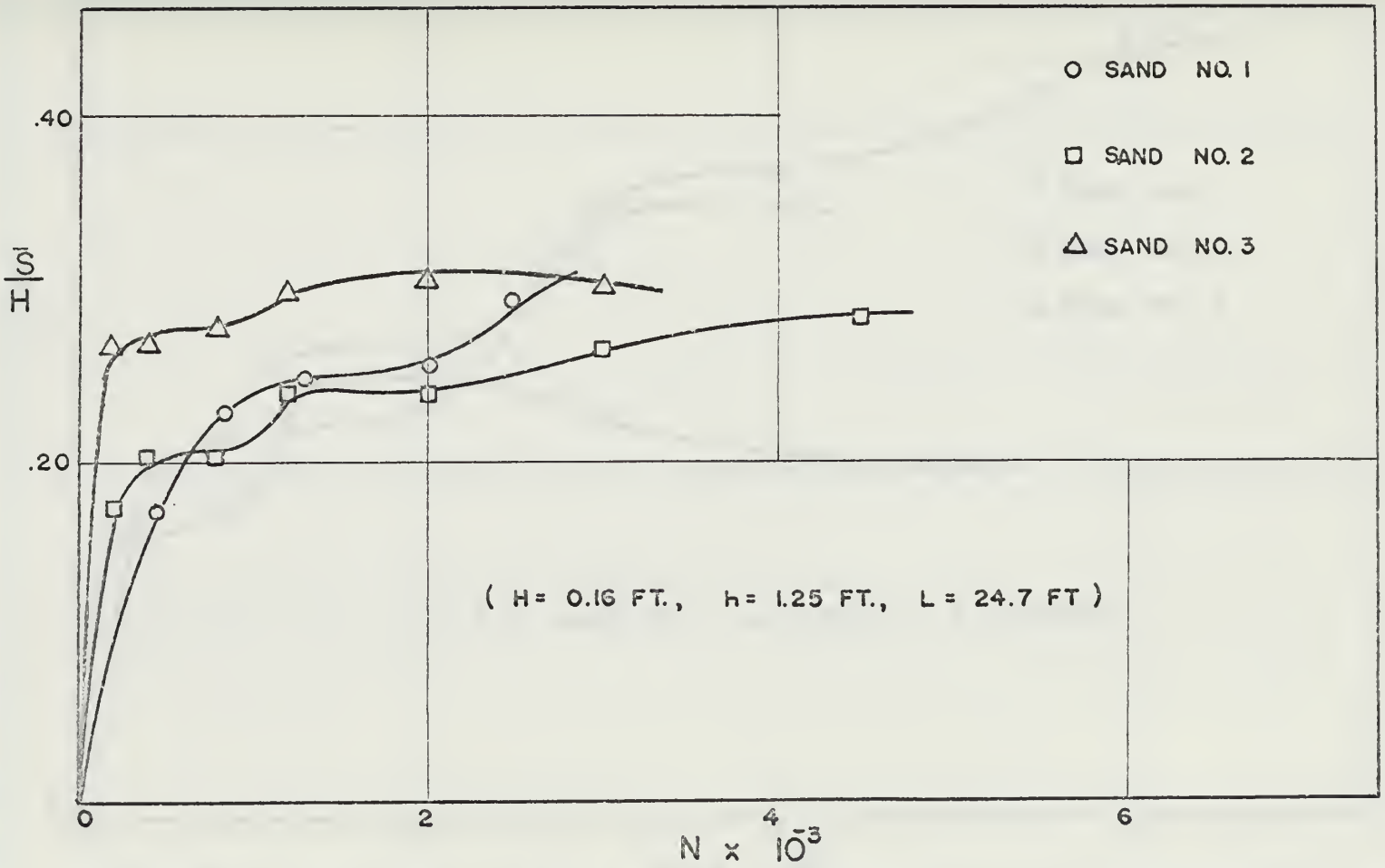

FIG. 24. RELATIVE DEPTH OF SCOUR AS A FUNCTION OF NUMBER OF WAVES

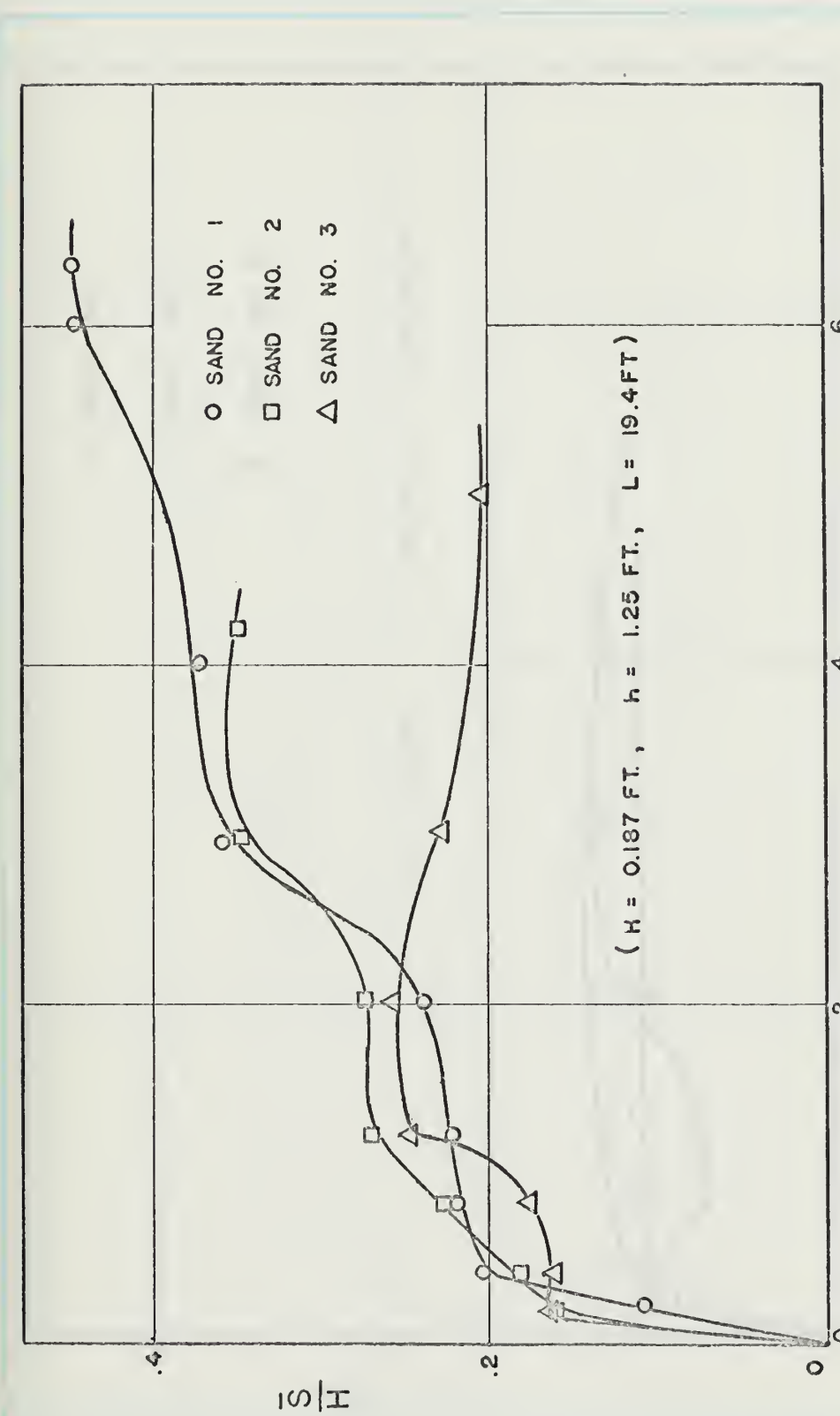

FIG. 25. RELATIVE DEPTH OF SCOUR AS A FUNCTION OF NUMBER OF WAVES

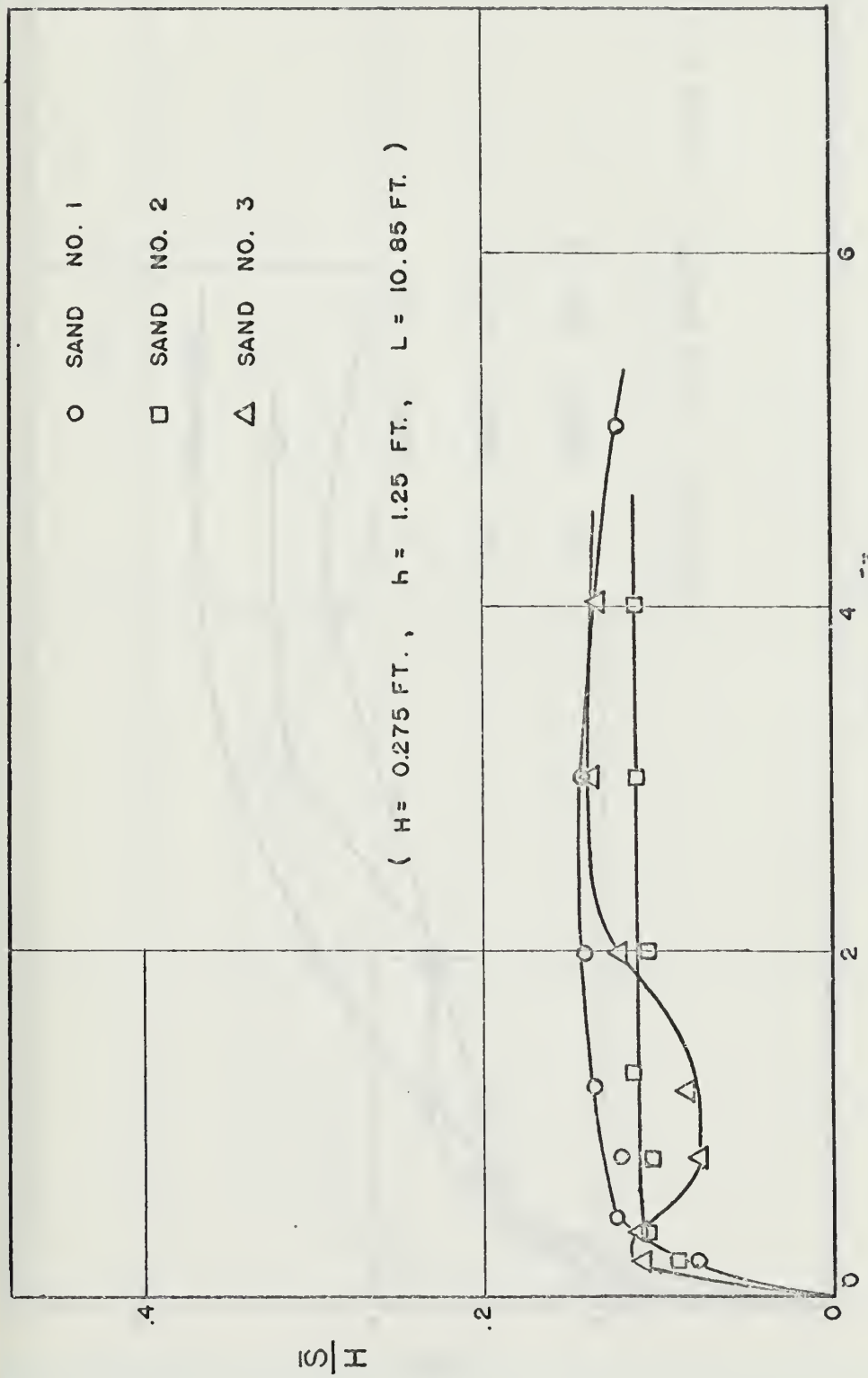

FIG. 26. RELATIVE DEPTH OF SCOUR AS A FUNCTION OF NUMBER OF WAVES

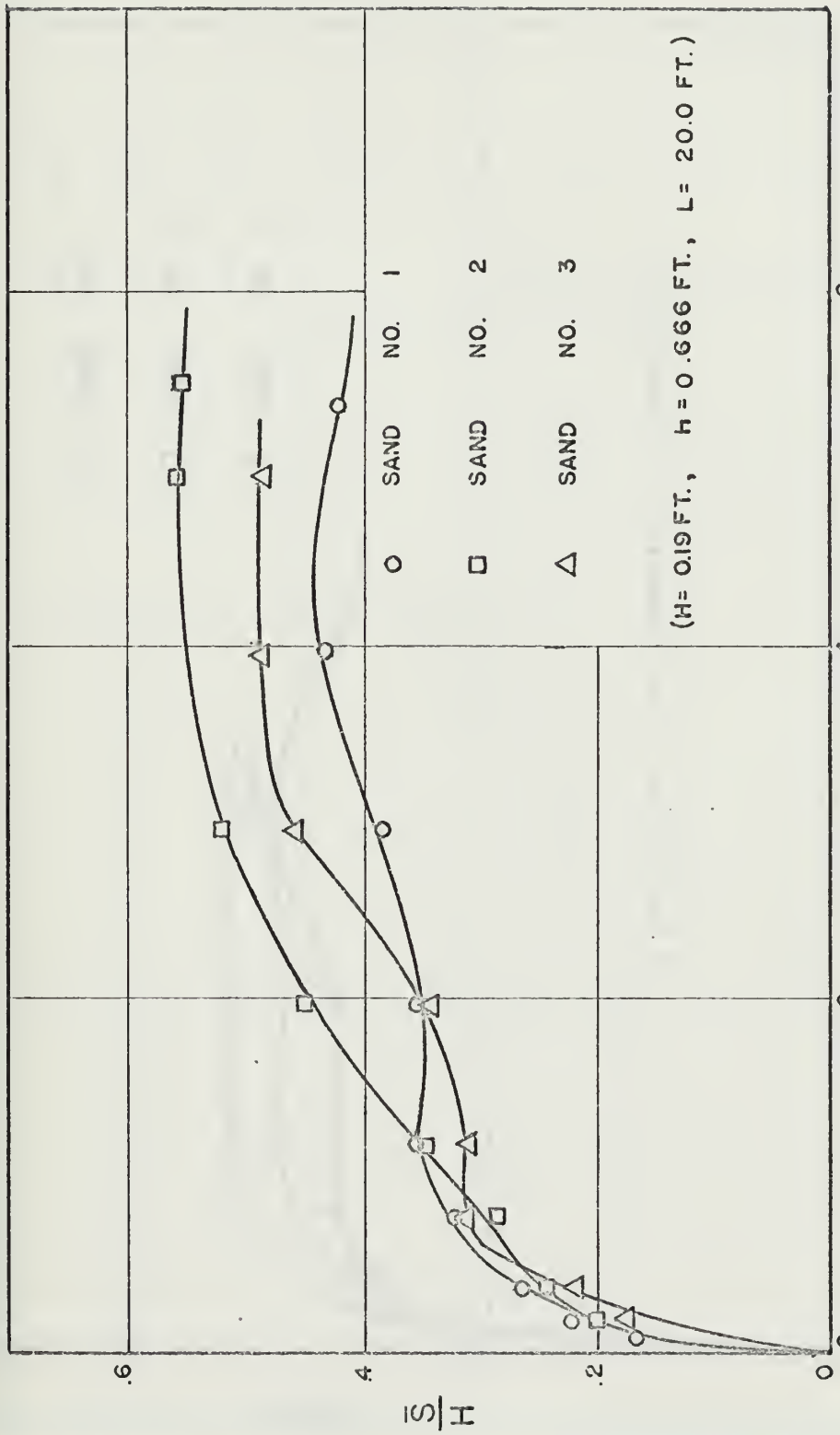

FIG. 27. RELATIVE DEPTH OF SCOUR AS A FUNCTION OF NUMBER OF WAVES

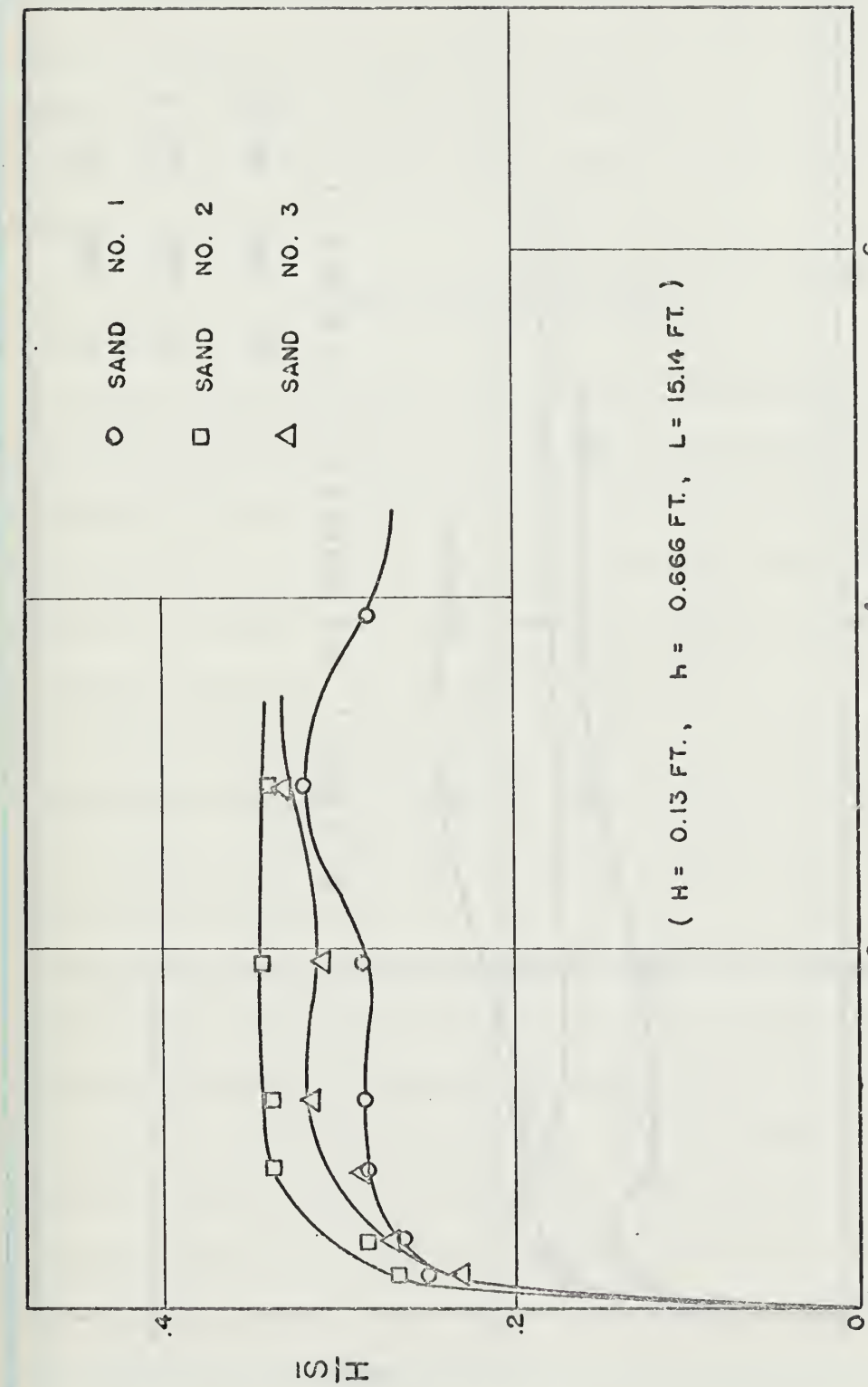

FIG. 28. RELATIVE DEPTH OF SCOUR AS A FUNCTION OF NUMBER OF WAVES

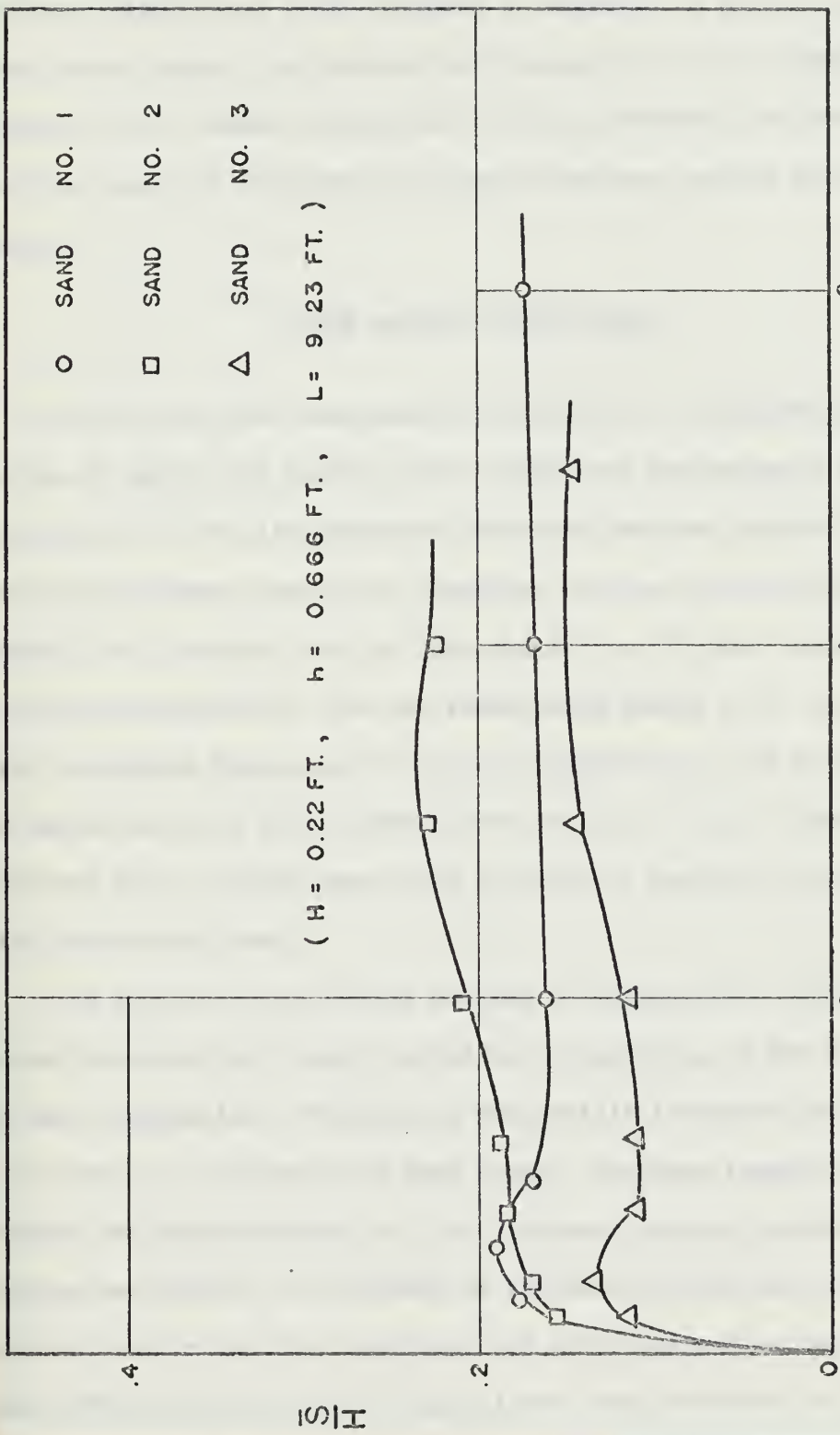

FIG. 29. RELATIVE DEPTH OF SCOUR AS A FUNCTION OF NUMBER OF WAVES

relative significant scour followed by Sands No. 2 and 3. However, this is not always the case and the reasons for it are unexplainable except for the reason pointed out by Roper, Schneider and Shen. For all the runs, the ultimate scour conditions are reached after 6000 waves.

SCOUR PATTERN OBSERVATIONS

For all the runs associated with wave No. 1 and especially those at the 8" depth, the initial scour action was concentrated around the front half of the pile periphery where the sand was scoured away and two relative deep scour holes formed at the rear of the pile approximately 1 to 2 inches from the pile and 30^{o} to 40^{o} from the normal to the wave direction. The two scour holes appear to be associated with the eddies being shed from the pile more so at the 8 inch depth. As the eddies were shed randomly from the pile slugs of sand could be observed being scoured away, more so with the smaller size sand than with the courser sand.

The general scour pattern was one of concentrated local scour around the pile with ripple formations progressing in the direction of wave propagation. The ripples were fairly irregular and in some cases were out of phase with each other. The wave length of the ripples was approximately 2-1/2 to 3 inches long and the shape of the ripples was similar to the shape of the wave in that the ripples had steep slopes on the down wave side and gentle slopes on the up wave side. The initial ripple in each of the scour patterns is formed by

the scour holes caused by the eddies. The eddy scour holes, after formation converge rapidly and form a front which starts the ripple activity. The rapidity of the formation of the ripples is dependent on the water depth, the wave characteristics and the sand size. The scour pattern was fairly symmetrical in all cases for wave No. 1.

The scour patterns resulting from wave No. 2 are fairly consistent in appearance in that the initial scour under the influence of eddy forces caused large elliptical holes to form on either side of the pile with some scouring around the periphery of the pile. As with wave No. 1, eddy scour holes are formed behind the pile at approximately 40^{o} from the normal to the wave propagation. Ripple activity starts relatively soon into the runs and due to the symmetry of the wave the ripples propagate in both directions away from the pile. The average wave length of the ripple patterns is 2 inches and the ripples are fairly parallel.

The scour patterns created by wave No. 3 are ones of total ripple formation having average ripple wave lengths of 2-3/4 inches at the 15 inch depth and 3-1/4 inch for the 8 inch depth. The initial scour is concentrated at the sides of the pile with the typical eddy scour holes forming as before, however, because of the steepness of wave No. 3 eddies do not seem to be of as much influence as with the previous experimental waves. Very little eddy shedding was observed. The ripple patterns form very rapidly consisting of a narrow band of ripples behind the pile and extending to the lower boundary of the sand after the 400th wave. Continued wave motion causes the ripple

pattern to expand outwards to cover the whole bed but little change in ultimate scour depth occurs. The pattern is fairly symmetrical in all cases with the ripples being parallel to each other.

Generally it can be said that the scour resulting is strongly influenced by the pile and the wave characteristics. In most of the runs very little to no bed movement could be observed away from the pile. The pile served as a catalyst to start the scour activity and once started around the pile it spread over a large area and extended in some cases great distances from the pile.

FIG. 30. SCOUR PATTERN WAVE NO. 1, 8 INCH DEPTH, SAND NO. 3

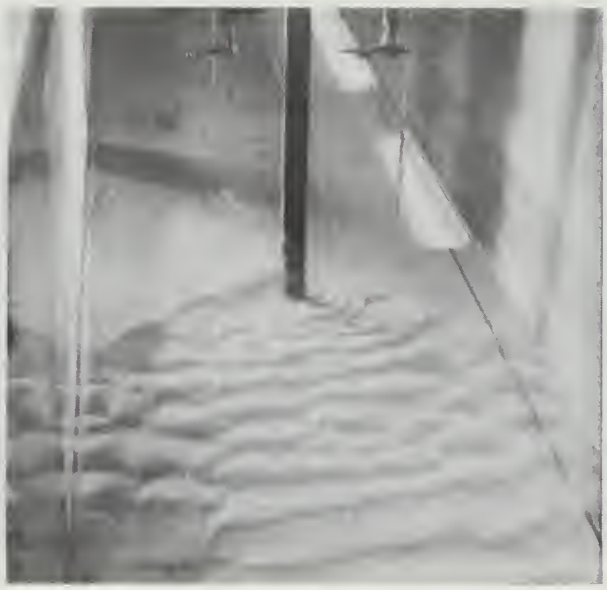

FIG. 31. SCOUR PATTERN WAVE NO. 1, 8 INCH DEPTH, SAND NO. 3

FIG. 32. SCOUR PATTERN WAVE NO. 1, 8 INCH DEPTH, SAND NO. 2

FIG. 33. SCOUR PATTERN WAVE NO. 2, 8 INCH DEPTH, SAND NO. 2

FIG. 34. SCOUR PATTERN WAVE NO. 2, 15 INCH DEPTH, SAND NO. 2

FIG. 35. SCOUR PATTERN WAVE NO. 3, 8 INCH DEPTH, SAND NO. 2

CHAPTER VIII

CONCLUSIONS AND REMARKS

1. The critical velocity necessary to cause incipient motion in oscillatory flow appears to be lower than that for steady state flow.

2. The ratio of the maximum velocity on the pile boundary and the initial free stream velocity is much less than the value of 2.0 for potential flow theory.

3. Incipient motion on the pile boundary appears to be independent of $\frac{H}{h}$ and directly dependent on the parameters $\frac{h}{gT^2}$ and $\frac{d}{h}$.

4. The drag coefficient for incipient motion of uniformly graded sands is much less than that predicted by Eagleson and Dean curve (Fig. 19).

5. $\frac{\bar{S}u}{H}$ appears to be directly related to the sediment number N_s and the pile Reynolds Number N_{RP}.

6. A maximum of only 6000 waves are required to reach an ultimate scour depth and in most cases 3000 waves are sufficient.

7. The relative ultimate significant scour depth increases very rapidly at first reaching three-fourths of its ultimate depth in the first 1000 waves and increases more slowly after that until it reaches its ultimate depth.

8. Eddy forces although initially influencing the scour patterns do not appear to be of significance in the final scour pattern.

9. The scour pattern resulting is primarily influenced by the pile and the wave characteristics.

10. In all the scour experiments the pile acted as a catalyst causing scour of the bed particles to be initiated whereas if the pile was not present little to no scour would have resulted.

To try and predict scour depths for a prototype case or relate these unconclusive results to a prototype would be presumptuous. To predict happenings or occurrences of a phenomenon in a prototype requires that there be similitude, both geometric and dynamic, between the model and prototype. This requires that similitude exists between the orbital velocities and orbital lengths (i.e. wave characteristics are similar), grain size and grain size distribution in the bed, roughness of the beds, and translation of the orbit due to drift. Without these similitudes, erroneous conclusions could be reached in attempting to predict prototype conditions. The difficulties in acquiring similitude between prototype and model were pointed out by Posey and Sybert (18) in their studies of scour around piles on offshore platforms. It required several years of study and experimentation before actual prototype conditions were duplicated in the model.

However, from the experiments conducted on scour it is felt that certain conjectures on prototype conditions can be made. The maximum scour measured in the experiments was approximately one pile diameter. It therefore is conjectured that the maximum scour observable in a prototype would be approximately equal to one pile diameter, which for a typical offshore pile of 4 to 6 ft would be approximately 5 ft. Kreig (13) has reported observed scour depths on offshore platforms in the Gulf of Mexico of 8 to 10 ft and Posey and Sybert (18) measured

maximum scour depths of 13 ft with average scour depths of 8 to 10 ft for offshore platforms in fine sands off Padre Island, Texas. The average pile diameter associated with the scour measurements made by Posey and Sybert (18) was approximately 3 ft and there was a fairly significant littoral current present. It is important to note from the above discussion that exact similitude is very important. Without every condition duplicated between model and prototype (i.e. the littoral current) erroneous results will be had. The scour patterns for the Padre Island platforms had a dish or saucer appearance, that was much larger in shape than the platform. Scour patterns such as these would not normally be expected.

The conclusion that the scour is very rapid at first and decreases thereafter has been verified by Posey and Sybert (18) who observed that the scour rate is high during the first year or two, and decreases thereafter.

The scour patterns observed in the experiments will be of little use for normal prototype conditions. However they might give some insight into prototype patterns caused by storms where the wave direction is unidirectional.

RECOMMENDATIONS FOR FURTHER RESEARCH

1. Further experimentation on ultimate scour depth should be conducted using different size sands and other non-cohesive materials. The experiments should include data in the area near the incipient motion point and in the area toward the breaking limit to better

define those parts of the ultimate scour curve.

2. Experimentation on scour should also be conducted using cohesive materials as the bed particles.

3. The pile diameter should be varied to ascertain its effect on the ultimate scour.

4. Continued studies on incipient motion associated with a circular pile would be worthwhile especially in determining the influence on the velocity ratio and ascertain the actual value.

5. Scour studies associated with circular pile should be conducted with currents against and with the wave direction.

BIBLIOGRAPHY

1. Abou-Seida, M., "Sediment Transport by Waves and Current," Hydraulic Engineering Laboratory, Wave Research Projects, Technical Report No. HEL2-7, Univ. of California, Berkeley, May, 1964.

2. Alger, G. R., Simons, D. B., "Fall Velocity of Irregular Shaped Particles," Journal of Hydraulics Division, ASCE, Vol 94, No. HY3, Proc. Paper 5949, May 1968.

3. Bagnold, R. A., "Sand Movement by Waves: Some Small-Scale Experiments with Sand of Very Low Density," Journal of the Institution of Civil Engineers, Vol 27-28 (1946-47), pp. 447.

4. Carstens, M. R., "Similarity Laws for Localized Scour," Journal of the Hydraulics Division, ASCE, Vol 92, No. HY3, Proc. Paper 4818, May 1966.

5. Chepil, W. S., "Equilibrium of Soil Grains at the Threshold of Movement by Wind," Proceedings of Soil Science, Society of America, Vol 23, pp. 422-428.

6. Coleman, N. L., "A Theoretical and Experimental Study of Drag and Lift Forces Acting on a Sphere Resting on a Hypothetical Stream Bed," Proceedings, Twelfth Congress, International Association for Hydraulic Research, Vol. 3, Section C18, 19, 1967.

7. Dean, R. G., "Relative Validities of Water Wave Theories," Proceedings, Conference on Civil Engineering in the Oceans, ASCE, 1967.

8. Eagleson, P. S., Dean, R. G., "Wave Inducted Motion of Bottom Sediment Particles," Transactions, ASCE, Vol. 126, 1961 Part 1, pp. 1162-1189.

9. Herbich, J. B., Murphy, H. D., Van Weele, B., "Scour of Flat Sand Beaches Due to Wave Action in Front of Sea Walls," Proceedings, Coastal Engineering Santa Barbara Specialty Conference, Chapter 28, Oct. 1965, pp. 703-726.

10. Huon Li, "Stability of Oscillatory Laminar Flow Along a Wall," Technical Memorandum No. 47, Beach Erosion Board, 1954.

11. Ippen, A. T., Estuary and Coastline Hydrodynamics, McGraw Hill Co., New York, 1966.

12. Ippen, A. T., Eagleson, P.S.," A Study of Sediment Sorting by Waves Shoaling on a Plane Beach," MIT Hydrodynamics Laboratory Report No. 18, 1955.

13. Kreig, J.L., "Criteria for Planning an Offshore Pipeline," Journal of the Pipeline Division, ASCE, Vol. 91, No. PL 1, July 1965, pp. 15-37.

14. Ko, S. C., "Scour of Flat Sand Beaches in Front of Seawalls," Fritz Engineering Laboratory Report No. 293.5, March, 1967.

15. Leliavsky, S., "An Introduction to Fluvial Hydraulics," Constable & Co., LTD, London, 1955, pp. 34-68.

16. Le Me'haute', B., Divoky, D., Lin, A., "Shallow Water Waves: A Comparison of Theories and Experiments," Proceedings, Eleventh Conference on Coastal Engineering, 1968.

17. Murphy, H. D., "Scour of Flat Sand Beaches Due to Wave Action," Fritz Engineering Laboratory Report No. 293.3, June, 1964.

18. Posey, C. J., Sybert, J. H., "Erosion Protection of Production Structures," Proceedings Ninth Congress, International Association for Hydraulic Research, 1961, pp. 1157-1162.

19. Raudkivi, A. J., Loose Boundary Hydraulics, Pergamon Press LTD, London, 1967.

20. Roper, A. T., Schneider, U. R., Shen, H. W., "Analytical Approach to Local Scour," Proceedings Twelfth Congress, International Association for Hydraulic Research, Vol. 3, Section C18, 19, 1967.

21. Skjelbreia, L., "Stokes Third Order Wave," Council on Wave Research, The Engineering Foundation of the California Research Corporation, June, 1958.

22. Vanoni, V. et al., "Sediment Transportation Mechanics: Initiation of Motion, Progress Report of the Task Committee on Preparation of Sedimentation Manual, Committee on Sedimentation," Journal of the Hydraulics Division, ASCE, Vol. 92, No. HY2, Proc. Paper 4738, March, 1966.

23. Van Weele, B., "Beach Scour Due to Wave Action on Seawalls," Fritz Engineering Laboratory Report No. 293.3, April, 1965.

24. Vincent, G. E., "Contribution to the Study of Sediment Transport on a Horizontal Bed Due to Wave Action," Proceedings, Sixth Conference on Coastal Engineering, ASCE, Dec. 1957, pp. 326-335.

25. Wiegel, R. L., Oceanographical Engineering, Prentice-Hall, Englewood Cliffs, N.J., 1964.

APPENDICES

APPENDIX I

INCIPIENT MOTION DATA

Sand No. 1

Run	h (ft)	T (sec)	H (ft)	L (ft)
1	1.25	1.155	.14	5.98
2	1.25	1.957	.185	11.79
3	1.25	.937	.23	4.40
3A	1.25	1.168	.255	6.18
4	1.25	1.0	.22	4.87
4A	1.25	1.2	.23	6.38
5	1.25	1.0	.19	4.84
6	.666	.8575	.12	3.31
7	.666	.889	.095	3.44
8	.666	.726	.12	2.57
9	.666	.75	.13	2.72
9A	.666	.9	.155	3.57
10	.666	.759	.13	2.77
10A	.666	.875	.155	3.43

Sand No. 2

Run	h (ft)	T (sec)	H (ft)	L (ft)
1	1.25	.91	.22	4.17
2	1.25	1.041	.155	5.12
3	1.25	.938	.205	4.38
3A	1.25	1.22	.215	6.51
4	1.25	.941	.25	4.45
4A	1.25	1.11	.305	5.79
5	1.25	.923	.24	4.28
5A	1.25	1.2	.25	6.40
6	.666	.75	.13	2.72
7A	.666	.857	.165	3.35
8	.666	.77	.13	2.83
8A	.666	1.0	.15	4.10
9	.666	.75	.125	2.71
10	.666	.762	.13	2.78
10A	.666	.875	.14	3.41

Sand No. 3

Run	h (ft)	T (sec)	H (ft)	L (ft)
1	1.25	1.06	.17	5.28
2	1.25	.947	.195	4.44
2A	1.25	1.333	.19	7.32
3	1.25	.889	.22	3.93
4	1.25	.889	.225	4.01
5	1.25	1.0	.22	4.87
6	1.25	0.9	.225	4.1
7	.666	.714	.115	2.50
8	.666	.733	.1125	2.61
8A	.666	.866	.18	3.42
9	.666	.769	.14	2.83
9A	.666	.909	.175	3.64
10	.666	.75	.115	2.70

SCOUR RUNS DATA

Run	Sand	Depth (ft)	Wave No.	H (ft)	T (sec)	L (ft)
1	1	1.25	1	.15	3.83	24.7
2	1	1.25	2	.18	3.05	19.37
3	1	1.25	3	.26	1.835	11.05
4	1	.666	1	.185	3.8	19.62
5	1	.666	2	.14	3.0	14.85
6	1	.666	3	.225	1.857	9.24
7	2	1.25	1	.16	3.8	24.58
8	2	1.25	2	.185	3.08	19.70
9	2	1.25	3	.30	1.75	10.56
10	2	.666	1	.19	3.83	20.30
11	2	.666	2	.13	3.08	15.14
12	2	.666	3	.22	1.835	9.07
13	3	1.25	1	.17	3.857	24.95
14	3	1.25	2	.195	3.0	19.19
15	3	1.25	3	.27	1.833	11.06
16	3	.666	1	.19	3.8	20.12
17	3	.666	2	.13	3.08	15.14
18	3	.666	3	.22	1.86	9.22

Run No. 1

Wave No. 1 Sand No. 1

No. of waves	Degree / Distance from pile	Depth of scour (ft)	$\bar{S}$ (ft)	$\frac{\bar{S}}{H}$
	30/0	.025		
	60/0	.025		
	90/0	.030		
450	0/1.0	.025	.027	.180
	120/1.0	.025		
	300/1.0	.030		
	345/1.0	.030		
	270/1.5	.030		
	0/0	.030		
	300/0	.025		
850	45/0.5	.040	.034	.226
	135/1.5	.045		
	270/1.5	.025		
	0/0	.033		
	300/0	.030		
1300	45/0.5	.040	.037	.246
	135/1.5	.045		
	270/1.5	.025		
	0/0	.030		
	300/0	.030		
2000	45/0.5	.040	.038	.253
	135/1.5	.055		
	300/1.75	.025		
	0/0	.030		
2450	300/1.5	.025	.043	.287
	135/1.5	.055		

Run No. 2

Wave No. 2 Sand No. 1

No. of waves	Degree / Distance from pile	Depth of scour (ft)	$\bar{S}$ (ft)	$\frac{\bar{S}}{H}$
200	225/0.75 270/0.5 90/1.25	.020 .015 .025	.020	.111
420	225/1.0 105/.75 60/1.0 195/2.5	.020 .040 .035 .020	.037	.205
800	105/0.5 30/1.0 210/3.0 240/1.0	.045 .035 .030 .020	.040	.222
1200	30/0.5 30/1.0 225/1.0 90/1.5 315/3.0 210/3.5	.025 .025 .025 .040 .030 .025	.037	.205
2000	165/1.0 210/4.75 210/5.75 225/1.5 30/0.0 30/1.5 90/0.5	.030 .030 .025 .020 .040 .030 .055	.044	.244
3000	150/0.0 135/2.0 180/1.0 195/3.75 210/6.0 255/1.0 0/0.5 30/0.5 105/0.5	.060 .025 .035 .030 .030 .025 .045 .060 .070	.065	.361

Run No. 2 (Continued)

Wave No. 2 Sand No. 1

No. of waves	Degree / Distance from pile	Depth of scour (ft)	$\bar{S}$ (ft)	$\frac{\bar{S}}{H}$
4000	90/0.5	.075	.067	.372
	30/0.5	.055		
	0/0.5	.050		
	180/0.5	.060		
	180/1.0	.040		
	240/1.5	.025		
	195/3.5	.025		
	240/7.0	.035		
6050	90/0.0	.080	.080	.444
6400	95/0.0	.080	.080	.444

Run No. 3

Wave No. 3 Sand No. 1

No. of waves	Degree / Distance from pile	Depth of scour (ft)	$\bar{S}$ (ft)	$\frac{\bar{S}}{H}$
200	120/1.5	.025	.022	.0847
	210/0.5	.020		
	315/1.0	.015		
	0/1.0	.000		
	75/1.5	.010		
450	120/1.5	.035	.0325	.125
	150/3.0	.010		
	210/3.0	.010		
	225/1.5	.030		
	285/2.0	.020		
	0/1.0	.005		
	75/1.5	.020		
800	120/1.5	.037	.033	.127
	150/3.0	.030		
	135/3.75	.035		
	180/5.5	.032		
	210/3.5	.030		
	210/6.0	.030		
	240/1.5	.035		
	315/1.5	.015		
1200	105/1.75	.033	.035	.1345
	150/3.5	.030		
	150/6.0	.035		
	180/2.75	.025		
	180/5.5	.035		
	210/6.0	.030		
	255/2.25	.035		
2000	105/2.0	.025	.037	.1425
	120/4.5	.040		
	135/6.75	.035		
	180/3.0	.025		
	180/5.5	.030		
	255/3.5	.030		
	300/2.5	.025		

Run No. 3 (Continued)

Wave No. 3 Sand No. 1

No. of waves	Degree / Distance from pile	Depth of scour (ft)	$\bar{S}$ (ft)	$\frac{\bar{S}}{H}$
	105/3.5	.035		
	135/6.25	.035		
	150/7.0	.040		
	120/7.0	.035		
3000	180/3.5	.020	.037	.1425
	180/5.75	.025		
	195/6.5	.035		
	255/4.25	.030		
	270/5.0	.025		
	0/1.25	.015		
	0/4.0	.015		
	240/1.5	.035		
5050	105/1.5	.030	.032	.1231
	180/.75	.005		
	180/2.5	.010		
	180/4.75	.030		

Run No. 4

Wave No. 1 Sand No. 1

No. of waves	Degree / Distance from pile	Depth of scour (ft)	$\bar{S}$ (ft)	$\underline{\bar{S}}$
100	0/0.0 210/2.0 135/2.0 90/0.0 270/0.0	.020 .035 .025 .020 .030	.0325	.176
230	0/0.0 90/0.0 270/0.0 135/2.5 210/2.5 180/4.5	.035 .025 .050 .030 .030 .035	.043	.232
400	0/0.0 270/0.0 90/0.0 135/3.0 190/5.5 200/3.0	.040 .060 .030 .030 .040 .040	.050	.270
800	0/0.0 270/0.0 90/0.0 140/3.25 195/3.25 180/7.0	.050 .055 .065 .033 .040 .040	.060	.324
1200	0/0.0 315/0.5 45/0.0 195/4.0 150/4.0	.060 .055 .070 .040 .042	.065	.351
2000	0/0.0 315/0.0 45/0.0 195/4.5 140/4.5	.060 .055 .073 .043 .045	.066	.357

Run No. 4 (Continued)

Wave No. 1 Sand No. 1

No. of waves	Degree / Distance from pile	Depth of scour (ft)	$\bar{S}$ (ft)	$\frac{\bar{S}}{H}$
3000	0/0.0	.070	.0725	.392
	315/0.0	.065		
	45/0.5	.075		
	195/5.5	.055		
	150/4.5	.060		
4000	0/0.0	.075	.080	.433
	330/0.0	.075		
	195/6.75	.060		
	150/5.0	.065		
	30/0.5	.085		
5440	0/0.0	.075	.0775	.419
	315/0.0	.075		
	240/3.5	.055		
	150/5.5	.075		
	30/0.5	.080		

Run No. 5

Wave No. 2 Sand No. 1

No. of waves	Degree / Distance from pile	Depth of scour (ft)	$\bar{S}$ (ft)	$\frac{\bar{S}}{H}$
200	210/1.75 120/1.0 0/0.0 180/0.0	.030 .035 .020 .020	.035	.250
400	210/1.25 180/0.0 135/1.25 0/0.0	.037 .030 .035 .025	.037	.264
800	225/1.5 180/0.0 135/1.75 0/0.0	.040 .025 .040 .015	.040	.286
1200	0/0.0 220/1.0 180/0.0 135/2.0	.030 .040 .015 .040	.040	.286
2000	0/0.0 300/0.0 210/1.5 135/2.0 180/1.0	.030 .040 .040 .040 .040	.040	.286
3000	0/0.0 300/0.0 225/1.75 180/1.0 120/2.5	.025 .045 .040 .040 .045	.045	.321
3600	0/0.0 30/0.0 225/1.5 120/3.5	.025 .030 .040 .040	.040	.286

Run No. 6

Wave No. 3 Sand No. 1

No. of waves	Degree / Distance from pile	Depth of scour (ft)	$\bar{S}$ (ft)	$\frac{\bar{S}}{H}$
320	125/1.5 240/1.0 195/4.5 165/4.0	.030 .040 .025 .025	.040	1775
600	125/1.25 190/0.5 130/1.75 150/4.5 195/4.5	.030 .045 .040 .025 .025	.0425	.189
1000	240/2.5 120/2.5 210/4.5 150/5.0 180/0.5	.033 .030 .025 .035 .040	.038	.1685
2000	240/3.0 120/3.0 210/.75 240/2.0 240/4.5 150/4.5	.025 .030 .035 .033 .030 .030	.036	.160
4000	250/3.0 225/3.75 180/.75 105/4.0 135/1.0 225/1.5	.025 .035 .030 .025 .040 .035	.038	.1685
6000	180/.75 220/1.25 180/4.25 120/1.25 105/5.5 255/5.5	.035 .040 .035 .038 .025 .020	.039	.1735

Run No. 7

Wave No. 1 Sand No. 2

No. of waves	Degree / Distance from pile	Depth of scour (ft)	$\bar{S}$ (ft)	$\frac{\bar{S}}{H}$
200	0/0.0	.020	.0275	.1715
	315/0.0	.020		
	230/1.0	.025		
	110/2.0	.030		
	60/1.5	.025		
400	0/0.0	.025	.0325	.203
	315/0.0	.024		
	220/1.5	.030		
	110/2.5	.035		
	60/1.5	.025		
800	270/0.0	.030	.0325	.203
	315/.75	.035		
	225/2.0	.030		
	110/3.0	.035		
	60/2.0	.020		
1200	315/0.0	.025	.038	.237
	270/0.0	.030		
	220/1.5	.035		
	110/3.0	.040		
	60/1.5	.025		
2000	315/0.0	.030	.038	.237
	270/0.0	.035		
	220/2.0	.040		
	110/3.0	.035		
	40/1.5	.025		
3000	315/0.0	.037	.042	.262
	270/0.0	.044		
	220/2.5	.040		
	120/3.5	.030		
	45/2.5	.030		

Run No. 7 (Continued)

Wave No. 1 Sand No. 2

No. of waves	Degree / Distance from pile	Depth of scour (ft)	$\bar{S}$ (ft)	$\frac{\bar{S}}{H}$
	315/0.0	.045		
	270/0.0	.044		
4500	220/1.5	.040	.0445	.278
	120/4.0	.032		
	30/2.0	.025		

Run No. 8

Wave No. 2 Sand No. 2

No. of waves	Degree / Distance from pile	Depth of scour (ft)	$\bar{S}$ (ft)	$\frac{\bar{S}}{H}$
200	280/0.5 240/1.0 115/2.5 45/2.5	.030 .030 .015 .015	.030	.162
400	0/0.0 270/1.0 240/1.5 110/2.0 40/2.0	.013 .033 .034 .025 .015	.0335	.181
800	270/1.5 190/0.5 240/1.5 110/1.0	.034 .042 .034 .020	.042	.227
1200	270/1.5 225/1.0 120/3.0	.035 .050 .025	.050	.270
2000	270/1.0 220/1.0 120/1.5 135/4.0	.040 .050 .025 .025	.050	.270
3000	310/0.5 260/0.5 230/1.0 120/2.0	.050 .065 .055 .025	.065	.351
4200	240/1.0	.065	.065	.351

Run No. 9

Wave No. 3 Sand No. 2

No. of waves	Degree / Distance from pile	Depth of scour (ft)	$\bar{S}$ (ft)	$\frac{\bar{S}}{H}$
200	320/0.5 285/0.5 220/1.5 130/1.5 100/1.0	.006 .010 .025 .021 .030	.0275	.0917
400	330/0.5 270/1.5 225/1.0 135/1.5 90/1.5 180/3.0	.005 .015 .030 .025 .035 .025	.0325	.1085
800	270/2.0 225/1.75 110/2.5 70/2.0 180/3.25 210/4.25 140/4.5	.020 .030 .030 .030 .020 .030 .035	.0325	.1085
1300	270/3.0 235/3.5 180/1.5 105/4.0 70/2.5 205/4.5	.030 .030 .030 .035 .035 .025	.035	.1165
2000	290/3.0 260/4.5 180/2.0 180/4.0 180/6.5 90/4.0 340/3.0	.020 .025 .025 .010 .025 .040 .020	.0325	.1085

Run No. 9 (Continued)

Wave No. 3 Sand No. 2

No. of waves	Degree / Distance from pile	Depth of scour (ft)	$\bar{S}$ (ft)	$\frac{\bar{S}}{H}$
3000	295/3.5	.010	.035	.1165
	255/3.5	.025		
	180/6.0	.020		
	110/5.5	.035		
	0/6.5	.000		
4000	0/4.0	.025	.035	.1165
	245/2.5	.030		
	100/2.5	.030		
	150/3.0	.035		
	200/3.0	.035		

Run No. 10

Wave No. 1 Sand No. 2

No. of waves	Degree / Distance from pile	Depth of scour (ft)	$\bar{S}$ (ft)	$\frac{\bar{S}}{H}$
200	0/0.5 270/0.5 200/2.5 140/2.5 90/0.5	.040 .035 .035 .035 .035	.0375	.1975
400	0/0.5 270/0.5 90/0.5 150/3.0 200/3.0 190/6.5 170/6.5	.043 .035 .050 .035 .040 .035 .045	.046	.242
800	0/0.5 315/0.5 45/0.5 200/4.5 160/4.5	.055 .055 .055 .050 .050	.055	.289
1200	0/0.0 45/0.5 315/0.5 195/5.25 165/5.0	.065 .070 .060 .060 .063	.0675	.355
2000	0/0.0 315/0.5 40/0.0 200/7.5 170/7.0	.070 .070 .087 .060 .080	.085	.447
3000	0/0.0 315/0.0 30/0.0	.095 .088 .100	.100	.526

Run No. 10 (Continued)

Wave No. 1 Sand No. 2

No. of waves	Degree / Distance from pile	Depth of scour (ft)	$\bar{S}$ (ft)	$\frac{\bar{S}}{H}$
5000	0/0.0 315/0.0 40/0.0	.095 .090 .105	.105	.553
5600	0/0.0 40/0.0 315/0.0	.095 .105 .090	.105	.553

Run No. 11

Wave No. 2 Sand No. 2

No. of waves	Degree / Distance from pile	Depth of scour (ft)	$\bar{S}$ (ft)	$\frac{\bar{S}}{H}$
200	0/0.0 180/0.0 220/1.0 130/1.0	.015 .025 .035 .035	.035	.269
400	0/0.0 180/0.0 225/1.5 135/1.5	.020 .025 .037 .035	.037	.284
800	0/0.0 180/0.0 225/2.0 135/2.0	.020 .030 .037 .044	.044	.339
1200	0/0.0 180/0.0 225/1.5 135/1.75	.020 .030 .037 .044	.044	.339
2000	0/0.0 180/0.0 220/1.5 135/1.5	.025 .030 .038 .045	.045	.346
3000	0/0.0 180/0.0 220/1.5 140/2.0	.026 .032 .038 .044	.044	.339

Run No. 12

Wave No. 3 Sand No. 2

No. of waves	Degree / Distance from pile	Depth of scour (ft)	$\bar{S}$ (ft)	$\frac{\bar{S}}{H}$
200	210/2.0 140/1.5 180/4.0	.035 .035 .025	.035	.159
400	225/1.5 135/1.5 180/4.0 180/7.0	.037 .037 .025 .025	.037	.168
800	225/1.5 135/2.25 180/4.5 180/7.5	.040 .040 .030 .025	.040	.182
1200	230/1.5 135/2.5 180/5.0 180/7.5	.042 .030 .025 .025	.042	.191
2000	240/2.5 130/3.5 180/5.0 180/7.5	.047 .020 .025 .025	.047	.213
3000	240/2.5 190/.75 120/5.0 180/5.5	.050 .044 .040 .025	.050	.227
4000	240/2.5 200/.5 120/5.0 180/6.0	.045 .044 .030 .023	.045	.205

Run No. 13

Wave No. 1 Sand No. 3

No. of waves	Degree / Distance from pile	Depth of scour (ft)	$\bar{S}$ (ft)	$\frac{\bar{S}}{H}$
200	0/0.0 180/0.0 210/2.5 135/2.0	.015 .020 .025 .045	.054	.265
400	0/.5 180/0.0 225/1.5 135/2.0 180/4.5	.010 .025 .040 .050 .040	.045	.265
820	0/.5 230/2.5 180/0.0 180/1.0 180/4.5 120/1.5	.010 .025 .035 .043 .035 .050	.047	.276
1200	0/0.5 180/0.0 180/0.5 180/4.5 105/1.5 45/0.5	.015 .040 .045 .035 .055 .040	.050	.294
2000	0/0.5 180/0.0 180/1.0 180/5.0 90/1.5	.025 .035 .063 .035 .045	.053	.312
3000	0/0.5 180/1.5 180/6.0 30/0.5 90/0.5 120/2.0	.020 .055 .044 .040 .045 .045	.050	.294

Run No. 14

Wave No. 2 Sand No. 3

No. of waves	Degree / Distance from pile	Depth of scour (ft)	$\bar{S}$ (ft)	$\frac{\bar{S}}{H}$
200	0/0.0 285/1.0 30/0.5 100/0.5 180/0.5	.020 .015 .020 .040 .025	.0325	.1665
400	0/0.0 285/1.0 225/1.75 95/1.0 45/1.0 120/2.0	.020 .020 .030 .033 .023 .025	.032	.164
800	0/0.5 280/1.5 225/2.0 180/0.0 90/1.5	.020 .020 .040 .035 .035	.035	.1795
1200	0/0.5 285/0.5 225/1.5 80/1.0 180/0.5 120/4.0	.010 .035 .045 .050 .035 .030	.0475	.243
2000	0/0.5 270/0.5 225/1.5 180/1.0 100/1.5 140/5.0	.015 .055 .045 .035 .040 .025	.050	.256
3000	0/0.5 315/0.75 245/1.0 120/2.0 170/3.0 130/4.0	.030 .045 .045 .020 .035 .025	.045	.230

Run No. 14 (Continued)

Wave No. 2 Sand No. 3

No. of waves	Degree / Distance from pile	Depth of scour (ft)	$\bar{S}$ (ft)	$\frac{\bar{S}}{H}$
5200	0/0.0	.035	.040	.205
	300/0.0	.045		
	285/4.5	.020		
	180/3.0	.035		
	250/4.5	.025		
	330/5.5	.010		

Run No. 15

Wave No. 3 Sand No. 3

No. of waves	Degree / Distance from pile	Depth of scour (ft)	$\bar{S}$ (ft)	$\frac{\bar{S}}{H}$
200	270/1.0 100/1.0 60/1.0	.020 .030 .030	.030	.111
400	260/1.5 300/1.0 45/1.0 120/0.5 180/4.5	.025 .020 .035 .020 .020	.030	.111
800	240/1.0 180/2.5 180/5.0 0/6.5 0/2.0	.015 .020 .020 .020 .015	.020	.0741
1200	0/1.0 0/3.5 0/5.5 180/2.5 180/5.0 180/7.5	.005 .015 .020 .025 .015 .015	.0225	.0834
2000	180/.75 180/3.0 180/5.0 225/2.0 0/2.5 0/5.0 0/7.5	.020 .025 .025 .035 .030 .015 .020	.0325	.120
3000	0/1.5 0/4.0 0/7.0 180/3.5 180/6.0	.030 .020 .020 .025 .025	.0375	.139

Run No. 15 (Continued)

Wave No. 3 Sand No. 3

No. of waves	Degree / Distance from pile	Depth of scour (ft)	$\bar{S}$ (ft)	$\frac{\bar{S}}{H}$
4000	0/1.0	.025	.037	.137
	0/4.5	.035		
	0/6.5	.020		
	180/2.0	.023		
	180/4.0	.040		

Run No. 16

Wave No. 1 Sand No. 3

No. of waves	Degree / Distance from pile	Depth of scour (ft)	$\bar{S}$ (ft)	$\frac{\bar{S}}{H}$
200	0/0.5	.035	.035	.184
	210/1.5	.035		
	125/2.5	.025		
	90/0.75	.020		
	180/6.5	.025		
	195/4.5	.025		
400	0/0.5	.040	.0425	.224
	290/0.5	.045		
	240/2.5	.025		
	160/5.5	.025		
	200/5.5	.020		
800	0/1.0	.045	.060	.316
	330/0.5	.070		
	285/0.5	.050		
	230/3.0	.040		
	120/2.5	.030		
	70/1.0	.040		
	190/4.5	.030		
1200	0/0.5	.040	.060	.316
	290/0.5	.060		
	290/1.0	.060		
	270/1.5	.060		
	240/2.0	.050		
	210/7.0	.045		
	165/7.0	.025		
	130/5.5	.055		
	195/2.0	.045		
	80/1.0	.045		
2000	0/0.0	.060	.070	.369
	290/0.5	.070		
	270/1.0	.065		
	245/1.0	.055		
	190/4.5	.030		
	140/5.25	.050		
	65/0.5	.070		

Run No. 16 (Continued)

Wave No. 1 Sand No. 3

No. of waves	Degree / Distance from pile	Depth of scour (ft)	$\bar{S}$ (ft)	$\frac{\bar{S}}{H}$
	0/0.0	.065		
	300/0.5	.080		
	255/1.0	.090		
3000	75/1.0	.080	.085	.447
	15/0.5	.075		
	125/7.0	.075		
	185/7.5	.045		
	0/0.0	.075		
	300/0.5	.095		
	260/1.0	.090		
4000	90/1.5	.085	.0925	.487
	45/0.5	.090		
	125/6.25	.060		
	215/7.0	.055		
	0/0.0	.075		
	270/1.0	.095		
5000	240/2.0	.085	.0925	.487
	90/1.0	.090		
	45/0.5	.090		

Run No. 17

Wave No. 2 Sand No. 3

No. of waves	Degree / Distance from pile	Depth of scour (ft)	$\bar{S}$ (ft)	$\frac{\bar{S}}{H}$
200	325/0.0 220/0.75 130/0.75 180/0.0 45/0.0	.013 .030 .030 .025 .015	.030	.231
400	0/0.0 320/0.0 220/1.0 135/1.0 180/0.0 45/0.0	.015 .015 .035 .035 .025 .015	.035	.269
800	0/0.0 330/0.0 220/1.0 125/1.25 180/0.0	.015 .015 .035 .040 .035	.037	.285
1200	0/0.0 330/0.0 230/1.0 180/0.0 180/0.5 120/1.0	.020 .020 .030 .035 .035 .044	.041	.315
2000	0/0.0 330/0.0 240/1.25 180/0.5 180/0.0 130/1.0	.020 .020 .030 .040 .037 .040	.040	.308
3000	0/0.0 320/0.0 240/1.5 180/0.0 180/0.5 130/1.0	.020 .015 .035 .043 .044 .038	.0435	.335

Run No. 18

Wave No. 3 Sand No. 3

No. of waves	Degree / Distance from pile	Depth of scour (ft)	$\bar{S}$ (ft)	$\frac{\bar{S}}{H}$
200	0/1.0	.000	.025	.1135
	225/1.5	.025		
	180/0.5	.025		
	135/2.5	.020		
	90/1.0	.015		
415	0/0.5	.000	.030	.1365
	0/2.0	.005		
	230/1.5	.020		
	210/0.75	.040		
	130/2.0	.020		
	60/1.0	.010		
	180/3.5	.020		
800	30/3.5	.005	.024	.109
	240/2.5	.012		
	180/3.0	.015		
	180/5.75	.020		
	135/1.5	.023		
	210/0.5	.025		
1245	30/3.0	.000	.025	.1135
	255/2.0	.010		
	240/1.0	.025		
	190/3.0	.020		
	190/6.0	.015		
	150/1.5	.025		
2000	250/1.0	.025	.025	.1135
	190/1.0	.025		
	185/4.0	.025		
	185/6.0	.020		
	135/2.0	.025		
	135/7.5	.005		

Run No. 18 (Continued)

Wave No. 3 Sand No. 3

No. of waves	Degree / Distance from pile	Depth of scour (ft)	$\bar{S}$ (ft)	$\frac{\bar{S}}{H}$
3000	250/1.0	.015	.032	.1455
	190/0.75	.040		
	180/4.0	.025		
	140/7.0	.020		
	100/7.0	.010		
	225/7.0	.015		
5000	250/1.0	.015	.032	.1455
	190/0.75	.040		
	180/4.0	.025		
	140/7.0	.020		
	100/7.0	.010		
	225/7.0	.015		

APPENDIX II. — SCOUR PATTERNS

The scour pattern drawings are presented only to give an indication of the possible resulting scour for a particular wave. The numbers shown on the drawings are the measured scour depths times 10^{-3} taken at the completion of the experimental run. The contour patterns shown are based on observations during the run and engineering judgement and should not be construed to be the exact contour patterns. No attempt should be made to extract cross-sections from the drawings.

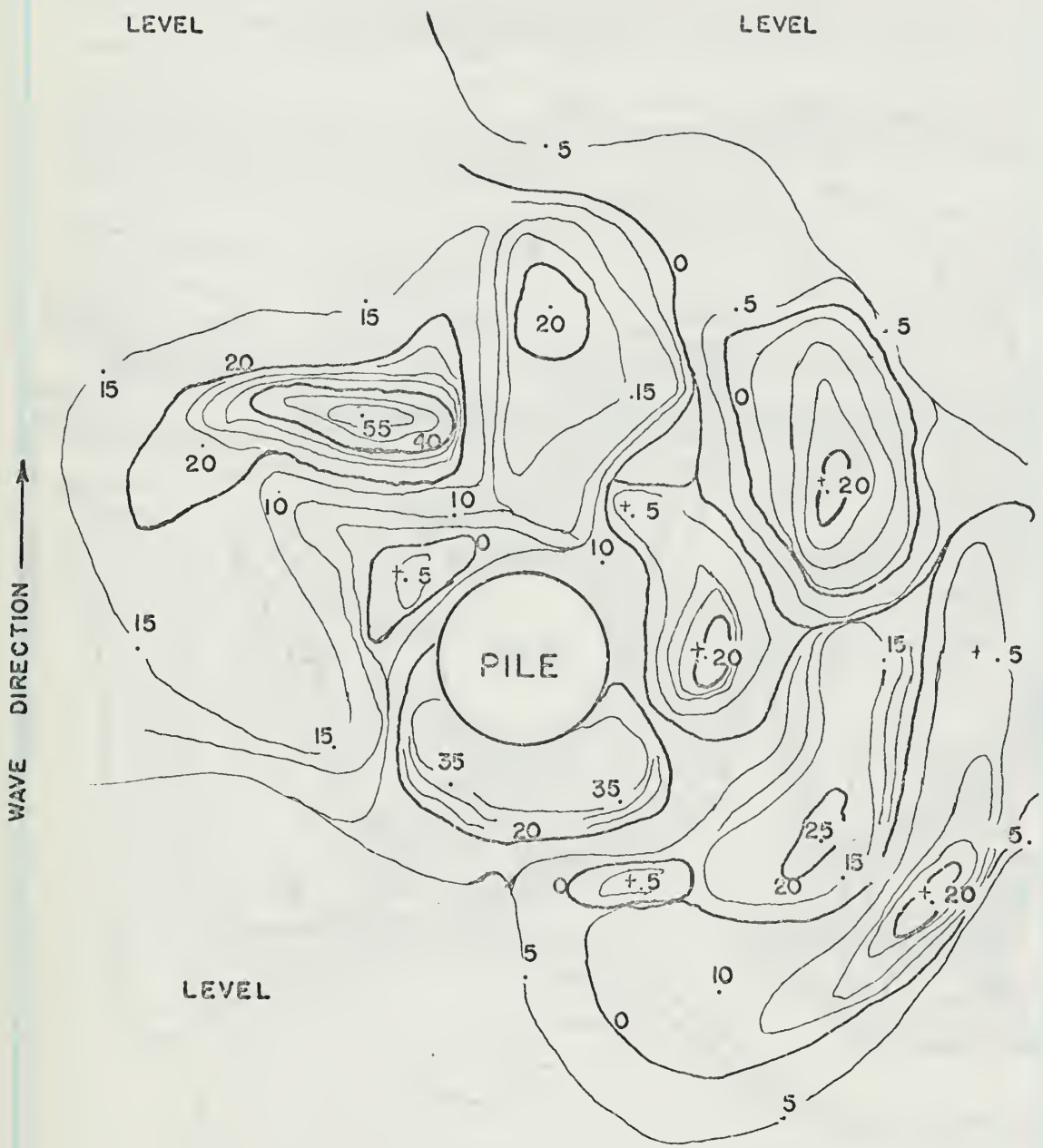

FIG. 36. SCOUR PATTERN FOR WAVE NO 1, SAND NO. 1, AND 1.25 FT. DEPTH

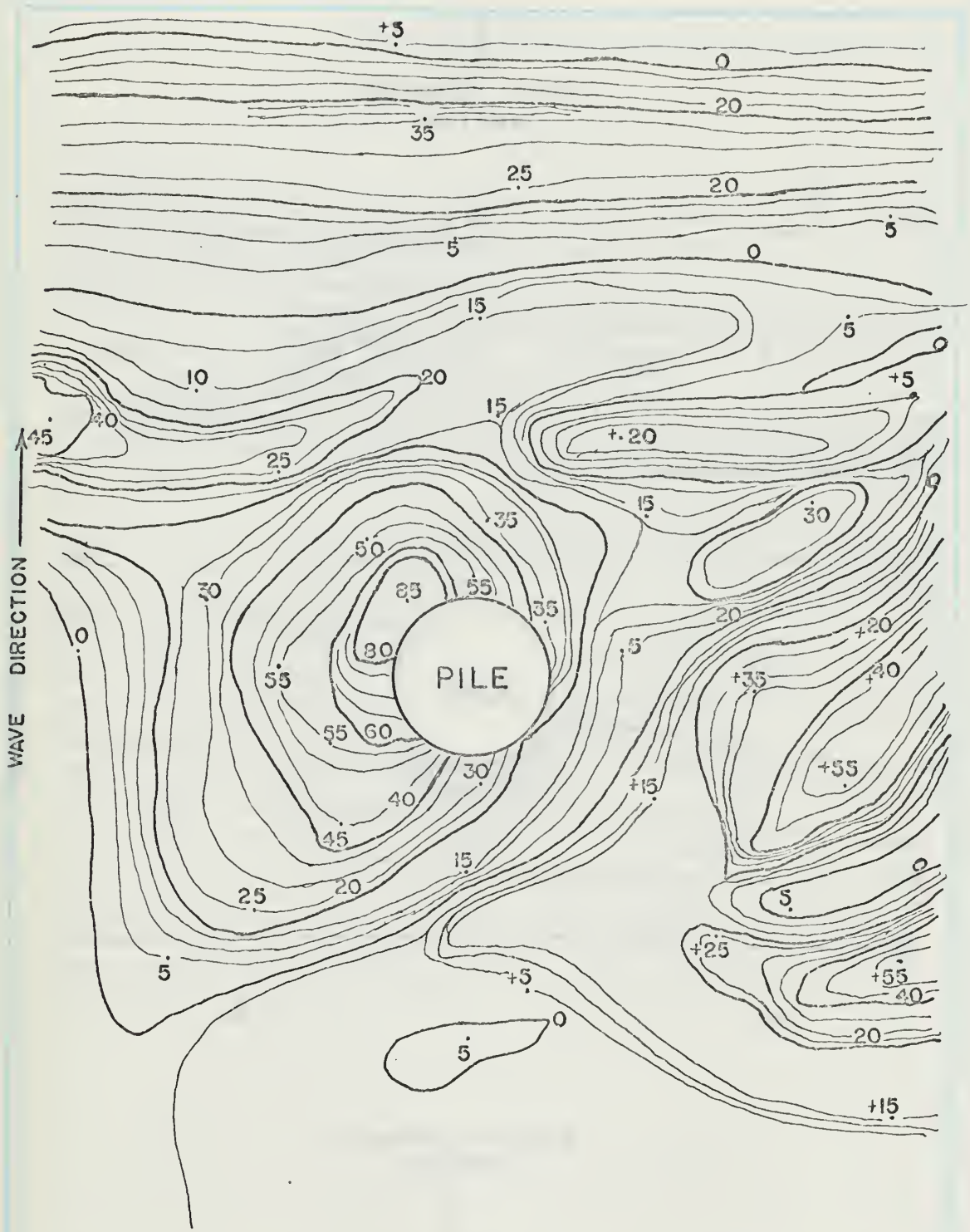

FIG. 37. SCOUR PATTERN FOR WAVE NO. 2, SAND NO. 1, AND 1.25 FT. DEPTH

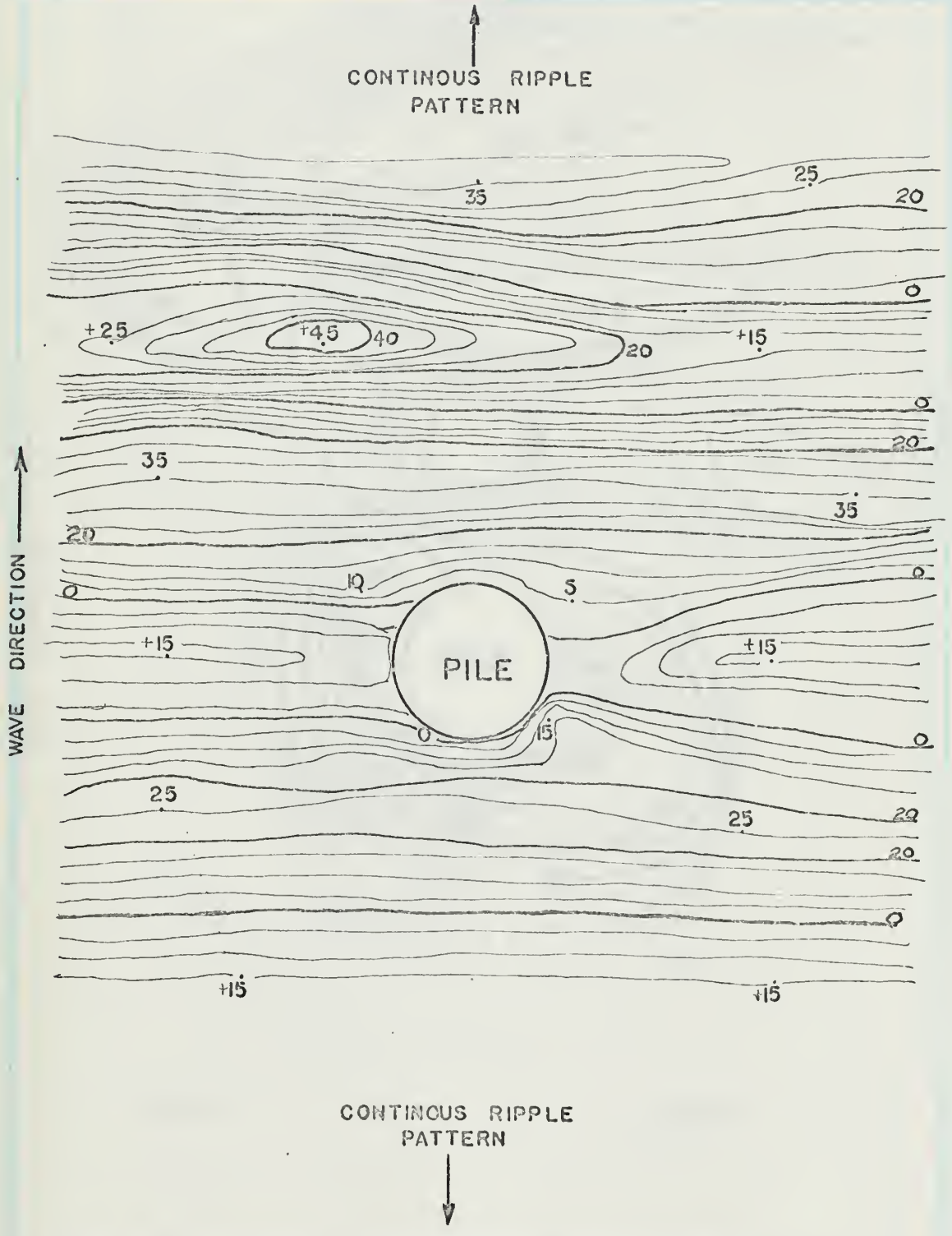

FIG. 38. SCOUR PATTERN FOR WAVE NO. 3, SAND NO. 1, AND 1.25 FT. DEPTH

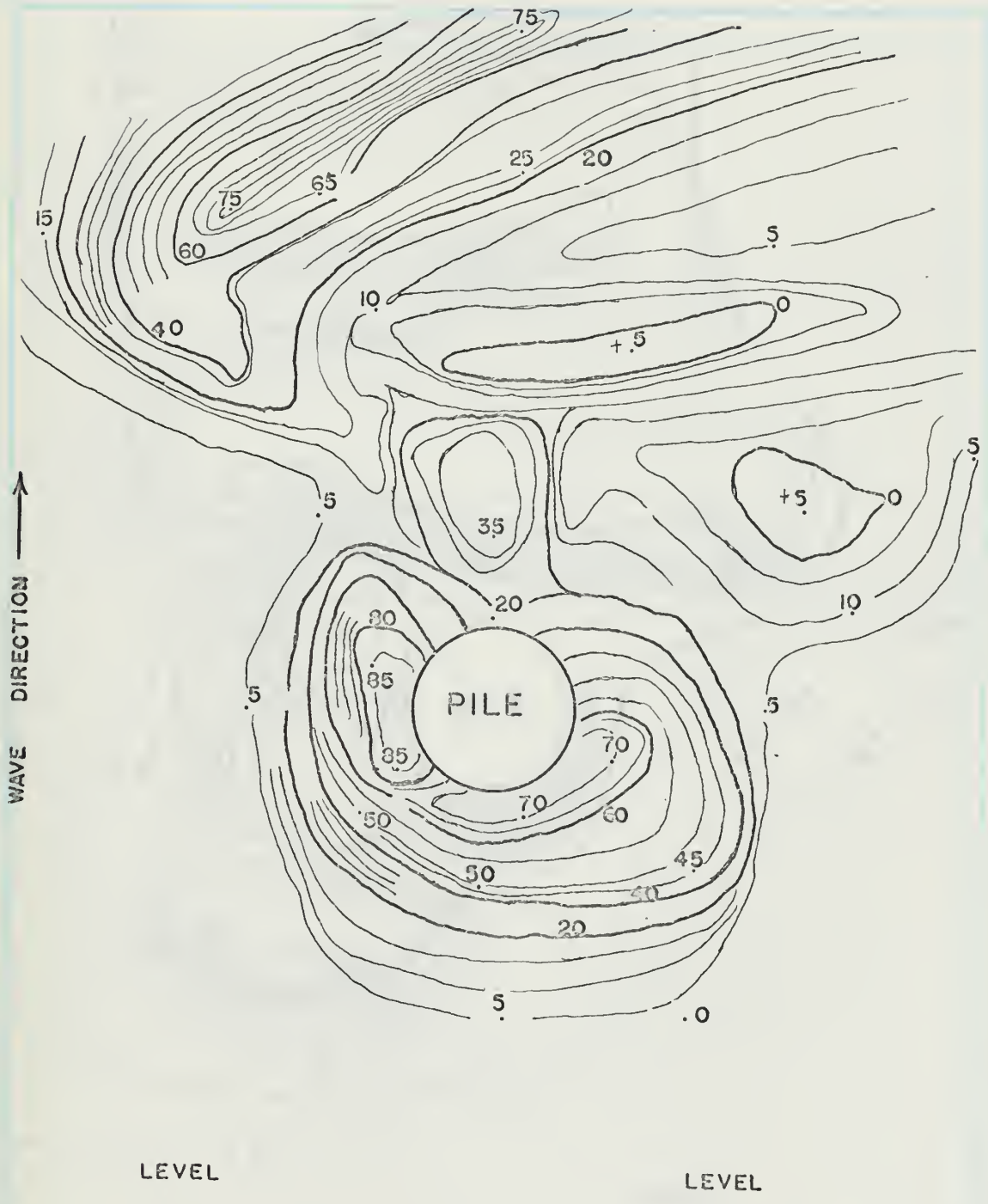

FIG. 39. SCOUR PATTERN FOR WAVE NO. 1, SAND NO. 1, AND 0.666 FT. DEPTH

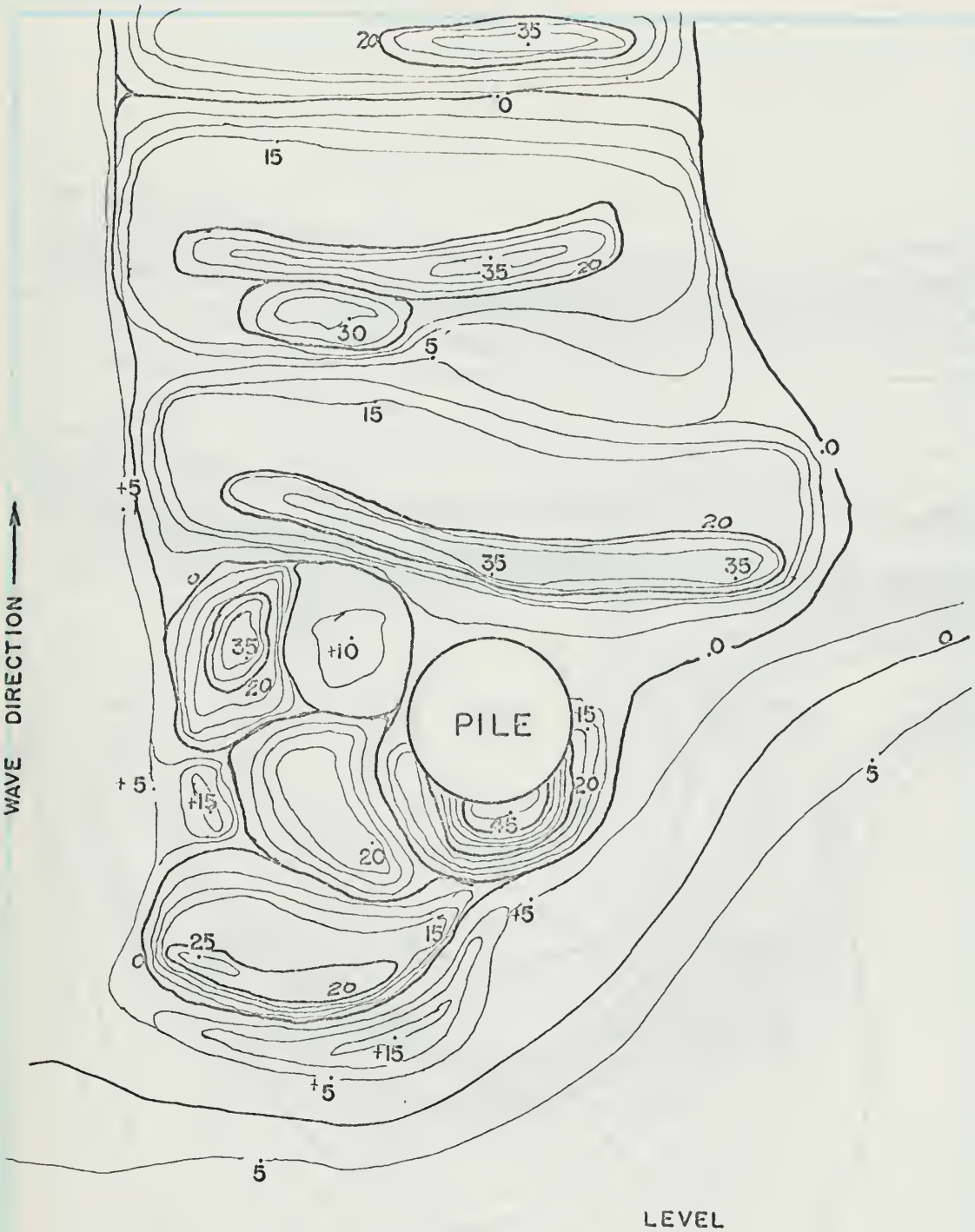

FIG. 40. SCOUR PATTERN FOR WAVE NO. 2., SAND NO. 1, AND 0.666 FT. DEPTH

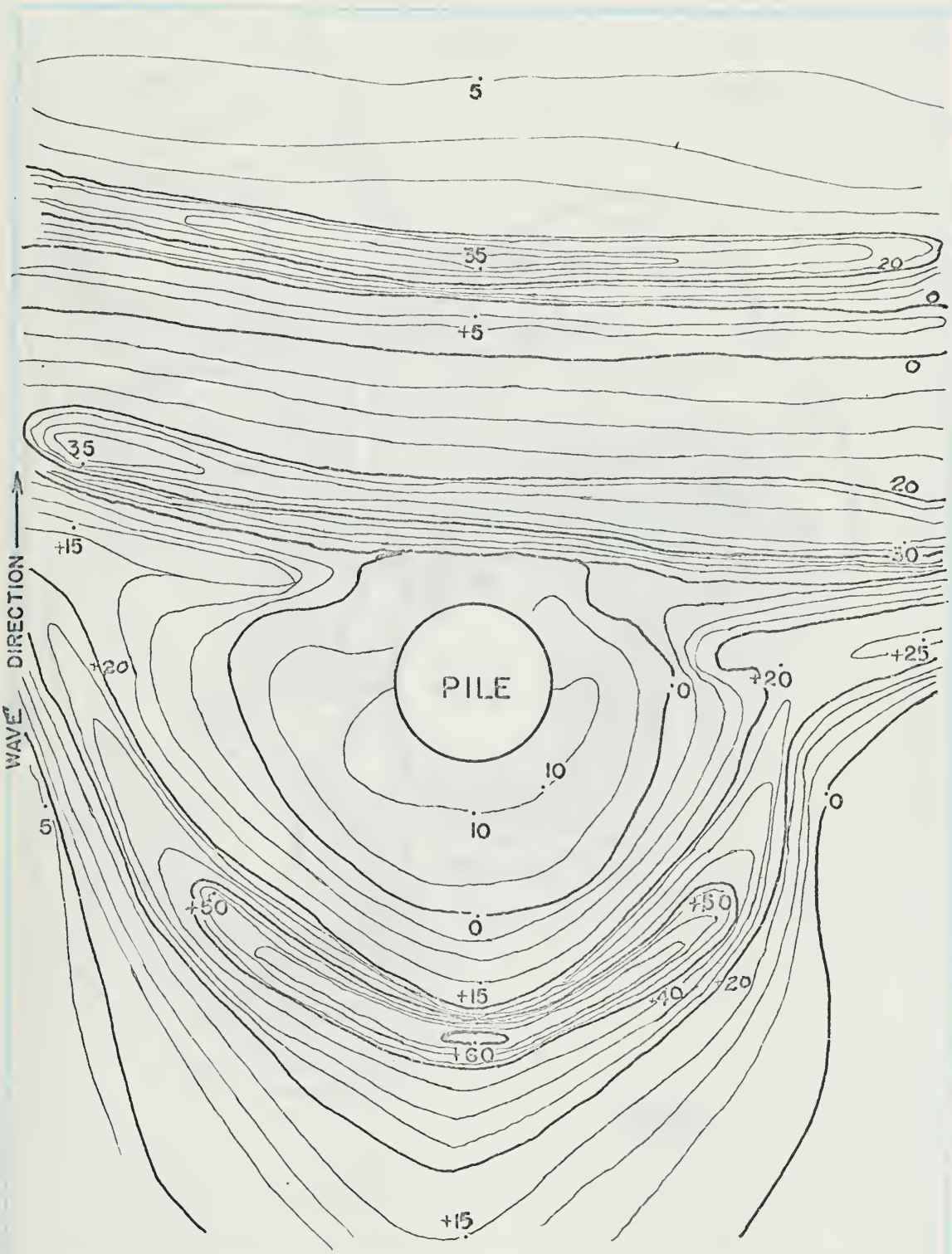

FIG. 41. SCOUR PATTERN FOR WAVE NO. 3, SAND NO. 1, AND 0.666 FT. DEPTH

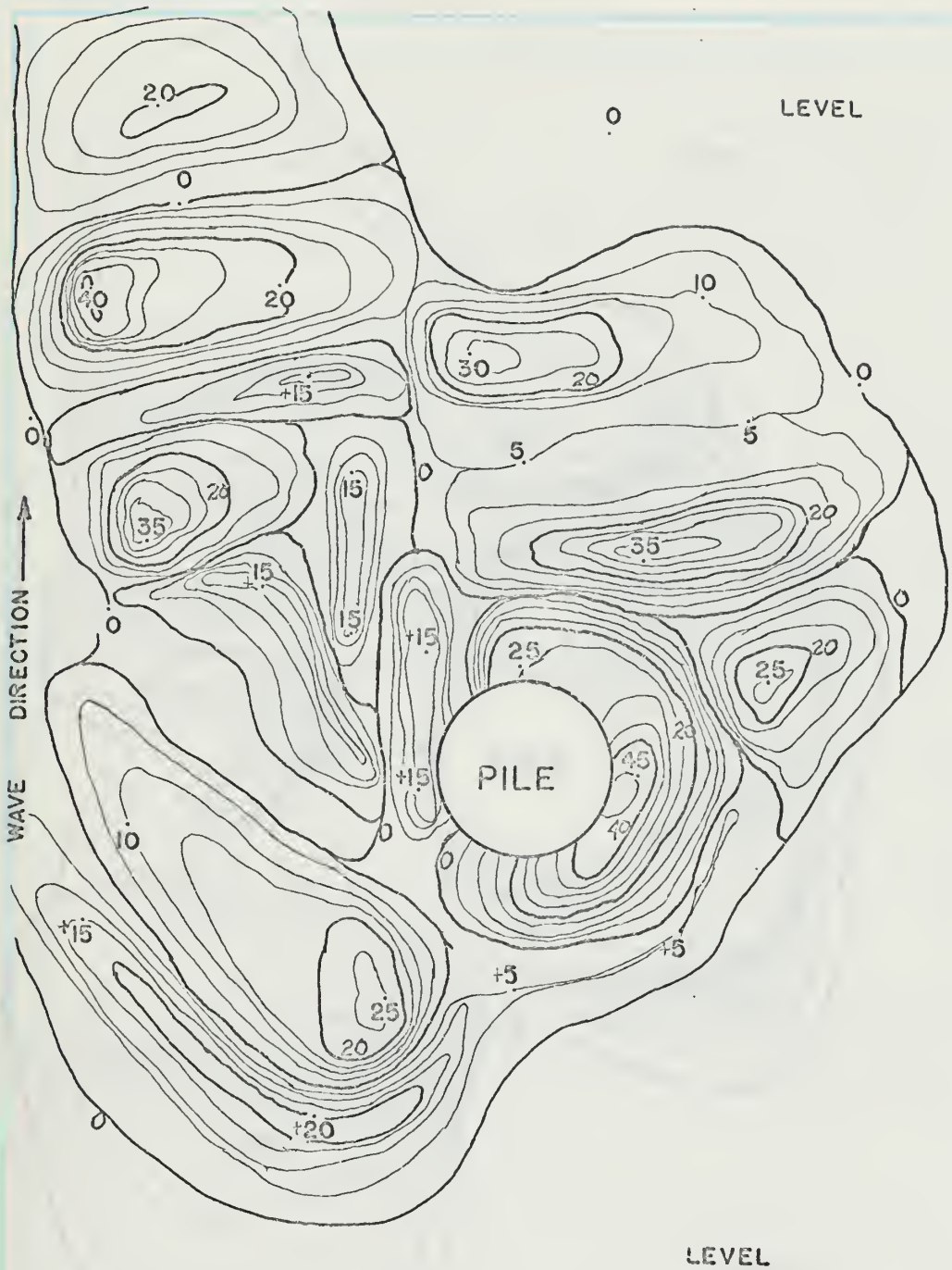

FIG. 42. SCOUR PATTERN FOR WAVE NO. 1, SAND NO. 2, AND 1.25 FT. DEPTH

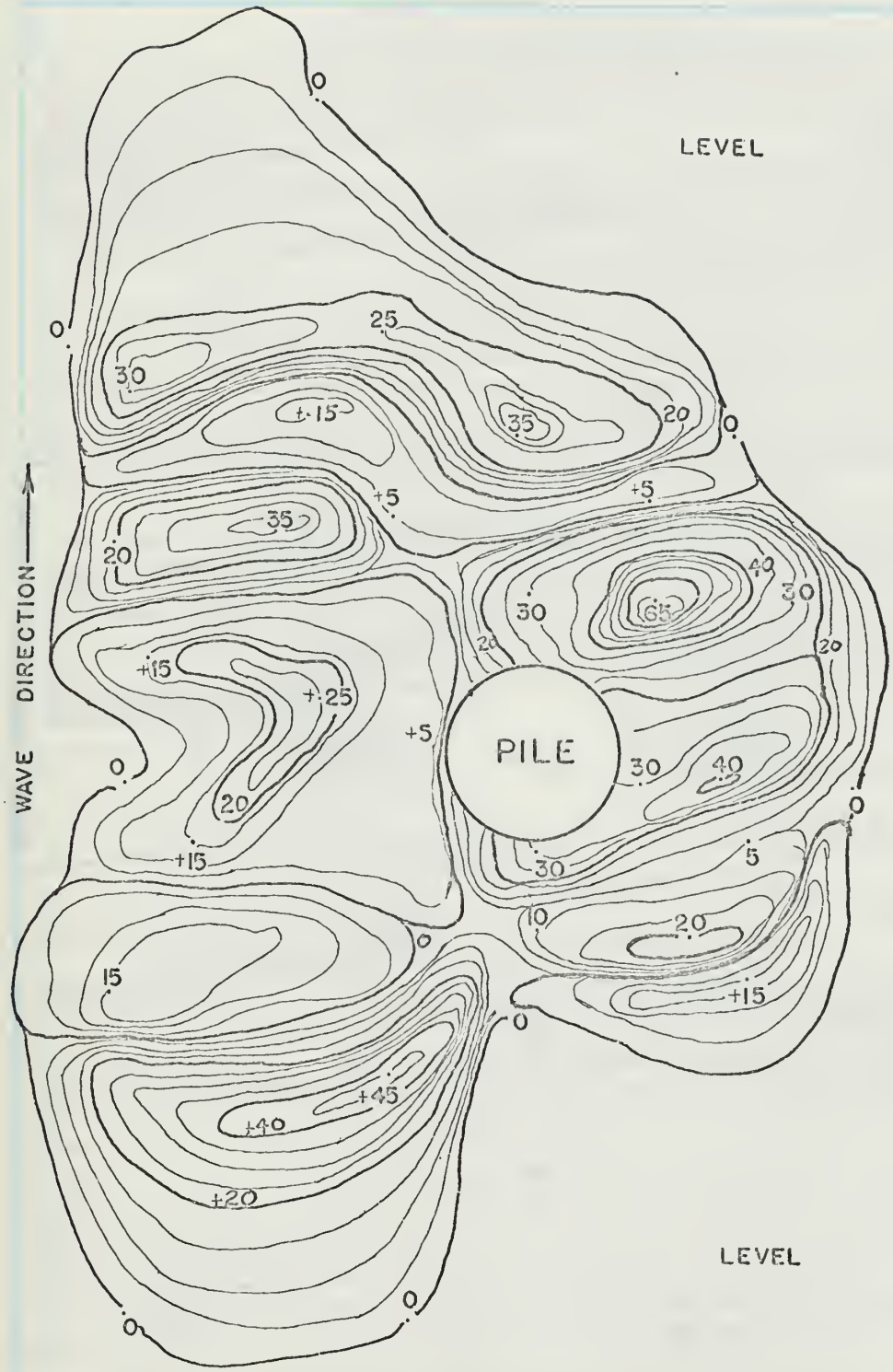

FIG. 43. SCOUR PATTERN FOR WAVE NO. 2, SAND NO. 2, AND 1.25 FT. DEPTH

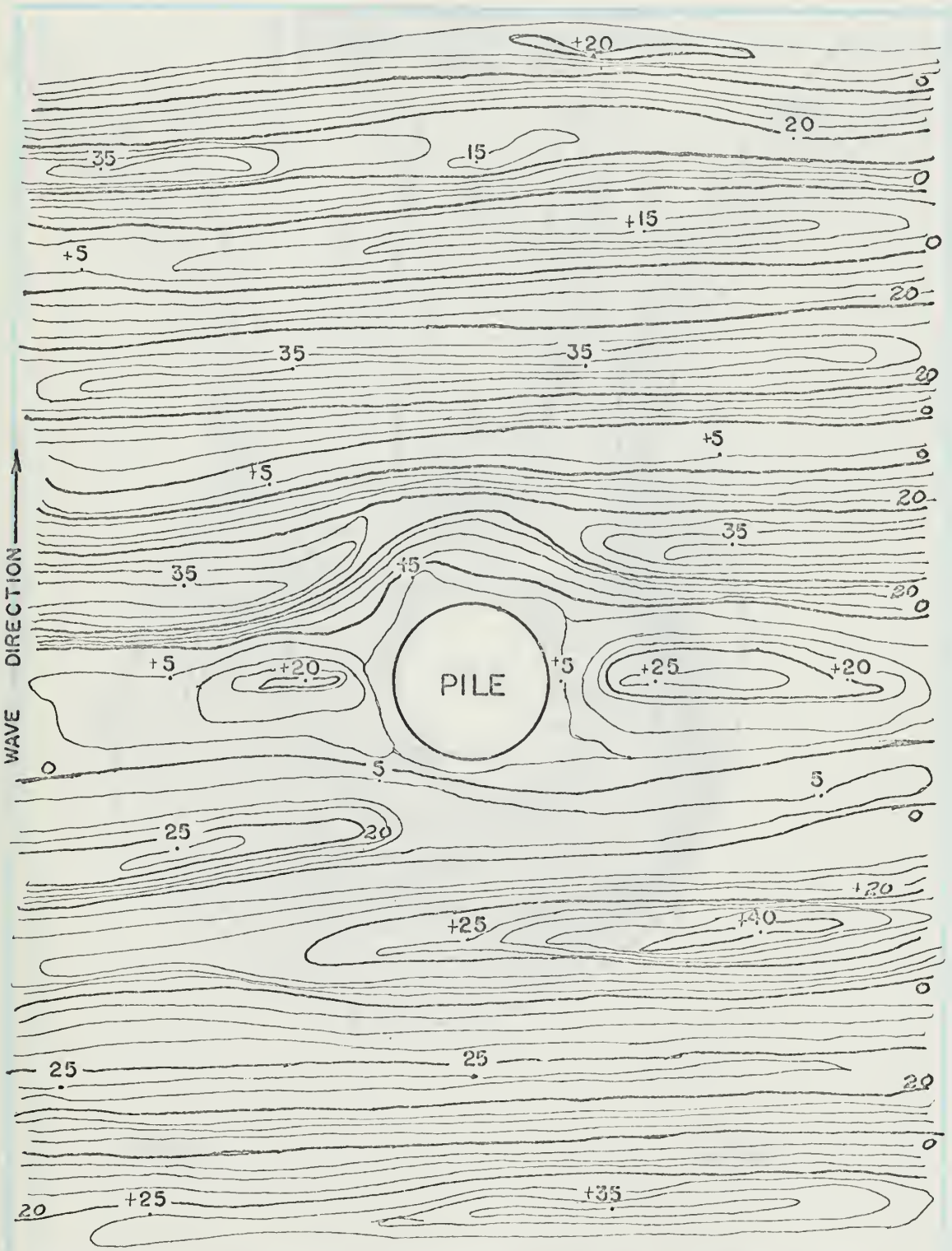

FIG. 44. SCOUR PATTERN FOR WAVE NO. 3, SAND NO. 2, AND 1.25 FT. DEPTH

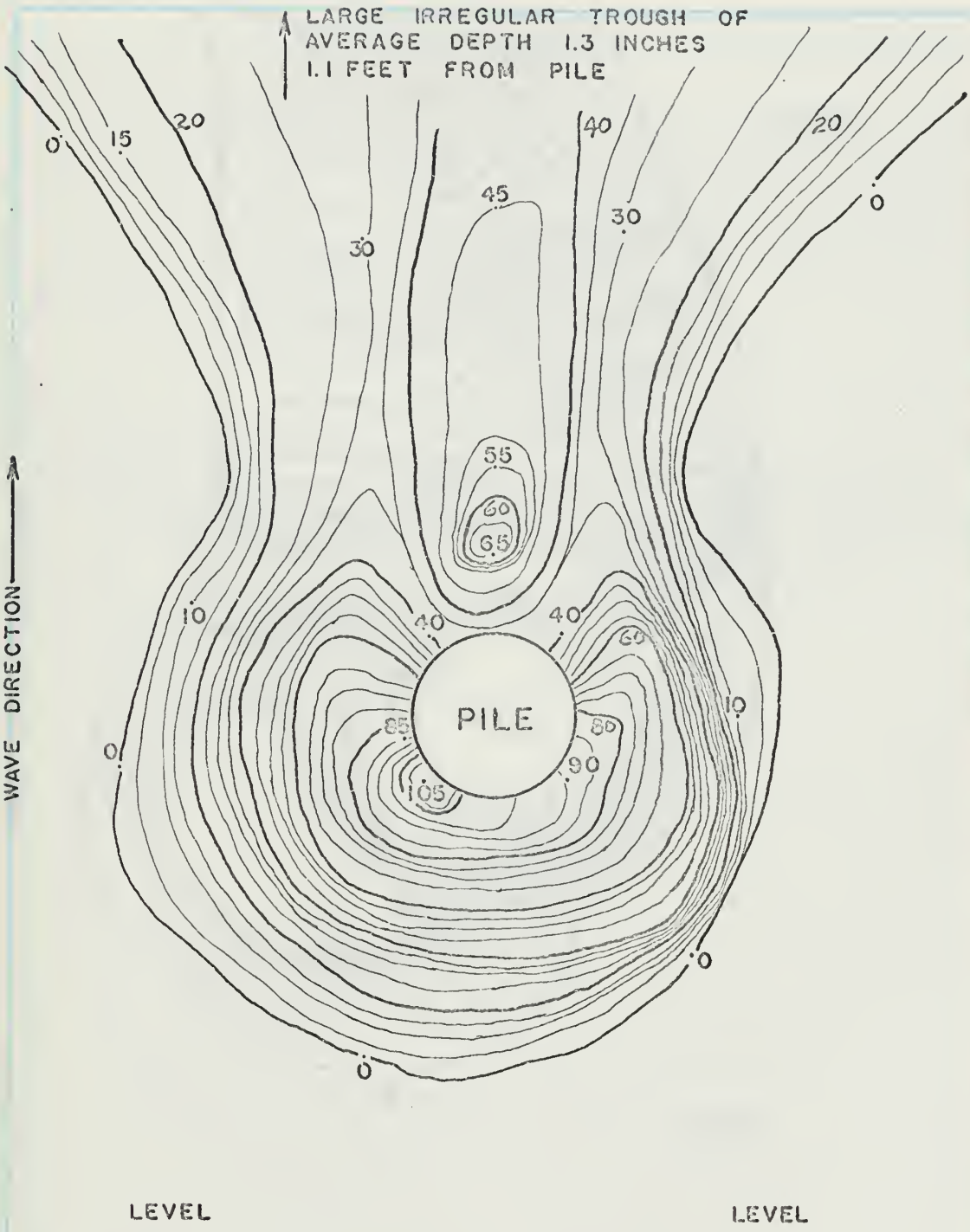

FIG. 45. SCOUR PATTERN FOR WAVE NO. 1, SAND NO. 2, AND 0.666 FT. DEPTH

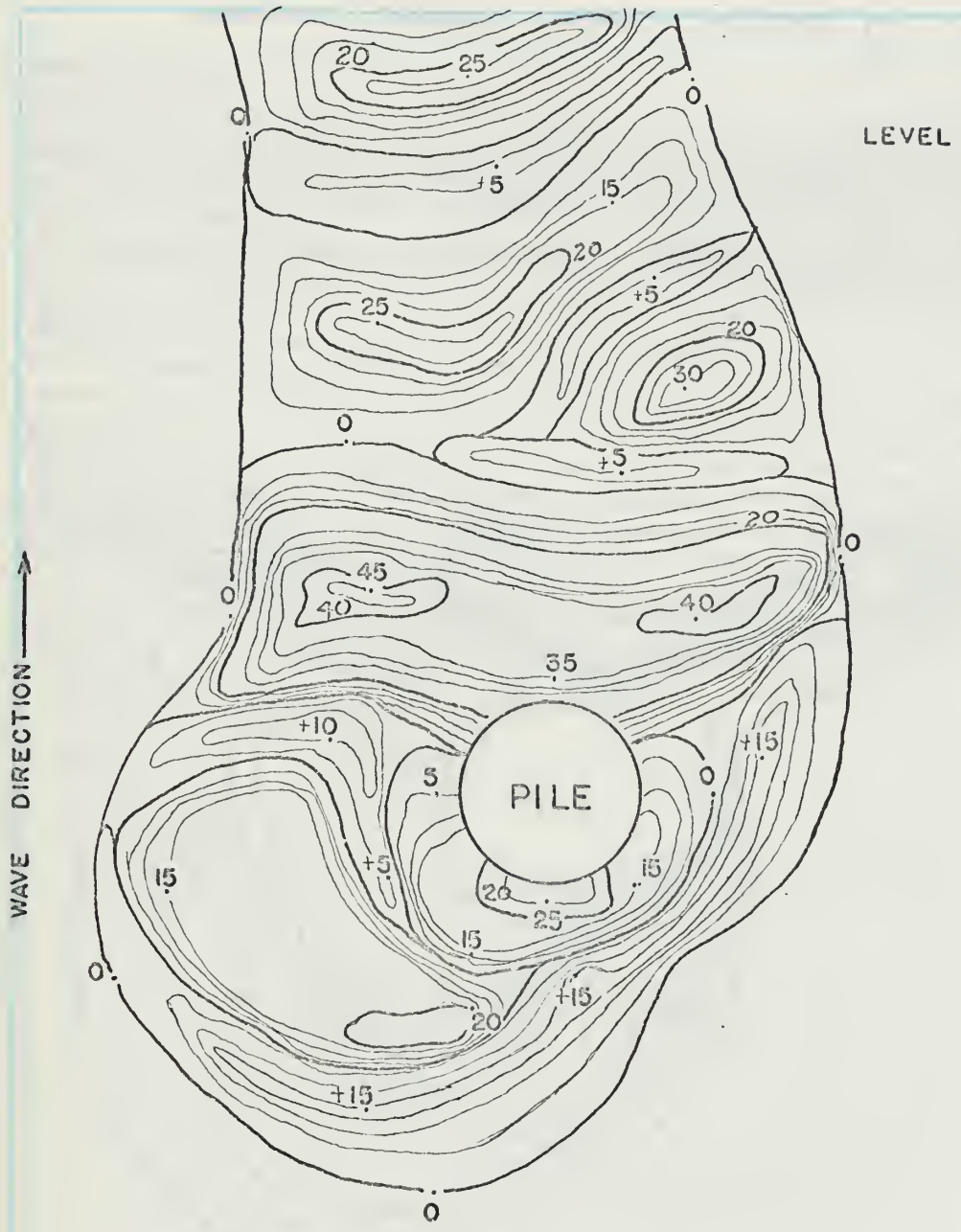

FIG. 46. SCOUR PATTERN FOR WAVE NO. 2, SAND NO. 2, AND 0.666 FT. DEPTH

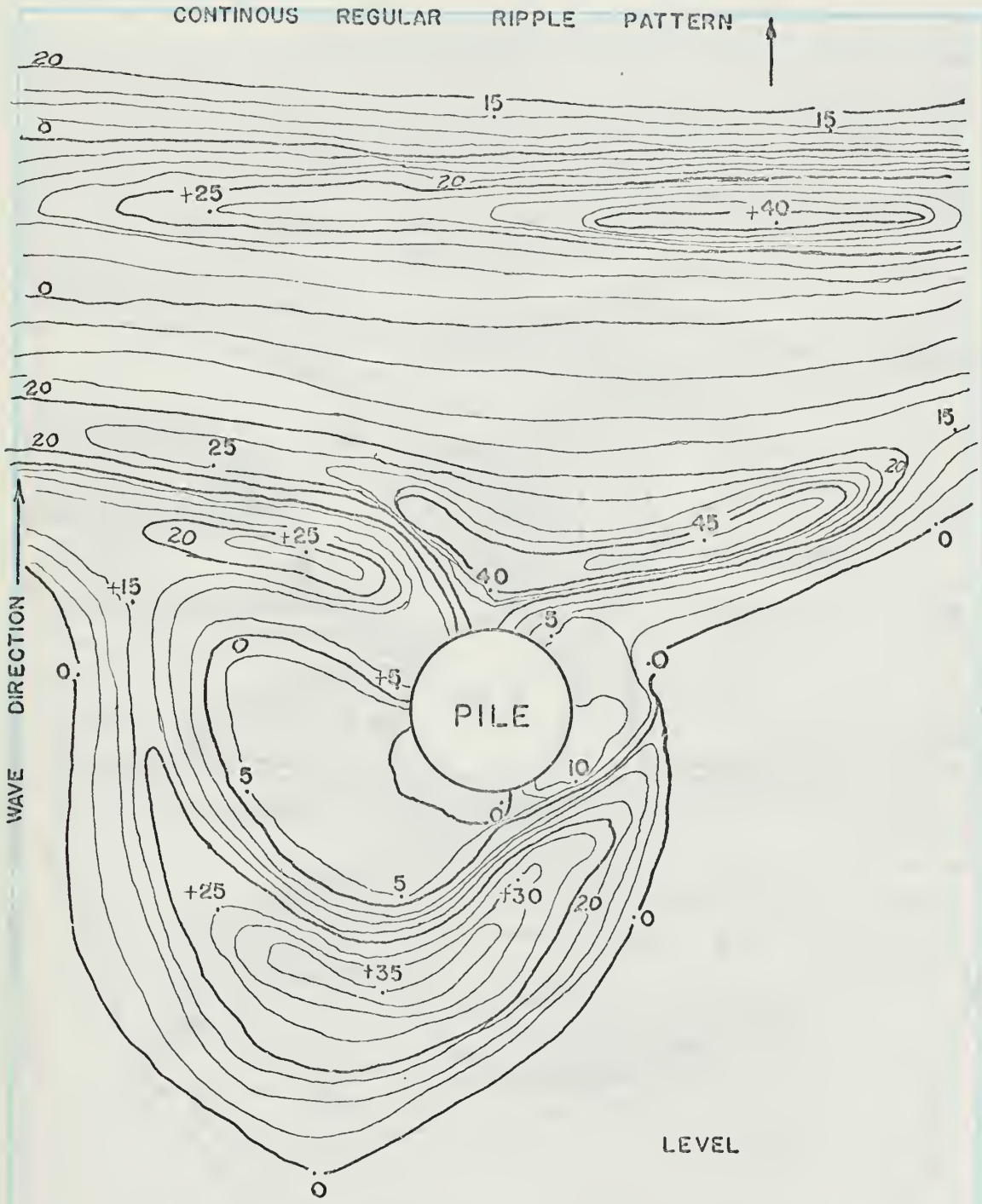

FIG. 47. SCOUR PATTERN FOR WAVE NO. 3, SAND NO. 2, AND 0.666 FT. DEPTH

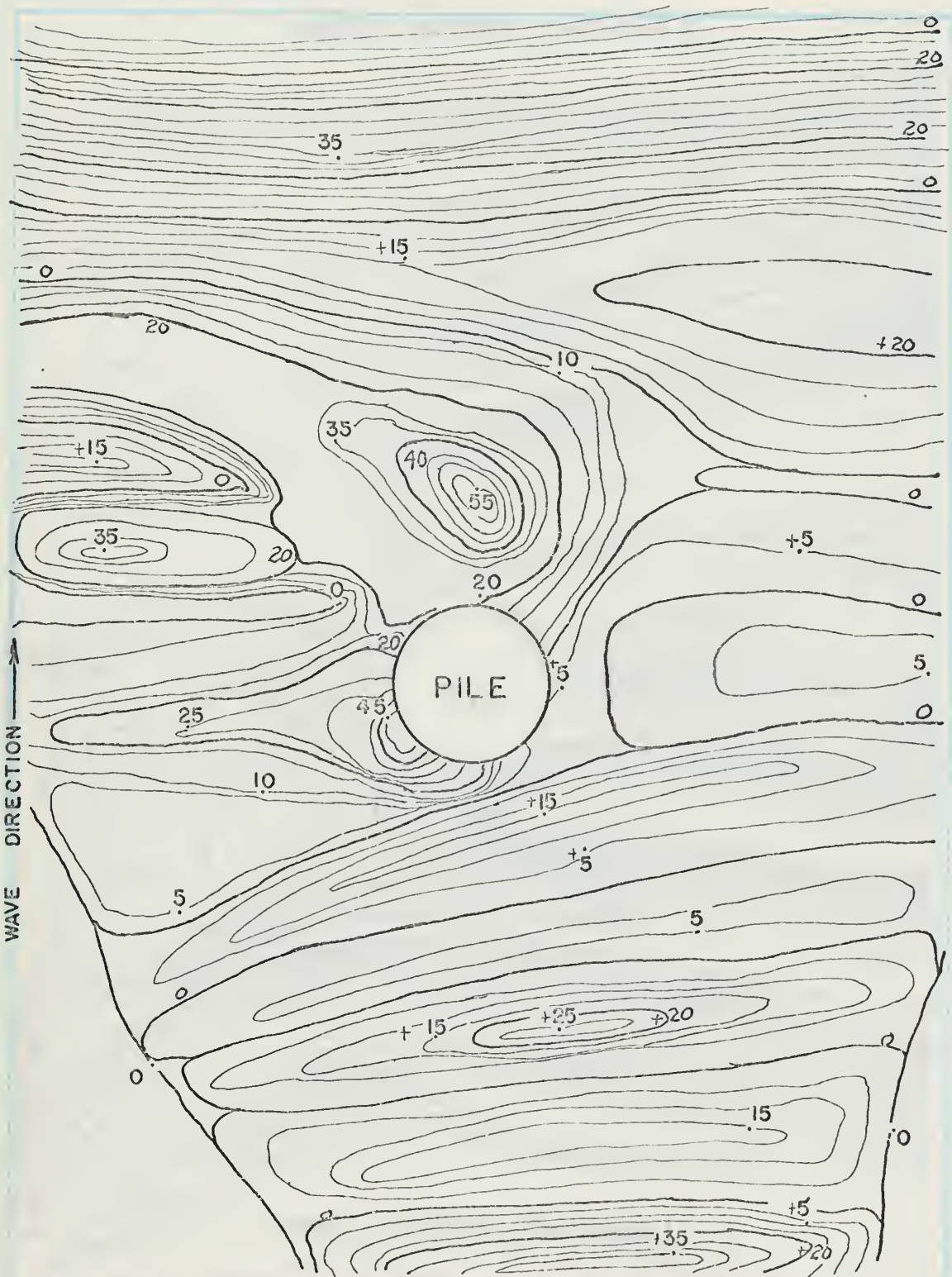

FIG. 48. SCOUR PATTERN FOR WAVE NO. 1, SAND NO. 3, AND 1.25 FT. DEPTH

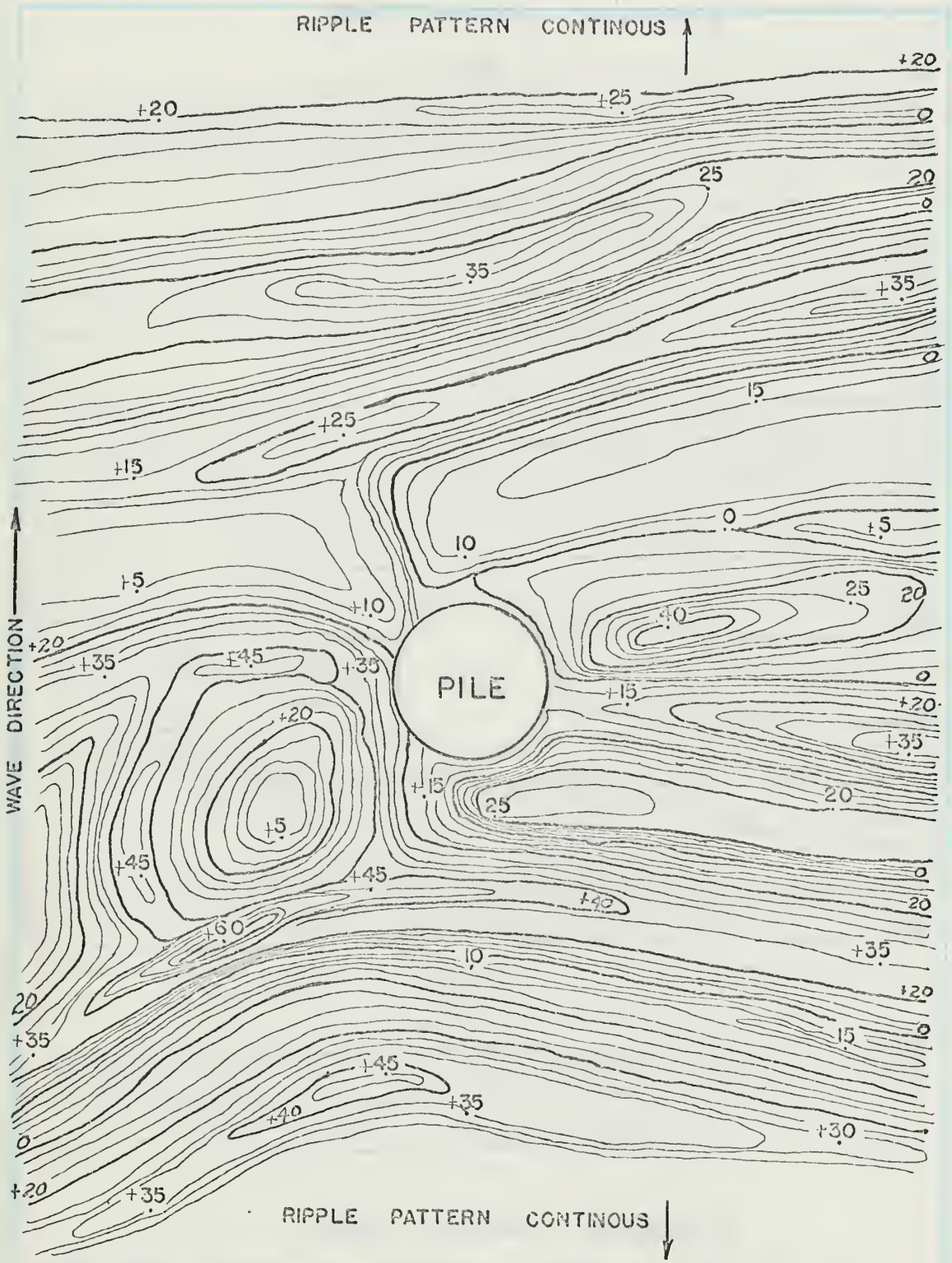

FIG. 49. SCOUR PATTERN FOR WAVE NO. 2, SAND NO. 3, AND 1.25 FT. DEPTH

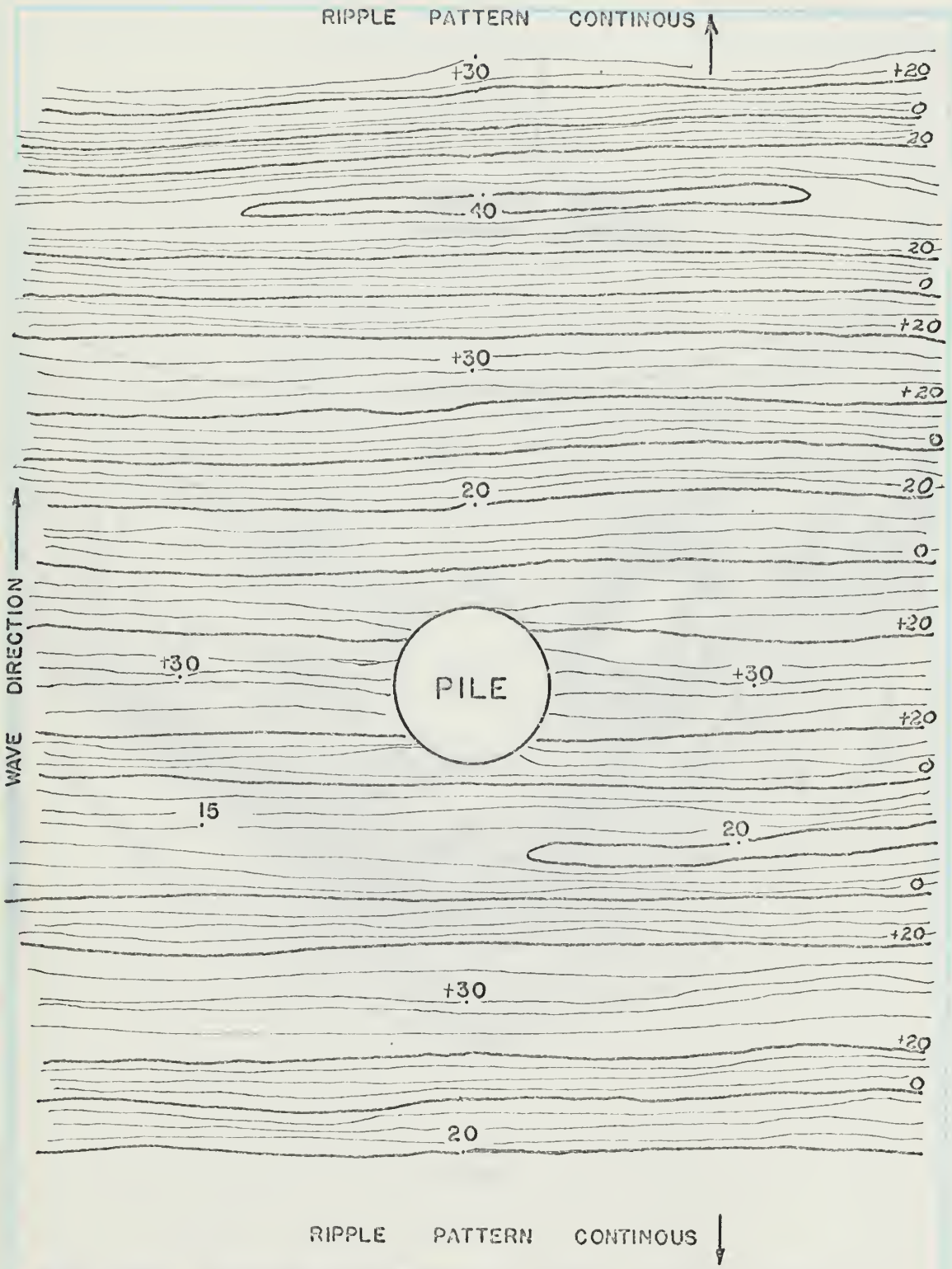

FIG. 50. SCOUR PATTERN FOR WAVE NO. 3, SAND NO. 3, AND 1.25 FT. DEPTH

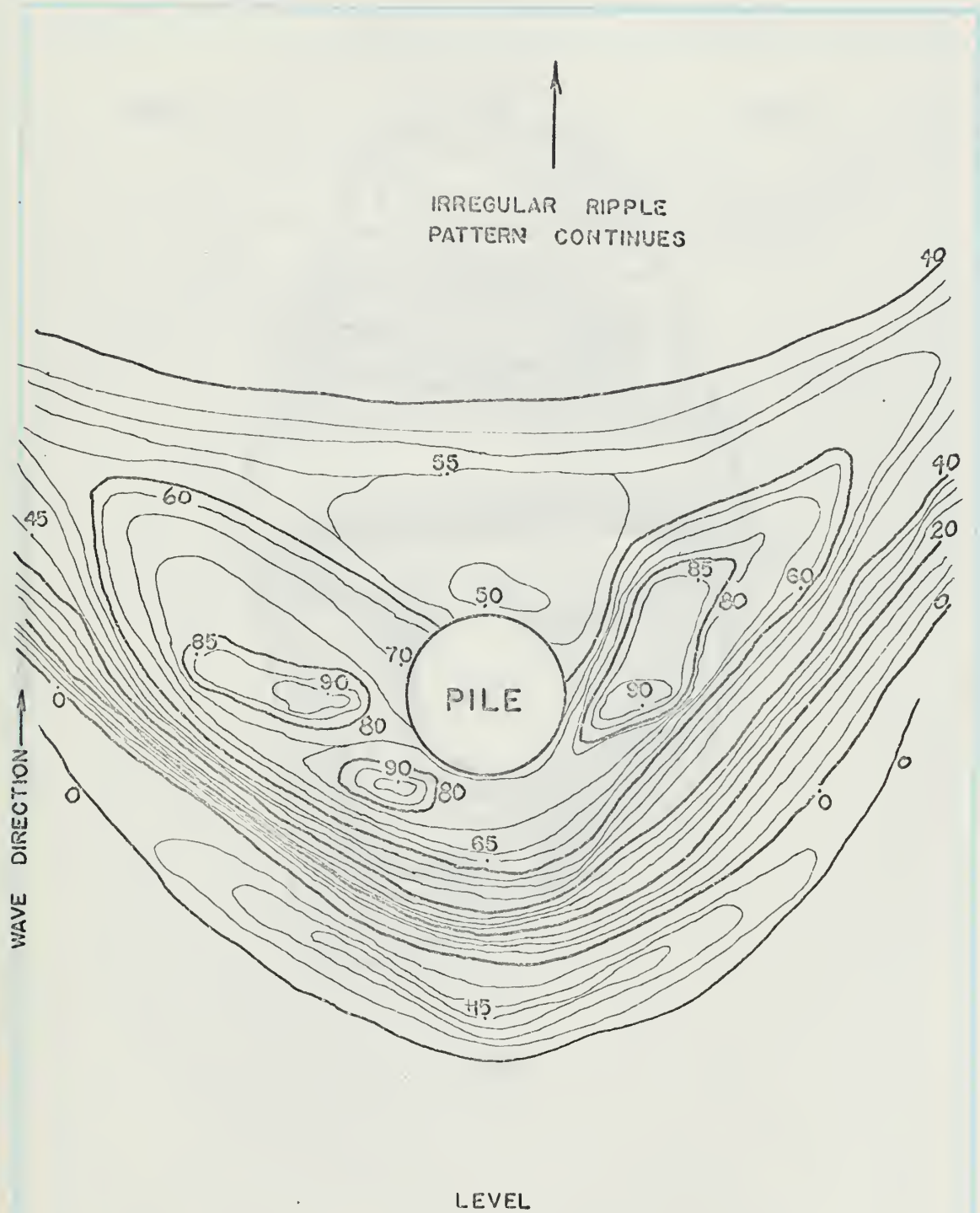

FIG. 51. SCOUR PATTERN FOR WAVE NO. 1, SAND NO. 3, AND 0.666 FT. DEPTH

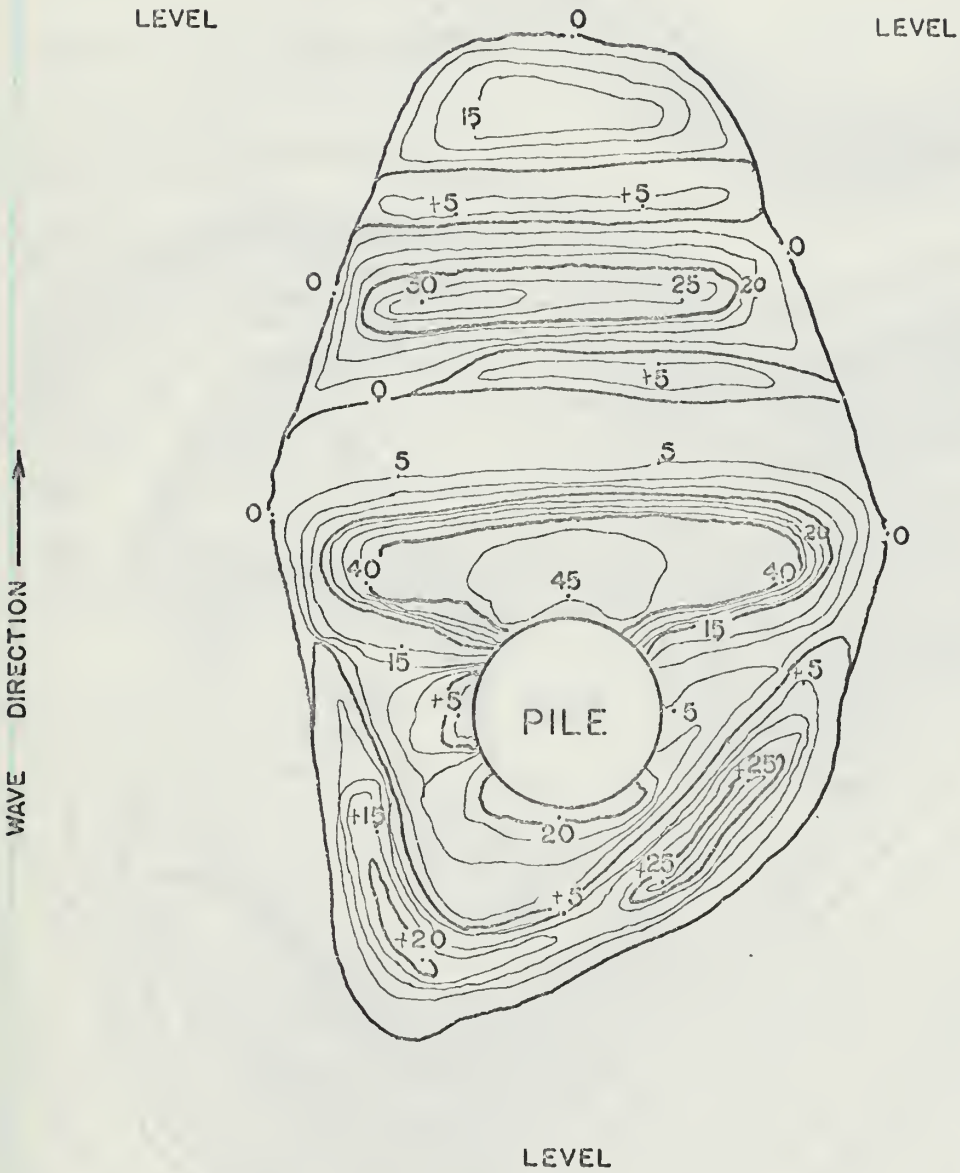

FIG. 52. SCOUR PATTERN FOR WAVE NO. 2, SAND NO. 3, AND 0.666 FT. DEPTH

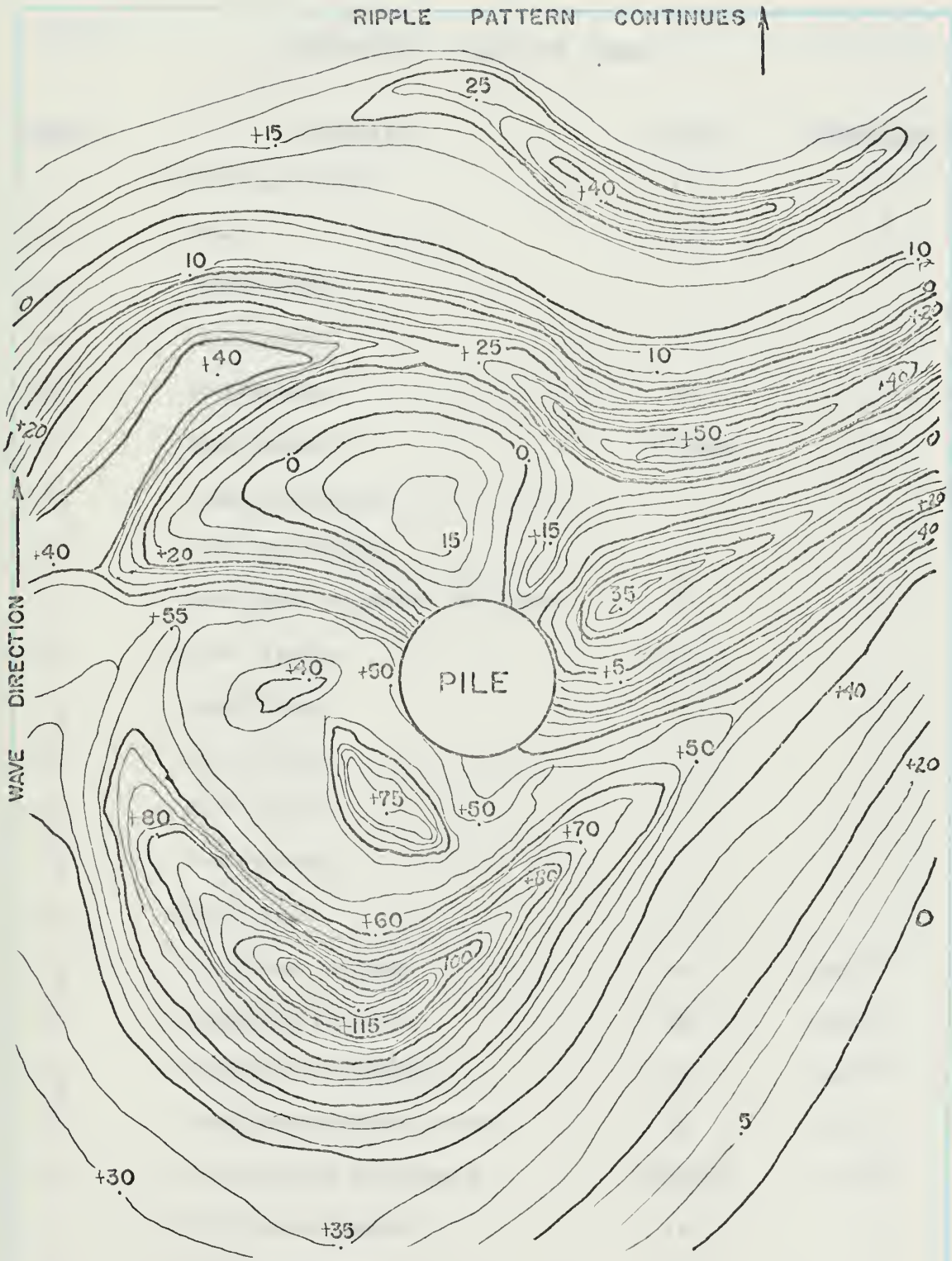

FIG. 53. SCOUR PATTERN FOR WAVE NO. 3, SAND NO. 3, AND 0.666 FT. DEPTH

APPENDIX III. — LIST OF SYMBOLS

Symbol	Quantity	Units	Dimension
a	Wave amplitude	ft	L
A	Area	ft^2	L^2
A_1	Coefficient	-	-
A_2	Coefficient	-	-
A_3	Coefficient	-	-
C	Wave celerity	ft/sec	L/T
C_D	Drag coefficient	-	-
C_L	Lift coefficient	-	-
d	Mean grain diameter 50% finer	ft	L
D	Pile diameter	ft	L
f_2	Coefficient	-	-
f_3	Coefficient	-	-
F_1	Coefficient	-	-
F_2	Coefficient	-	-
F_3	Coefficient	-	-
F_d	Force due to drag	lb	ML/T^2
F_L	Force due to lift	lb	ML/T^2
F_g	Force due to gravity	lb	ML/T^2
F_T	Total hydrodynamic force	lb	ML/T
g	Acceleration of gravity	ft/sec^2	L/T^2
h	Still water depth	ft	L
H	Wave height	ft	L

Symbol	Quantity	Units	Dimension
K	Coefficient	-	-
L	Wave length	ft	L
N_R	Reynolds number	-	-
N_{RP}	Pile Reynolds number	-	-
N_s	Sediment number	-	-
N	Number of waves	-	-
$\bar{S}_u$	Ultimate significant scour depth	ft	L
$\bar{S}$	Significant scour depth	ft	L
S_b	Distance from bottom to water particle under consideration	ft	L
S	Specific gravity of water	-	-
S_s	Specific gravity of sand	-	-
T	Wave period	secs	T
t	Elapse time	secs	T
U	Maximum free stream horizontal velocity	ft/sec	L/T
u	Instantaneous horizontal water particle velocity	ft/sec	L/T
V	Terminal fall velocity	ft/sec	L/T
v	Instantaneous vertical water particle velocity	ft/sec	L/T
x	Horizontal distance	ft	L
y	Vertical distance	ft	L
γ	Specific weight	lb/ft^3	M/L^2T^2
σ	Boundary layer thickness	ft	L
θ	Phase angle	-	-
λ	Wave length of ripple	ft	L

Symbol	Quantity	Units	Dimension
μ	Viscosity of water	lb-sec/ft^2	$\frac{M}{LT}$
ν	Kinematic viscosity	ft^2/sec	L^2/T
ϕ	Angle of repose	-	-
π	Dimensionless parameter	-	-
ρ	Density of water	slug/ft^3	M/L^3
ρ_s	Density of sand	slug/ft^3	M/L^3
ω	Angular velocity of oscillation	rad/sec	$1/T$

VITA

Donald Wells was born in East Orange, New Jersey on April 29, 1939 of Ernest and Dorethea Wells. He received an NROTC Scholarship in 1958 and attended the University of South Carolina from which he received his B.S. in Civil Engineering in 1962. Upon graduation he was commissioned in the U.S. Navy as an Ensign and has remained on active duty since that time. He was sent to Texas A&M University in 1968 to continue his studies in Civil Engineering and will receive his M.S. degree in January 1970. His permanent address is 1031 Summit Drive, Albany, Georgia.

The typist for this thesis was Mrs. J.C. Glidewell, Glidewell Printers, Bryan, Texas.